Title
Mechanisms of Mechanotransduction in Merkel cells

Author
Haeberle, Henry

Publication Date
2008-01-04

Peer reviewed|Thesis/dissertation

Mechanisms of mechanotransduction in Merkel cells

by

Henry Haeberle III

DISSERTATION

Submitted in partial satisfaction of the requirements for the degree of

DOCTOR OF PHILOSOPHY

in

Neuroscience

in the

GRADUATE DIVISION

of the

UNIVERSITY OF CALIFORNIA, SAN FRANCISCO

UMI Number: 3289324

ProQuest Information and Learning Company
300 North Zeeb Road
P.O. Box 1346
Ann Arbor, MI 48106-1346

To my mother and father,

and to Hans van Riel.

ACKNOWLEDGEMENTS

My parents have provided unremitting support and encouragement. My father's laid-back humor has always put the disappointing experiments in perspective and his enthusiasm has made the exciting ones that much more interesting. My mother continues to work harder than I do. Her dedication to her job, her fascination with current research, and her inquisitive mind in general, I have strived to emulate. Both have said that they are lucky to have me in the family. I always knew that I was the one, in fact, that was lucky.

I would very much like to thank David Julius and the members of the Julius lab. I set a rather unorthodox precedent by choosing a fellow as my thesis advisor. David was kind enough to sign on as my official thesis advisor, and furthermore allowed the members of the Lumpkin lab and me to participate in their laboratory meetings. Graduate education does not occur in the classroom. It occurs in the day-to-day interactions with your peers and colleagues, and I learned more in the Julius lab meetings than any other forum in graduate school.

I would like to thank my colleagues in the Lumpkin lab. First and foremost, I would like to thank Becky Piskorowski, who taught me more about electrophysiology than anyone else. She was particular, exacting, and thorough- all the positive traits that I lacked entering graduate school. Mika, Michael, Mayuri, Jodi and Carla were technicians in the lab that provided enthusiastic work and friendly camaraderie.

I would like to especially thank Diana Bautista and Janet Altman for their comments on my written manuscripts. They are the rock stars of my literary world. Janet also provided an invaluable sounding board during my qualifying exam. Diana taught me more of the experimental techniques in this thesis than any other person and I deeply appreciate her help.

My dissertation committee provided invaluable help during my PhD. Every member had useful comments that helped bring my research to fruition. Roger Nicoll, especially, was a great mentor, and together with David Julius pushed me to try the hypotonic experiments described in chapter 3. These experiments formed the core of my thesis, and I thank them for guiding me in the right direction.

Finally I would like to thank my thesis advisor Ellen Lumpkin. I was Ellen's first graduate student, and I think we learned from each other: she learned how to be an advisor, and I learned how to be a student and scientist. She is a thorough, insightful and ethical scientist, and her work can be assumed to be of the highest quality. I hope that my work equally reflects these qualities. If only more scientists could be like her, we would not have to wade through so much questionable research in the literature.

CONTRIBUTIONS

The work in Chapters 2, 3 and 4 was conducted in collaboration with other authors.

The data presented in Chapter 3 was collected by Henry Haeberle, Mika Fujiwara, Michael Medina, Mayuri Panditrao, and Ellen Lumpkin in her laboratory. Specifically, Ellen Lumpkin and Mika Fujiwara developed the Merkel dissociation and purification procedure, and derived the mRNA for the microarray experiments. Ellen Lumpkin performed the microarray experiments. Michael Medina, Ellen Lumpkin and I performed microarray analysis. Michael Medina and Ellen Lumpkin performed RT-PCR. Mayuri Panditrao and Ellen Lumpkin performed immunohistochemistry. I developed the conditions for culturing Merkel cells and performed the live-cell imaging of Merkel cells. Reprinted with permission from Haeberle *et al.* (2004). Molecular profiling reveals synaptic release machinery in Merkel cells. Proceedings of the National Academy of Sciences, volume 101 pp. 14503-14508. Copyright 2004, The National Academy of Science of the USA.

The data presented in Chapter 4 was collected by Henry Haeberle, Leigh Ann Bryan from the laboratory of Ellen Lumpkin and Tegy Vadakkan from the laboratory of Mary Dickinson. Specifically, Tegy Vadakkan contributed the strategy for measuring the volume of Merkel cells. Leigh Ann Bryan performed the RNA isolations of Merkel cells and performed the RT-PCR. Ellen Lumpkin performed the rodamine-phalloidin staining and imaging. Henry Haeberle performed the live-cell imaging and the BODIPY imaging. Submitted as Haeberle *et al.* (2007) Swelling-activated Ca^{2+} channels trigger Ca^{2+} transients in Merkel cells. Copyright 2007 Public Library of Science ONE.

ABSTRACT

Merkel cell-neurite complexes are highly sensitive touch receptors comprising sensory afferents and epidermal Merkel cells. Based on morphological and molecular studies, Merkel cells are proposed to be mechanosensory cells that signal afferents via neurotransmission; however, functional studies testing this hypothesis in intact skin have produced conflicting results. To ask whether Merkel cells are genetically programmed to be excitable cells, we purified Merkel cells from touch domes and used DNA microarrays to compare gene expression in Merkel cells and other epidermal cells. We identified 362 Merkel-cell-enriched transcripts including neuronal transcription factors, presynaptic molecules and ion-channel subunits. Antibody staining of skin sections showed that Merkel cells are immunoreactive for presynaptic proteins, including piccolo, Rab3C, VGLUT2 and cholecystokinin. These data indicate that Merkel cells are poised to release glutamate and neuropeptides. Finally, using Ca^{2+} imaging, we discovered that Merkel cells have L-type and P/Q-type voltage-gated Ca^{2+} channels, which have been shown to trigger vesicle release at synapses.

We also asked whether purified Merkel cells are directly activated by mechanical stimulation. Cell shape was manipulated with anisotonic solution changes and direct indentation with probes while responses were monitored by Ca^{2+} imaging with fura-2. We found that hypotonic-induced cell swelling, but not hypertonic solutions, triggered cytoplasmic Ca^{2+} transients. Several lines of evidence indicate that these signals arise from swelling-activated Ca^{2+}-permeable ion channels. First, transients were reversibly abolished by chelating extracellular Ca^{2+}, demonstrating a requirement for Ca^{2+} influx

across the plasma membrane. Second, Ca^{2+} transients were initially observed near the plasma membrane in actin-filled processes. Third, voltage-activated Ca^{2+} channel (VACC) antagonists reduced transients by half, suggesting that swelling-activated channels depolarize plasma membranes to activate VACCs. Finally, emptying internal Ca^{2+} stores attenuated transients by 80%, suggesting Ca^{2+}-induced Ca^{2+} release amplifies signals from swelling-activated cation channels. To identify candidate mechanotransduction channels, we used RT-PCR to amplify ion-channel transcripts whose pharmacological profiles matched those of Merkel-cell hypotonic responses. Collectively, these results directly demonstrate that Merkel cells are mechanosensitive, identify cellular signaling mechanisms that mediate mechanically evoked responses, and support the hypothesis that Merkel cells contribute to touch reception in the Merkel cell-neurite complex.

TABLE OF CONTENTS

LIST OF FIGURES

CHAPTER 1:

GENERAL INTRODUCTION

The mechanisms by which the skin senses touch, temperature and pain have been the subject of scientific inquiry since at least the third century BCE, when Aristotle included touch in his five cardinal senses. Anatomical experiments in the 19th century revealed a remarkable assortment of sensory structures within the dermis and underlying tissues of the skin. Concurrently psychophysical experiments discovered the presence of sensory spots that were highly sensitive to specific modalities of stimuli in the skin of man (Hamann, 1995). The spatial localization of structure and function lead von Frey and others to postulate the specificity theory of somesthesis (Boring, 1942), which states that each of the cutaneous senses are subserved by sensory neurons sensitive to only one sensory modality and encoding only one perceptual quality.

The sensory modalities of somesthesis are innocuous touch, cool, warm and pain (nociception). What sensory modalities were mediated by the various cutaneous sensory structures was the subject of much speculation: most sensory structures are not visible in live humans, and the inability to record the activity of sensory neurons in animals prevented definite attribution of individual sensory modalities to individual neuronal populations. Consequently, the strict labeled-line doctrine of somesthesis was controversial.

Physiological analysis of cutaneous sensation awaited the development of single unit recordings of primary afferent fibers. In 1926, Adrian and Zottermann developed the first live, semi-intact nerve recordings of primary sensory afferents and their associated cutaneous targets (Adrian and Zotterman, 1926; Zotterman, 1939). They discovered individual afferents specifically activated by light touch, supporting von Frey's

specificity theory. Subsequent work confirmed the presence of specific thermosensitive and nociceptive afferents (Zotterman, 1939; Dodt and Zotterman, 1952; Hensel and Boman, 1960).

The presence of different labeled lines mediating different sensory modalities suggested that stimulus intensity might be encoded by firing patterns of individual neurons. Mountcastle tested this theory by recording from sensory afferents while applying quantitative indentations of the skin (Werner and Mountcastle, 1965). He described mechanically sensitive fibers responding to indentation of mechanosensitive touch-domes with the following power function: $R = K \bullet S^n$ where R is the mean response number, K is a constant, S is the stimulus intensity measured as net skin indentation and the exponent n is a constant. Mechanosensitive afferents in hairy skin have negative power functions (n<1) (Werner and Mountcastle, 1965), while mechanosenstive afferents in glabrous skin have linear power functions (n=1) (Mountcastle, 1967). These power functions permit glabrous skin to accurately encode degree of mechanical stimulation, while hairy skin is highly sensitive to mechanical stimuli just above threshold. Mountcastle extended his work by recording similar mechanically induced stimulus-response functions in the spinal cord and the primary somatosensory areas of the brain, indicating that stimulus intensity was primarily encoded by the sensory afferent terminal and that transformations at more central areas of the nervous system were in sum linear (Mountcastle, 1967; Knibestol and Vallbo, 1980).

Cutaneous afferent stimulus response profiles

Further studies of cutaneous sensory afferents in various vertebrates revealed five consistent stimulus-response profiles (Hamann, 1995). These response profiles are

characterized by their adaptive properties (Fig. 1). Rapidly adapting afferents fire bursts of action potentials to skin movement and vibration, but are insensitive to sustained skin deformation. Slowly adapting afferents, by contrast, continue to respond to sustained skin deformation for upwards of half an hour and are relatively insensitive to high frequency vibration (Iggo and Muir, 1969). Both rapidly adapting and slowly adapting response profiles are further subdivided into two categories: type I and type II. Type I responses have receptive fields with small, sharp borders while type II responses have large, poorly defined receptive fields.

Rapidly adapting type I (RA I) afferents respond to bending of hairs, gentle rubbing of skin, and vibration (Brown and Iggo, 1967; Petit and Burgess, 1968; Iggo and Findlater, 1984). They are also the most sensitive mechanosensors in the hand, responding to surface features as small as 2 μm. Rapidly adapting type II responses (RA II or PC), which have been definitively correlated with Pacinian corpuscles (Iggo and Findlater, 1984; Bell et al., 1994), respond most robustly to high frequency vibration (Hunt and Mc, 1960). Slowly adapting type I (SAI) afferents respond specifically to indentation of touch-domes containing Merkel cell-neurite complexes (Iggo and Muir, 1969), and have the highest spatial resolution of the afferent response profiles. Slowly adapting type II (SAII) afferents are spontaneously active, and respond somewhat to indentation but more effectively to skin stretch (Brown and Iggo, 1967; Leem et al., 1993). Finally, c-mechanorecptors are rapidly adapting c-fibers that respond to both skin indentation and bending of hairs (Nordin, 1990).

Definitive correlation of cutaneous stimuli with afferent responses and perception was not possible until the advent of a novel technique in awake humans called primary

afferent microneurography. In this experimental paradigm, extremely thin electrodes record electrical impulses from nerves. Mechanical stimuli such as a pen point are applied to the hand and single afferent responses associated with a tactile unit are identified. The electrode is then used to stimulate the single afferent fiber, and the subject reports the quality of sensation generated. Most of these studies have been done in the hand, which has a high density of mechanosensitive afferents (Vallbo and Johansson, 1984; Johnson and Hsiao, 1992). Such studies, combined with traditional electrophysiological recordings in primates, have indicated that rapidly adapting afferents transmit information of skin motion. They are integral to transmitting information related to low frequency vibration and the sensation of slip when between skin and a gripped object (Johnson et al., 2000). Microstimulation of RA afferents in humans was described as a "wobbling" or "fluttering feeling" with very short electrical trains described as a "tap" (Vallbo et al., 1984). RAII or PC afferents respond best to vibratory stimuli, and are described by human subjects not surprisingly as a "vibration" sensation. Since SAII responses are more sensitive to forces tangential to the skin than indentation, they likely encode skin stretch. Microstimlation of SAII afferents has been described as percepts ranging from sustained lateral pulling of the skin to flutter (Vallbo et al., 1984). By contrast, slowly adapting type I afferents encode texture and small feature discrimination, and are necessary for fine tactile discrimination tasks, such as reading braille (Johnson et al., 2000). They are extremely sensitive to local deformations: a single brail dot will elicit 20 times more firing than a smooth surface of equal indentation (Phillips and Johnson, 1981). Microstimulation of single SAI afferents innervating the hand induced humans to

feel a faint and uniform pressure, much like "a leaf held against the skin" or of a "soft painting brush held tangentially against the skin" (Vallbo et al., 1984).

The Merkel-cell neurite complex underlies the SAI response profile

In 1969, Iggo and Muir identified highly touch-sensitive domes in hairy skin, called touch domes, as the source of a slowly adapting response (Iggo and Muir, 1969). These structures are visible in de-haired rodents and felines, and Iggo and Muir were able to characterize the highly spatially sensitive response profile. They noted that SAI fibers are completely silent in the absence of mechanical stimulation of the touch dome (Fig 1). Sustained touch dome indentation elicits a burst of action potentials followed by a slowly adapting response. The sustained element of the response is characterized by an irregular firing pattern, with interspike intervals ranging from <20 to 220 ms. This characteristic in particular differentiates SAI responses from SAII responses, which have a highly regular sustained firing pattern. Iggo and Muir noted that the dome of the touch dome was highly sensitive to indentation, with firing rates dropping precipitously with indentation of the surrounding tissue. Measurement of conduction velocity by electrical stimulation of touch dome indicated that they were innervated by rapidly conducting, highly myelinated afferents (A-β fibers).

Touch dome are generally innervated by a single, highly myelinated axon that branches repeatedly, ultimately contacting specialized epidermal cells called Merkel cells (Munger, 1965; Iggo and Muir, 1969). The axon has large terminal elaborations, called axon termini, at its point of contact with Merkel cells. These axon termini envelop the deep half of Merkel cells. This anatomy is reminiscent of other sensory structures, consistent with a role as a touch receptor (Fig 2A). The Merkel cells are located just

above the basement membrane, at the border of the epidermis and dermis. The Merkel cells have processes that interdigitate among the overlying keratinocytes, which have more layers in the touch dome, contributing to its dome-like appearance. The dermal portion of the dome contains collagen bundles woven in a tight mesh. The dermis beneath the dome is well vascularized, suggestive of high-energy use by the axon and its associated Merkel cells, which together are termed the Merkel cell-neurite complex.

Recent experiments by Woodbury and Koerber have confirmed Iggo and Muir's original correlative work indicating that the Merkel cell-neurite complex underlies the SAI response (Woodbury and Koerber, 2007). In a technical *tour de force* they developed a mouse semi-intact preparation in which they obtained whole-cell recordings of dorsal root ganglia somata with their cutaneous afferents intact. By filling electrodes with fluorescent dye, they were able to trace the axonal projections of the cell bodies they were recording from. Cells with SAI response profiles had dye present in the axons of 1 or 2 Merkel cell-neurite complexes.

Merkel cell Anatomy and Ultrastructure

Merkel cell anatomy suggests a contribution to touch reception in the touch dome. For Merkel cells to be formally categorized as sensory cells, however, they must fulfill two basic criteria: they must be intrinsically mechanically sensitive and they must signal to the underlying afferent terminal through synaptic transmission. Merkel-cell ultrastructure provides some evidence for both functions (Fig 3). Merkel cells have, thin, 1–2 μm microvilli that project into overlying keratinocytes (Iggo and Muir, 1969). These processes are reminiscent of steriocilia in hair cells and are hypothesized to help detect shearing deformations due to indentation of the touch dome (Iggo and Muir, 1969).

Additionally, Merkel cells and keratinocytes are linked by many small desmosomes, suggesting stiff structural attachment (Munger, 1965; Iggo and Muir, 1969). Additional ultrastructural evidence supports the notion of synaptic transmission between Merkel cells and the afferent terminal. There is a close association between Merkel cells and the axon terminus, with the afferent terminal expanding to cover the entire deep half of the Merkel cell (Iggo and Muir, 1969). Between Merkel cells and the afferent terminal there is a synapse-like granular cleft and a postsynaptic-like thickening of the afferent terminal membrane (Iggo and Muir, 1969; Hartschuh and Weihe, 1980). Additionally, Merkel cells have large, dense-core granules clustered between the nucleus and the afferent terminal. The synapse-like structures always have associated granules, with some directly contacting the synapse-like structure (Mihara et al., 1979; Hartschuh and Weihe, 1980). The axon termini contain an abundance of mitochondria and have small clear-core vesicles (Munger, 1965). In one report, a second synapse-like structure was observed with an asymmetrical electron density facing the Merkel cell, accompanied by a cluster of small clear-core vesicles in the neuron (Mihara et al., 1979), which the authors interpreted as a possible reciprocal synapse.

The presence of synapse-like structure suggests that Merkel cells are sensory cells that function in the skin much as hair cells and photoreceptors function in hearing and vision; however, Merkel cells do not contain the small clear-core vesicles characteristic of these other sensory synapses and fast, excitatory neurotransmission in general. Large dense-core vesicles are generally thought to release neuropeptides or hormones, although they also may contain the excitatory neurotransmitter glutamate (Morimoto et al., 2003). Therefore it is possible that Merkel cells employ large dense-core vesicles for

mechanically triggered, excitatory synaptic transmission. The recent discovery that Merkel cells express vesicular glutamate transporters further supports the presence of glutamate mediated synaptic transmission (Hitchcock et al., 2004; Nunzi et al., 2004). Furthermore, electrophysiological recordings of cultured Merkel cells revealed voltage-activated K^+ and Ca^{2+} currents (Yamashita et al., 1992), indicating that Merkel cells are excitable cells.

Do Merkel cells contribute to mechanotransduction?

These anatomical findings have lead to a long-standing controversy over whether mechanotransduction occurs in Merkel cells or the axon termini in the Merkel cell-neurite complex. Iggo and Muir hypothesized that the irregular firing pattern characteristic of the SAI response could be explained if each Merkel cell, operating independently, could induce action potentials in the afferent nerve (Iggo and Muir, 1969). Such independent excitation of the nerve would generate the binomial distribution of interspike intervals observed in the SAI response. On the other hand, such firing patterns could be generated by spike generation in the axon termini. Indeed, Gottschaldt and Vahle-Hinz observed SAI mechano-electric response latency between 0.2 and 0.3 ms., which they interpreted as being too fast for chemical synaptic transmission (Gottschaldt and Vahle-Hinz, 1981). Unfortunately, Merkel cells' location in the skin prevents direct electrophysiological recordings with microelectrodes in slice preparations. Instead, several groups have attempted pharmacological manipulations of semi-intact skin-nerve preparations to determine if synaptic transmission is required for normal SAI response. Pacitti and Findlater reported that skin nerve-preparations bathed in voltage-activated calcium channel blockers have impaired SAI responses (Pacitti and Findlater, 1988). Fagan and

Cahusac found that the NMDA receptor antagonist MK-801 inhibited the static element of the SAI response, but the AMPA receptor antagonist NBQX had no effect (Cahusac et al., 2005). Other blockers of neuromodulators had no effect (Gottschaldt and Vahle-Hinz, 1982).

Studies asking whether Merkel cells are required for the SAI response have produced conflicting results. Eliminating Merkel cells by photoablation greatly diminished SAI responses in one study ((Mills and Diamond, 1995)), but not another (Ikeda et al., 1994)). The contradictory outcomes likely resulted from incomplete photoablation of Merkel cells, or collateral damage of the nerve afferent (Senok et al., 1996). Another study characterized mice deficient in the low affinity neurotrophin receptor p75 (Kinkelin et al., 1999). The authors noted a dramatic reduction in the number of visible touch domes beginning two weeks after birth in deficient animals, but no change in slowly adapting responses, however, the remaining touch domes had only slightly reduced numbers of Merkel cells. This report also did not distinguish between SAI and SAII response profiles, confounding their interpretation considerably.

Several groups have attempted to determine if Merkel cells are directly responsive to mechanical stimulation. Chan *et al*. used a semi-intact sinus hair preparation to investigate Merkel cells *in situ* (Chan et al., 1996). They incubated the entire sinus-hair in the fluorescent Ca^{2+} indicator, fura-2, and treated the preparation with mechanical stimuli and solutions containing depolarizing concentrations of potassium. Unfortunately, Merkel cells were unlabeled, so the [Ca^{2+}] transients observed could reflect any cell in the preparation (Chan et al., 1996). A second group analyzed osmotic induced [Ca^{2+}] responses in an acutely dissociated Merkel cell, labeled with the

fluorescent Merkel cell marker, quinacrine. Though promising, the rigors of dissociation likely prevented analysis of additional cells (Tazaki and Suzuki, 1998).

To test for mechanosensitivity in the Merkel cell, and by extrapolation their potential role as a sensory cell, we have developed a protocol to isolate, enrich, and culture Merkel cells *in vitro* by employing transgenic mice with GFP expressed specifically in Merkel cells in the skin. I demonstrate that cultured Merkel cells are sensitive to the mechanical forces induced by both hypotonic solutions and direct touch *in vitro*. Furthermore, this mechanical sensitivity is likely bestowed by force-sensitive, Ca^{2+} permeable ion channels clustered in Merkel cell processes. The mechanically induced Ca^{2+} influx is amplified by voltage-activated Ca^{2+} channels and Ca^{2+}-induced Ca^{2+} release. Along with my colleagues, I also demonstrate that Merkel cells express presynaptic machinery required for synaptic transmission indicating the synapse-like structures observed ultrastructurally are most likely synaptic active zones. The presence of such zones supports the hypothesis that Merkel cells excite or modulate neurons via chemical synaptic transmission. We also identify two potential neurotransmitters: glutamate and CCK8. Together these results support the hypothesis that Merkel cells are a functional component of mechanotransduction in the Merkel cell-neurite complex.

Figures

Figure 1. Representation of response profiles of PC (RA II), RA I, SAI and SAII afferents to a compound mechanical stimulus (Mollon, 1982).

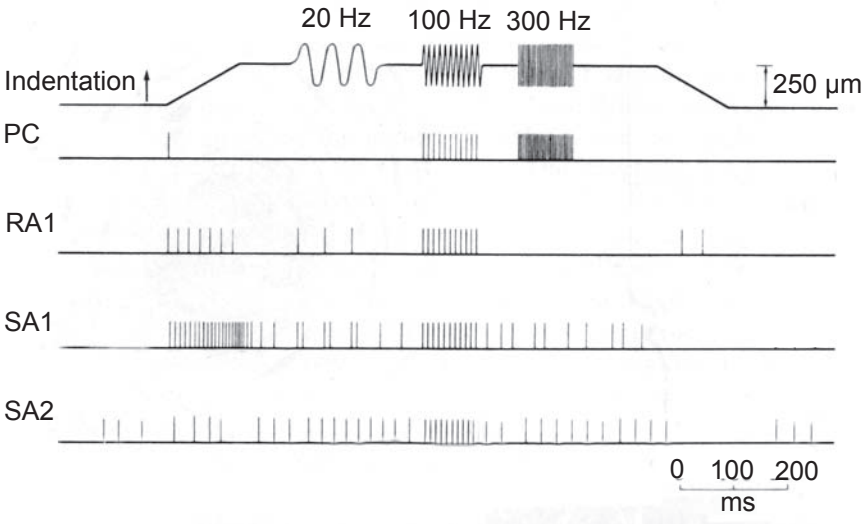
20 Hz
100 Hz
300 Hz
Indentation
250 µm
PC
RA1
SA1
SA2
0
100
200
ms

Figure 2. Touch domes contain Merkel cell-neurite complexes. Diagram displays the Merkel cell-neurite complex and surrounding touch dome of the cat (A; adapted from Iggo and Muir 1969). Touch-domes are raised areas of the skin in rodents and cats. They have areas of thickened epidermis, consisting of elongated keratinocytes (yellow), and contain from a dozen to more than 30 Merkel cells (green). Merkel cells are located on the superficial surface of the basement membrane, which separates the dermis from the epidermis. Most Merkel cells are contacted by a myelinated nerve fiber (blue), which branches, loses its myelin sheath (dark blue), and forms an afferent terminal on the deep surface of Merkel cells. Touch domes are well vascularized, containing at least one blood vessel coursing through the dermis (red). Many touch-domes are also innervated by an unmyelinated nerve fiber (dark blue). A confocal image displays Merkel cells with associated nerve fiber in the touch dome (B). Green labels GFP, which is expressed in Merkel cells of a *math1:nGFP* transgenic mouse. Blue labels neurofilement 200, a cytoskeleton protein present in myelinated neurons. Fibrous structures in green in the dermis are autofluorescent fibrils and not GFP labeling.

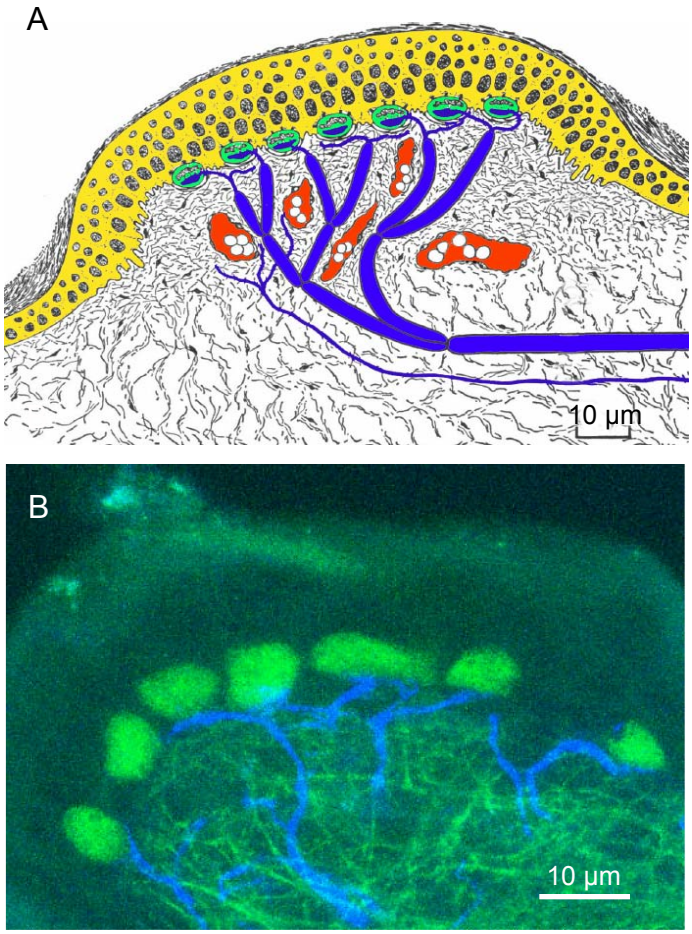
A
10 µm
B
10 µm

Figure 3. Tracing of an electron micrograph showing the Merkel cell and its associated nerve afferent (Adapted from Iggo and Muir, 1969). Merkel cells share desmosomes (D) with overlying keratinocytes, and have actin-filled processes (P) that protrude into overlying keratinocytes. Large, dense core vesicles (G) are evident in the basal part of the Merkel cell, deep to the characteristically lobulated Nucleus (N). These vesicles are in close apposition to the afferent terminal (AT), and often cluster around synapse-like densities. Merkel cells are contacted exclusively by myelinated axons (A).

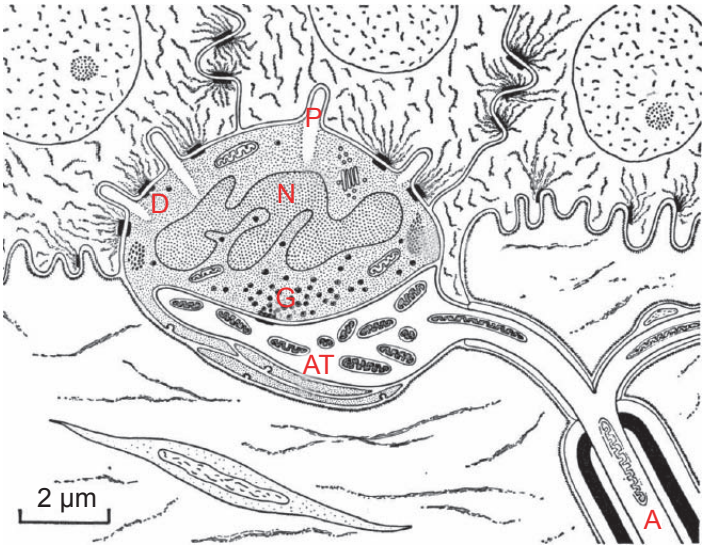
P
D
N
G
AT
2 µm
A

CHAPTER 2:

METHODS

Cell preparation. All animal research was conducted according to protocols approved by Institutional Animal Care and Use Committee (IACUC) of Baylor College of Medicine (BCM) and the University of California, San Francisco (UCSF). Merkel cells were dissociated from the skin of post natal day 3–6 (P3–P6) *Math1/nGFP* (Lumpkin et al., 2003; Haeberle et al., 2004) mice after euthanization by decapitation with sharp scissors. The skin from the body and face was dissected and washed in 10% Hibiclens (Regent Medical) and Hank's balanced salt solution (HBSS) supplemented with penicillin, streptomycin and amphotericin B. Tissue was cut into 1-cm^2 pieces and incubated for 1 h at 23ºC in dispase (BD Biosciences) suspended to 25 U/mL in Ca^{2+} and Mg^{2+} free HBSS. The epidermis was peeled from the dermis with sharp forceps and incubated in 0.1% trypsin and 1 mM EDTA-4Na solution (Gibco) for 15 min with periodic vortexing. Trypsin was neutralized with fetal bovine serum (FBS) and cells were triturated with a 5-ml seriological pipette. Cells were filtered with 70- and 40-μm cell strainers, spun at 400 x *g* for 12–15 min, and then resuspended in keratinocyte media (CNT-02, Chemicon) with 10% FBS. GFP-positive Merkel cells were enriched to approximately 85% from epidermal-cell suspensions by FACS into a landing media containing 50% FBS and 50% keratinocyte media (CNT-02, Chemicon). Merkel cells were spotted onto either collagen-coated coverslips for Ca^{2+} imaging or collagen-coated eight-well chamber slides (LAB-TEK) for cell volume-analysis and grown with 5% CO_2 at 37 ºC in antibiotic-free keratinocyte media (CNT-02, Chemicon).

Fluorescence-activated cell sorting (FACS). Cells were purified using a multi-parameter cell sorter. We excluded dead cells by setting gates on plots of forward versus

side scatter. Next, we used plots of green fluorescent protein (GFP) fluorescence (530/30 nm) versus red autofluorescence (580/30 nm) to set gates around GFP-positive (GFP^+) cells and GFP-negative (GFP^-) cells. Equal numbers of GFP^+ and GFP^- epidermal cells were collected with each sort so that cells from the same animals could be compared directly. Cells were sorted into lysis buffer for RNA isolation or into S-MEM/50% FBS for culture. The isolation procedure (from skin harvesting to lysis buffer) typically lasted ~4 h.

Microarray RNA amplification. Total RNA was harvested from epidermal cells using a Mini RNA isolation kit (Zymo Research) and DNA was removed using RNase-free DNase (Promega). RNA was amplified from matched numbers of GFP^+ and GFP^- cells (P2 – P5; $1 – 2 \times 10^4$ per reaction). To prepare samples for screening cDNA microarrays, we used published linear amplification methods ((Klebes et al., 2002)). Two rounds of reverse transcription (RT) and *in vitro* transcription (IVT) produced 7 – 28 μg amplified RNA per reaction. For screening Affymetrix arrays, amplification through the second round of cDNA synthesis was performed as described ((Klebes et al., 2002)), then IVT was accomplished with a kit (Enzo BioArray HighYield). These methods yielded 5 – 40 μg biotinylated RNA per reaction. Biotinylated RNA was pooled from three amplification reactions for each Affymetrix array.

Microarray analysis. Glass-slide cDNA microarrays were generated by the UCSF Mouse Microarray Consortium. Fluorescent cDNAs were produced from amplified RNA (2 μg) and microarrays were screened as described (ref. (DeRisi et al., 1997). Affymetrix GeneChips (Murine Genome Array U74v2) were hybridized and analyzed. Enrichment thresholds were chosen to yield a manageable number (<300) of elements for further

analysis. Detailed protocols for producing and screening cDNA microarrays are available at http://derisilab.ucsf.edu/. Affymetrix GeneChips (Murine Genome Array U74 version 2) were hybridized with 11 - 15 μg of biotinylated RNA, washed, and scanned according to manufacturer's protocols with a GeneArray 2500 scanner (Affymetrix). GeneChip data were analyzed with Microarray Suite (version 5, Affymetrix). For each trial, signals from GFP^+ cells (experimental sample) were normalized and compared with those from GFP^- epidermal cells (baseline sample), and $\log_2$ ratio values (GFP^+ cells/GFP^- cells) were calculated. The identities of probe sets were ascertained by querying the Net Affx database (http://www.affymetrix.com/analysis/index.affx), Entrez Gene and UniGene. To exclude transcripts that gave low hybridization signals, we analyzed probe sets whose signals in GFP^+-cell samples were scored as 'present' by the absolute-call algorithm. Glass-slide cDNA microarrays containing 21,300 mouse clones were generated by the UCSF Mouse Microarray Consortium using published methods (DeRisi *et al.,* 1997, *Science* **278**,680-686). Cy3- and Cy5-labeled cDNA samples were combined and competitively hybridized to microarrays for 18 – 19 h at 65°C. Fluorescence signals were visualized with a microarray scanner (GenePix 4000B, Axon Instruments). Data were analyzed with GenePix Pro (version 4.1, Axon Instruments), NOMAD (http://ucsf-nomad.sourceforge.net/), Excel (version X, Microsoft) CLUSTER (version 1.6) and TREEVIEW (version 2.2; Eisen *et al.,* 1998, *Proc Natl Acad Sci USA* **95,**14863-14868). To omit elements with low signal-to-background ratios, data were filtered to exclude array elements whose summed Cy5 and Cy3 signals were less than 500 units.

Five experimental trials from two biological replicates (independent sorts and amplifications) were performed. In two trials, a Cy5-labeled cDNA sample from GFP^+

cells was directly compared to a Cy3-labeled cDNA sample from GFP^- epidermal cells by competitive hybridization. In the remaining three trials, Cy5-labeled samples from GFP^+ or GFP^- epidermal cells were hybridized against Cy3-labeled cDNA from reference tissues. For those trials, reference RNA was amplified from total RNA (10 ng per reaction) extracted from brain, skin, heart, spleen, liver and kidney. When experimental samples were compared to reference samples, fold enrichment values (GFP^+ cells/GFP^- epidermal cells) were calculated by dividing the fluorescence ratios from GFP^+ trials by the corresponding ratios from GFP^- trials. To determine the mean fold enrichment for an element, we calculated means for the data derived from each biological replicate and then calculated the mean of means. The identities of RIKEN clones were determined by querying the RIKEN FANTOM database (http://fantom.gsc.riken.go.jp/db/search/), Entrez gene and Unigene.

Comparison of RIKEN and Affymetrix data. In addition to the database queries described above, BLAST searches were performed to determine whether elements on the RIKEN and Affymetrix arrays represented the same transcripts. When we identified multiple array elements or probe sets that represented the same transcript, we calculated the mean fold enrichment for each array type by averaging the fold enrichment values from all independent elements and all biological replicates. Because hybridization signals were calculated differently for RIKEN and Affymetrix arrays, we did not average together data from the two types of arrays.

Of 362 unique genes identified by our thresholds, 41 genes (11%) were scored as Merkel-cell-enriched on both array types. This number underestimates the

reproducibility of the data because we set conservative enrichment thresholds that could have excluded genes that were only moderately enriched on one of the two array types.

To better estimate reproducibility, we determined whether the 206 positive clones from the RIKEN screen (criteria: detectable hybridization signals and ≥3-fold enriched in Merkel cells in 3/5 RIKEN trials) were also likely to be enriched in the Affymetrix data. 108/206 clones were annotated with their RIKEN ID in the Affymetrix database. Of these clones, 68 gave detectable hybridization signals in both of the Affymetrix trials. Fifty-nine of the RIKEN clones were scored as likely to be enriched (change $P \leq 0.10$) in both of the Affymetrix trials. Thus, 55% of the annotated RIKEN clones that were included on both array types were reliably scored as Merkel-cell-enriched on both types of arrays.

Calcium channel RT-PCR. Total RNA from 1 – 2 X 10^4 sorted cells served as the template for RT. First-strand cDNA was synthesized using oligo$(dT)_{12\text{-}18}$ primers at 42°C for 2 h using SuperScriptII (Invitrogen). PCR products were amplified with touchdown PCR; 1/100 – 1/20 of an RT reaction was used for each PCR. In all experiments, control PCRs lacking cDNA template were performed to confirm that products were not due to contamination. $Ca_V2.2/\alpha_{1B}$ and keratin primers were designed to span introns to demonstrate that products were amplified from cDNA and not genomic DNA.

Immunohistochemistry. Hairy skin from P15 – P19 mice was fixed, embedded and stained as described (Lumpkin et al., 2003). Tissue was cryosectioned at 10 – 50 μm. Sections were permeabilized and blocked overnight at 4°C or 1 – 4 h at room temperature with 0.1% (wt/vol) TritonX-100 and 3% (wt/vol) non-fat dry milk in PBS. Sections were incubated overnight at 4°C or 3 h at room temperature in primary antibodies, then rinsed

with PBS. To detect bound antibodies, sections were incubated for 30 – 70 min at room temperature in secondary antibodies conjugated to Alexa 546, Alexa 594 or Alexa 660 (2 μg/ml; Molecular Probes, Eugene, OR). Fluorescence of GFP, DAPI and secondary antibodies were excited sequentially and visualized by confocal microscopy. Unless noted, images represent a single plane of focus. Primary antibodies were: mouse anti-KRT1-18 (RGE 53; ICN Pharmaceuticals), mouse-neurofilament 200 (N52; Sigma), rabbit anti-Rab3C (Calbiochem), rabbit anti-cholecystokinin 26 – 33 (CCK8; Phoenix Pharmaceuticals), rabbit anti-VGLUT2 (gift from Dr. Robert Edwards, UCSF) and rabbit anti-Piccolo (Synaptic Systems).

Live-cell Ca^{2+} imaging. After 2 days in culture, Merkel cells were loaded for 20 min with 2 μM fura-2 acetoxymethyl ester (Molecular Probes) and 0.02% pluronic F-127 (Molecular Probes) in a modified Ringer's solution containing (in mM): 110 NaCl, 5 KCl, 10 HEPES (pH 7.4), 10 D-Glucose, 2 $MgCl_2$, 2 $CaCl_2$ and 30 mannitol (290 mmol·kg^{-1}). Cells were allowed to digest the ester bonds for 30 min and were imaged in modified Ringer's solution. Twenty percent hypotonic solutions contained all the same elements as modified Ringer's solution except mannitol. At these concentrations, mannitol did not fluoresce significantly in the fura-2 excitation or emission range. To make 30% hypertonic solution, modified Ringer's solution was supplemented with an additional 45 mM mannitol (377 mmol·kg^{-1}). For dose-response experiments, solutions contained (in mM): 95 NaCl, 5 KCl, 10 HEPES (pH 7.4), 10 D-Glucose, 2 $MgCl_2$, 2 $CaCl_2$ and 45 mannitol (290 mmol·kg^{-1}, isotonic); 30 mannitol (10% hypotonic, 261 mmol·kg^{-1}); 15 mannitol (20% hypotonic, 232 mmol·kg^{-1}) or no mannitol (30% hypotonic, 203 mmol·kg^{-1}). Osmolality of all solutions was verified to within 1% of

target values with a Vapro 5520 vapor pressure osmometer (Wescor). Merkel cells were depolarized with high-K^+ Ringer's solution containing (in mM): 70 NaCl, 75 KCl, 10 HEPES (pH 7.4), 10 D-glucose, 2 $MgCl_2$ and 2 $CaCl_2$. Large conductance Ca^{2+} activated K (B_K) channels were blocked with 3 mM TEA. All K^+ channels were blocked with 30 mM TEA. To maintain osmolality, solutions with 30 mM TEA contained 30 mM less NaCl. L-, P/Q- and N-type VACCs were blocked by a mixture of 10 μM nimodipine and 10 μM ω-conotoxin MVII-C. Internal stores were depleted by application of 1 μM thapsigargin followed by repeated high-K^+ pulses to activate store release. Cells were viewed with a BX61WI epiflourescence upright microscope (Olympus) equipped with XLUMPlanFI 20X, 0.95 NA and 60X, 0.9 NA dipping objective lenses. Cells were illuminated with a 300-W Xenon lamp equipped with a high-speed excitation filter wheel (Sutter). Emission was captured with a cooled CCD camera (Hamamatsu). Data were acquired with Metafluor software of Meta Imaging series (version 6.4.7, Molecular Devices), and analyzed with custom algorithms written in Igor Pro (Version 5.03, Wavemetrics). The region around each Merkel cell was defined such that the fura-2 signals from the entire cell were averaged.

The Ca^{2+} dissociation constant of fura-2 in Merkel cells was determined by performing a three point calibration *in situ* with solutions containing (in mM): 135 KCl, 2 $MgCl_2$, 10 HEPES, and one of the following: 10 EGTA (for R_{min}), 10 $CaCl_2$ (for R_{max}), and 8.5 EGTA, 1.5 $CaCl_2$ (for R_{mid}, effective free [Ca^{2+}] 0.9 μM as measured *in vitro* by fura-2 imaging). Merkel cells were rendered Ca^{2+} permeable by ionomycin (1 μM) and triton X-100 (0.01–0.015%). Cellular respiration was inhibited with 2 mM 2-deoxy-D-glucose to block active pumps. Only cells with stable F_{340}/F_{380} and fura-2 dye

concentrations were considered to be clamped at extracellular [Ca^{2+}] and included in the analysis. Resting [Ca^{2+}] was found to range from 40-150 nM in healthy cells, consistent with resting [Ca^{2+}] in other sensory cells (Ikeda et al., 1991; Hayashi et al., 1996).

Mechanical Stimulation. Merkel cells were indented with a blunt, 1 μm wide, glass probe coated with sylgard (Dow Corning) driven by a MP-285 micromanipulator (Sutter). Merkel cells were stimulated with ≈0.4 μm displacements parallel to the coverslip. To generate stretch, Merkel cells were cultured on elastic, silicon membranes (Specialty Manufacturing) coated with cell-Tak (BD Biosciences), than fitted to a StageFlexer (Flexcell international), which pulls the membranes over a circular post. The bottom of the membranes was lubricated with "extreme" bicycle lubricant (Rock and Roll). By varying line pressure, radial stretch of 0–18% was applied to the membranes. While dynamic changes in membrane stretch generated focal artifacts, static membranes were observable with an upright microscope.

Volume imaging and analysis. Merkel cells were cultured for two days in an eight-well coverglass chamber (Lab-Tek). Cells were imaged in modified Ringer's solution described above containing 0.1-μm fluorescent microspheres (TetraSpeck, Invitrogen). Microspheres were allowed to settle onto the surfaces of Merkel cells and coverslips for 20–30 min. Merkel cells were imaged with an LSM 5-LIVE imaging system with a Plan-Apocromat 63X, 1.4 NA oil-immersion objective lens (Zeiss). Microsphere fluorescence was excited at 532 nm, a 535-nm dichroic beam splitter was used and emitted light was filtered with a 550-nm long-pass filter. Stacks of confocal sections were imaged once every 7 s. Microsphere locations were determined with the

"spot" identifying utility in Imaris 5.0.1 software (Bitplane AG). Volume calculations and graphs were generated in custom programs written for MATLAB (Mathworks).

Confocal imaging of Merkel-cell morphology. Cells were imaged in a modified Ringer's solution described above containing 1 μM BODIPY FL C5-ceramide (Molecular Probes) and 0.02% pluronic F-127 (Molecular Probes). Fluorescent sphingolipids were allowed to diffuse into cell membranes for 5 min and then were imaged with the system described for volume imaging. For visualizing filamentous actin, Merkel cells were fixed with 4% paraformeldehyde for 10 min and washed with phosphate buffered saline (PBS). Cells were incubated with rhodamine-phalloidin for 30 min, rinsed in PBS, mounted with Vectashield (Vector Laboratories) and imaged with an LSM 510 confocal microscope equipped with a 63X, 1.4 NA oil-immersion objective lens (Zeiss).

RT-PCR of TRP channels. GFP^+ Merkel cells were purified from P3–P6 mice using FACS with strict gating conditions to achieve ≥ 95% purity. Cells from two to six mice were used for each sort. Total RNA from 2–10 X 10^4 GFP^+ cells was isolated using commercially available reagents (Qiagen RNeasy kit) and DNAse treated according to manufacturer's instructions to remove contaminating genomic DNA. First-strand cDNA was synthesized using oligo$(dT)_{12\text{-}18}$ primers at 42°C for 2 h using SuperScriptIII (Invitrogen). PCR products were amplified with touchdown PCR using a PTC-200 Peltier thermal cycler (MJ Research); cDNA from ~1000 cells was used for each PCR. To evaluate reproducibility, each primer pair was tested on two to four independent biological samples, that is, cDNA produced from cells isolated and sorted in separate experiments. We considered amplicons robust if they were present in at least half of

biological samples tested. In all experiments, control PCRs lacking cDNA template were performed to confirm the absence of contamination, and primer performance was verified with positive control cDNA template from brain, skin, or a mixture of liver, heart, spleen and kidney tissue. To ensure that amplicons were not derived from genomic DNA, primers were designed to span introns, with the exception of PKDREJ whose TRP channel isoform is not predicted to have any introns (Entrez Gene accession number NM_011105).

Statistical analysis. Cells whose resting [Ca^{2+}] was 30% higher than average resting [Ca^{2+}] (for all cells in an experiment) and cells whose [Ca^{2+}] remained elevated post stimulus were considered unhealthy and excluded from analysis. Cells were considered responsive if [Ca^{2+}] increased above threshold, where threshold= $3 \bullet \Delta + \bar{x}$. Δ represents the range of values recorded during 30 s of control, and $\bar{x}$ is the mean of control values. Response latency was defined as the amount of time elapsed between solution change and the time when cellular [Ca^{2+}] first exceeded threshold. Because peak hypotonic responses in individual experiments were not normally distributed, we used the non-parametric Wilcoxon signed rank test to analyze cellular responses in individual experiments. Mean peak hypotonic-induced responses of cells in individual wells were near-normally distributed (*N*=20 means, skewness=0.35, excess kurtosis=0.75, *N*=7–28 cells per experiment); therefore we used paired Student's *t* tests to compare paired mean responses.

CHAPTER 3:

MOLECULAR PROFILING REVEALS SYNAPTIC RELEASE MACHINERY IN MERKEL CELLS

Introduction

Whether the Merkel cell, the afferent or both are sites of mechanotransduction is a controversial issue raised more than a century ago (Merkel, 1875). Because somatosensory terminals often contact them, Merkel cells have been proposed to be mechanosensory cells that activate sensory afferents. This role would be analogous to that of hair cells, specialized epithelial cells that mediate transduction in the acousticolateralis system.

Parallels between Merkel cells and hair cells have fueled the idea that Merkel cells are mechanosensory cells (Iggo and Findlater, 1984). For example, Merkel cells have microvilli that are reminiscent of stereocilia, the sites of mechanotransduction in hair cells. Also, both cell types express the transcription factors Math1 and Gfi1 (Ben-Arie et al., 2000; Helms et al., 2000; Wallis et al., 2003).

If Merkel cells are sensory receptor cells, then they must transmit signals through synaptic contacts with somatosensory neurons. Consistent with this notion, Merkel cells contain dense-core vesicles that resemble neurosecretory vesicles (Hartschuh et al., 1990). Moreover, Merkel cell-neurite complexes have membrane densities like those at synaptic active zones (Mihara et al., 1979); however, some have argued that these are merely sites of adhesion (Gottschaldt and Vahle-Hinz, 1981).

Studies that asked whether Merkel cells are required for touch sensitivity have produced conflicting results (Halata et al., 2003). For example, removing Merkel cells by enzymatic treatment, photoablation or genetic modification abolished the responses of slowly adapting afferents in some studies (Mills and Diamond, 1995; Kinkelin et al.,

1999) but not in others (Ikeda et al., 1994). Reports of the involvement of synaptic transmission in SAI responses are likewise contradictory (Gottschaldt and Vahle-Hinz, 1981; Pacitti and Findlater, 1988). Recent evidence for excitatory neurotransmission is the finding that an inhibitor of ionotropic glutamate receptors reduces SAI responsiveness (Fagan and Cahusac, 2001). Additionally, sinus hair follicles, which are rich in Merkel cell-neurite complexes, show immunoreactivity for vesicular glutamate transporters (VGLUTs), which fill synaptic vesicles with glutamate (Hitchcock et al., 2004).

Because the question of whether Merkel cells are sensory cells is unresolved, other functions have been proposed. For example, Merkel cells may play a passive role in touch by efficiently transmitting force to mechanosensitive afferents (Gottschaldt and Vahle-Hinz, 1981). Alternatively, they may release neuromodulators to regulate the sensitivity of mechanoreceptive neurons (Tachibana and Nawa, 2002). Merkel cells have also been proposed to influence the development or innervation of epithelia (Pasche et al., 1990).

To ask whether Merkel cells express genes that are indicative of excitable cells that play a direct role in touch, we used DNA microarrays to profile gene expression in Merkel cells. Our results show that Merkel cells express the molecular tools to send both excitatory and modulatory signals to sensory neurons.

Results

Isolating Merkel cells.

Merkel cells represent a miniscule fraction of cells in the skin; we therefore developed a strategy to genetically label these rare cells and purify them by FACS. To obtain labeled Merkel cells, we used a transgenic mouse strain (*Math1/nGFP*) in which

math1 enhancer sequences drive expression of GFP. In these animals, Merkel cells are the only skin cells with detectable GFP fluorescence (Lumpkin et al., 2003).

We dissociated epidermal cells from neonatal *Math1/nGFP* mice for FACS. To identify GFP-expressing cells, we plotted the red versus green fluorescence of viable epidermal cells (Fig. 1*A*). Whereas signals of autofluorescent epidermal cells fell near a line of slope unity (R2), the signals of GFP^+ cells were displaced along the abscissa (R1). GFP^+ cells constituted 0.08% of viable epidermal cells (n = 141 animals).

Three lines of evidence confirmed that sorted GFP^+ cells were highly enriched. First, using flow cytometry to analyze FACS-purified GFP^+ cells, we found that 85 - 95% of the cells expressed GFP, which corresponds to an enrichment of >1000-fold (n = 3 experiments). Second, epifluorescence microscopy showed that most cells in the sorted GFP^+ population displayed GFP fluorescence (Fig. 1*B*), whereas GFP^- cells did not (Fig. 1*C*). Third, using PCR, we amplified transcripts that are known to be expressed specifically in either Merkel cells or keratinocytes (Fig. 1*D*). We amplified robust PCR products for GFP and the Merkel-cell marker keratin 1-18 (KRT1-18) only from GFP^+ cells. By contrast, the keratinocyte marker KRT2-1 (Chu and Weiss, 2002) was more abundant in GFP^- cells than in GFP^+ cells.

Profiling gene expression in Merkel cells**.**

To identify molecules that define the specialized role of the Merkel cell in the epidermis, we compared the gene-expression profile of GFP^+ Merkel cells with that of an equivalent number of GFP^- epidermal cells. This comparison may identify transcripts that are specifically upregulated in Merkel cells or those that are specifically downregulated in other epidermal cells. The latter population primarily consisted of keratinocytes, as

evidenced by the expression of keratin 2-1, keratin 1-14 and Integrinβ1 (Brakebusch et al., 2000).

We screened cDNA microarrays containing ~20,000 murine clones including the RIKEN FANTOM 1.1 set (Kawai et al., 2001). GFP^+ Merkel cells and GFP^- epidermal cells were collected by FACS in two independent experiments. Total RNA was harvested and linearly amplified. One FACS collection (1.9×10^4 cells) yielded sufficient fluorescent cDNA probe to screen microarrays in triplicate. A second FACS collection (1.1×10^4 cells) produced sufficient cDNA to screen two additional microarrays. For each replicate, we determined a transcript's enrichment in Merkel cells over GFP^- epidermal cells by dividing the hybridization signal from the Merkel-cell probe by that of the GFP^--cell probe (Fig. 2*A* and Table 1). For further analysis, we chose 206 clones that exceeded an enrichment of three-fold in at least three trials.

We also screened Affymetrix arrays representing ~36,000 probe sets (Fig. 2*B* and Table 2). Two replicates were performed from sorts and amplification reactions independent of each other and those used for screening cDNA arrays. For further analysis, we chose 269 probe sets that were at least six-fold enriched in Merkel cells in both experimental trials.

Some transcripts were represented by multiple array elements in the two types of microarrays; we therefore compared the datasets of Merkel-cell-enriched genes from the RIKEN and Affymetrix array screens to identify 362 unique genes whose mean fold enrichment in Merkel cells ranged from 3 to 1748 (Table 3). These included 225 named genes and 137 transcripts of unknown function. Eighty-five transcripts were identified with at least two independent elements on the arrays.

Nine of the Merkel-cell-enriched transcripts in the dataset encoded proteins that have been previously shown by immunostaining to be expressed in Merkel cells (Dalsgaard et al., 1989; Pasche et al., 1990; Moll et al., 1995; Vielkind et al., 1995; Garcia-Caballero et al., 1997; Ben-Arie et al., 2000; Helms et al., 2000; Tachibana et al., 2001; Szeder et al., 2003; Wallis et al., 2003). These included transcription factors (Math1 and Gfi1), intermediate filament subunits (*e.g.,* keratin1-18) and a dense-core vesicle protein (7B2/Sgne1). These results demonstrate that our approach is suitable for identifying transcripts that are enriched in Merkel cells *in vivo*.

Merkel cells express neuronal transcription factors**.** A cell's identity is determined largely by its complement of cell-type-specific transcription factors. Our microarray analysis identified 14 transcription factors that are enriched in Merkel cells. Thirteen of these, including Math1 and Gfi1, act in neuronal development (Table 1). These data support the idea that Merkel cells function as excitable cells.

Merkel cells express synaptic proteins**.** Consistent with a neuron-like fate for Merkel cells, our dataset of Merkel-cell-enriched transcripts included a number of molecules that regulate cell adhesion, synaptic transmission and electrical excitability (Table 1). For example, cadherin 10, which we found to be 25-fold enriched in Merkel cells, is an adhesion molecule that is thought to regulate the formation of specific neuronal connections (Bekirov et al., 2002).

Moreover, we identified 17 new Merkel-cell-enriched transcripts encoding presynaptic and neurosecretory molecules (Table 1). These included active-zone molecules such as Piccolo, and molecules required for Ca^{2+}-triggered vesicle release, such as synaptotagmin I and the SNARE protein SNAP25. We also found that Merkel

cells express molecules that modulate release, such as Rab3C and synapsin II. Moreover, our array data showed that the neuropeptide-precursor CCK and the transporter VGLUT2 are highly enriched in Merkel cells.

To test whether the enrichment we observed at the transcript level translates into differences in protein abundance, we labeled skin cryosections with antibodies against presynaptic proteins (Fig. 3). An antibody against the vesicle protein Rab3C showed immunoreactivity only in Merkel cells in the skin (Fig. 3*B*). This immunoreactivity was concentrated on the lower half of the Merkel cell (Fig. 3*C*), which is where afferent fibers make contact (Fig. 3*A*). Antibodies against the neuropeptide CCK8 (Fig. 3*D*) and the active-zone-matrix protein Piccolo also stained Merkel cells specifically (Fig. 3*E*). Similar staining patterns were seen with antibodies against SNAP25, RIM2 and synaptotagmin 13 (data not shown). The latter is an unconventional synaptotagmin (von Poser and Südhof, 2001) that we found to be enriched in Merkel cells (42-fold, Affymetrix; 64-fold, RIKEN).

We additionally used an antibody against VGLUT2 to determine whether *in vivo* Merkel cells express this glutamate transporter (Fremeau et al., 2001). Like other presynaptic proteins (Fig. 3), VGLUT2 immunoreactivity in the skin was most intense in Merkel cells and was strongest on the side of the cell that abuts sensory nerve terminal s (Fig 4*A* – *D*). We also observed weak VGLUT2 staining in DRG fibers, including those that contacted Merkel cells (Fig. 4*E*). Notably, our array data revealed that Merkel cells express receptors that monitor glutamate release, including the ionotropic receptor GluR2 (29-fold enriched). Furthermore, we found that Merkel cells express Homer2 (7-fold enriched, Affymetrix; 15-fold, RIKEN), which regulates metabotropic glutamate

receptors. The expression of such receptors has recently been detected in Merkel cells (Tachibana et al., 2003).

Merkel cells have voltage-gated ion channels. Our array data revealed that Merkel cells preferentially express six ion-channel subunits that may control signaling between Merkel cells and sensory afferent terminal s (Table 1). These include three voltage-gated K^+ channel subunits.

We also observed that Merkel cells preferentially express the $\alpha_2\delta_1$ subunit of voltage-gated Ca^{2+} channels. To determine which pore-forming subunits are expressed in Merkel cells, we performed PCRs with subtype specific primers (Fig. 5*A*, $n = 6 – 9$ experiments). We consistently amplified products for the P/Q-type Ca^{2+} channel $Ca_V2.1/\alpha_{1A}$, the N-type channel $Ca_V2.2/\alpha_{1B}$ and the L-type channel $Ca_V1.2/\alpha_{1C}$. Products from other α_1 subunits were detected only sporadically or not at all (data not shown).

To determine whether voltage-gated Ca^{2+} channels are functional in Merkel cells, we used the ratiometric Ca^{2+} indicator fura-2AM to monitor the cytoplasmic free Ca^{2+} concentration in FACS-purified Merkel cells (Figs. 5*B – G*). In normal Ringer's solution, Merkel cells exhibited a low ratio of fura-2 fluorescence when excited at 340 nm and 380 nm (Fig. 5*C*). When depolarized with high-K^+ Ringer's solution after 2 d in culture, ~90% of Merkel cells exhibited robust increases in fura-2 ratio (Fig. 5*D*). On average, the peak fura-2 response was four-fold that of baseline signals ($n = 30$ experiments).

To delineate the voltage-gated Ca^{2+} channels that mediate depolarization-evoked Ca^{2+} influx in Merkel cells, we used specific antagonists (Catterall, 2000) of L-type (nimodipine), P/Q-type (ω-agatoxin IVA) and N-type Ca^{2+} channels (ω-conotoxin GVIA). We observed that Merkel cells' peak fura-2 ratios were reduced by

10 μM nimodipine (Figs. 5*E, H*) and by 1 μM ω-agatoxin IVA (Figs. 5*F, H*). Together, nimodipine and ω-agatoxin IVA blocked almost all of the response to high-K^+ solution in cultured (93 ± 3%; Figs. 5*G, H*) and acutely dissociated Merkel cells (93 ± 1%; Fig. 7). By contrast, 1 μM ω-conotoxin GVIA had no effect on Ca^{2+} signals in Merkel cells (Figs. 5*H*).

Discussion

Our principal finding is that Merkel cells express presynaptic active-zone constituents, synaptic vesicle proteins and molecules required for neuropeptide production and glutamate release. Moreover, our live-cell imaging experiments revealed that Merkel cells have functional voltage-gated Ca^{2+} channels; such channels are essential for synaptic transmission. Together, these data demonstrate that Merkel cells are excitable cells and designate glutamate and CCK8 as candidate neurotransmitters at synapses between Merkel cells and sensory afferents *in vivo*. Our conclusion that Merkel cells function as excitable cells is strengthened by the abundance of neuronal transcription factors that we found to be enriched in Merkel cells (Table 1).

The discovery of molecules that are necessary for touch reception has been hindered by the paucity of somatosensory mechanoreceptors and by the fact that their mechanosensitive structures are scattered throughout target tissues. In this study, we have surmounted these obstacles by combining genetic labeling, *in vitro* methods and microarray techniques to identify 362 transcripts that are enriched in Merkel cells. A similar strategy has been used to discover genes expressed in worm touch receptors (Zhang et al., 2002). To our knowledge, this report represents the first extensive

molecular profiling of Merkel cells, and it provides a rich dataset of molecules that help to define the Merkel cell's function in the epidermis.

These data afford an assessment of the molecules expressed by Merkel cells at the message level. For 16 of the named genes, we and others have used antibodies to demonstrate protein enrichment *in vivo*. Such verification is important because the correlation between transcript abundance and protein levels is imperfect. Furthermore, technical limitations may have led to the inclusion of false positives in our dataset. For example, it is conceivable that Merkel cells co-purified with fragments of somatosensory afferents that contained neuronal transcripts. By directly demonstrating that Merkel cells express presynaptic proteins *in vivo*, we have ruled out the possibility that synaptic molecules are found only in somatosensory afferents.

Along with describing molecular components of Merkel-cell synapses, our expression data offer a means for discovering targets of transcription factors. Interestingly, three of the Merkel-cell-enriched transcription factors we found have been implicated in mechanosensory cell development. For example, Math1 and Gfi1, which are expressed in Merkel cells at the protein level (Helms et al., 2000; Wallis et al., 2003), are essential for proper hair-cell differentiation (Bermingham et al., 1999; Wallis et al., 2003). Atonal, the *Drosophila* ortholog of Math1, is a proneural gene for chordotonal organs, which mediate hearing and proprioception (Jarman, 2002). Additionally, expression of Brn3B has been shown in lateral-line hair cells (DeCarvalho et al., 2004). Brn3B's closest homolog in *C. elegans*, UNC-86, is needed for differentiation of neurons that respond to gentle body touch (Duggan et al., 1998).

Our data also support the idea that Merkel cells or their precursors give rise to Merkel-cell carcinoma, a skin tumor whose origin is controversial (Haag et al., 1995). Comparison of our expression data with those from Merkel-cell carcinomas (Van Gele et al., 2004) identifies five transcripts that are enriched in both cell types: SNAP25, CPE, PCSK2, SNGE1 and protein phosphatase 2A B56β.

As well as molecular profiles, we have developed *in vitro* methods for purifying and imaging the activity of living Merkel cells. These methods represent a significant advance because they allow signal transduction in Merkel cells to be characterized with high resolution techniques. Such dissociated cell preparations have been essential for discovering mechanisms of sensory signaling in hair cells and thermosensitive nociceptors (Lewis and Hudspeth, 1983; Caterina and Julius, 2001). In this study, we used these methods to ascertain which voltage-gated Ca^{2+} channels are active in murine Merkel cells. Our results extend a previous report of Ca^{2+} currents in Merkel cells (Yamashita et al., 1992). We found that almost all of the depolarization-induced Ca^{2+} influx in Merkel cells is through two types of channels. These are L-type channels, which trigger neurotransmission in hair cells and retinal bipolar cells (Roberts et al., 1990; Tachibana et al., 1993), and P/Q-type channels, which are found at central synapses (Reuter, 1996). Although we found that Merkel cells expressed transcripts encoding $Ca_V2.2/\alpha_{1B}$, these channels did not significantly contribute to Ca^{2+} entry. This suggests that, under our experimental conditions, either such channels are not activated or significant protein is not expressed.

Our finding that Merkel cells express presynaptic molecules indicates that the sites of Merkel cell-afferent contact observed ultrastructurally are most likely synaptic

active zones. The presence of such active zones is consistent both with the idea that Merkel cells are sensory receptor cells that signal afferents through neurotransmission and with the hypothesis that Merkel cells release neuromodulators to influence the sensitivity of mechanoreceptive afferents.

How might neurotransmitter release be stimulated from Merkel cells? Merkel cells may be mechanoreceptive cells that are directly activated by touch. Alternatively, Merkel cells may receive input from active afferent terminal s. The latter conjecture is bolstered by reports of reciprocal connections in Merkel cell-neurite complexes (Mihara et al., 1979).

By identifying molecular components of Merkel-cell synapses, our results strongly suggest that Merkel cells are active participants in somatosensory signaling. Moreover, this study provides tools for interfering with synaptic transmission so its role in touch reception can be defined.

Figures

Figure 1. Purifying Merkel cells. (*A*) A plot of red versus green fluorescence of 5 X 10^5 epidermal cells from *Math1/nGFP* mice was used to set regions around GFP^+ cells (R1) and GFP^- cells (R2). (*B – C*) Confocal micrographs show epidermal cells collected from R1 (*B*) or R2 (*C*). Nuclei were stained with DAPI (shown in red). GFP^+ cells appear yellow. Scale bar: 50 μm. (*D)* PCR products were amplified from sorted cells. Templates: dH_2O, GFP^+-cell cDNA, GFP^--cell cDNA, and whole-skin cDNA (control cDNA). Cell-type-specific markers were amplified with the primers indicated. GAPDH product confirmed that comparable amounts of template was used from sorted cells.

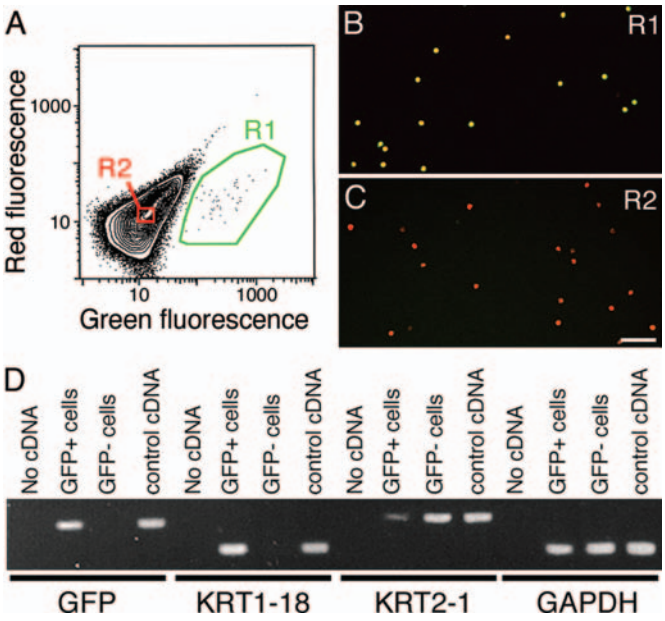
A
Red fluorescence
1000
10
R1
R2
10
1000
Green fluorescence
B
R1
C
R2
D
No cDNA
GFP+ cells
GFP- cells
control cDNA
GFP
KRT1-18
KRT2-1
GAPDH

Figure 2. Histograms of the $\log_2$ ratio of signals from GFP^+ cells to GFP^- cells (GFP^+/GFP^-) for microarray elements. Data from each trial is plotted in a different color. Gray bars indicate the enrichment values exceeded by clones that were analyzed further. (*A*) Results from five trials with glass-slide cDNA microarrays. Elements shown had sums of median Cy3 and Cy5 signals ≥500 fluorescence units. (*B*) Results from two trials with Affymetrix oligonucleotide microarrays. Elements shown were scored as 'present' by the absolute-call algorithm.

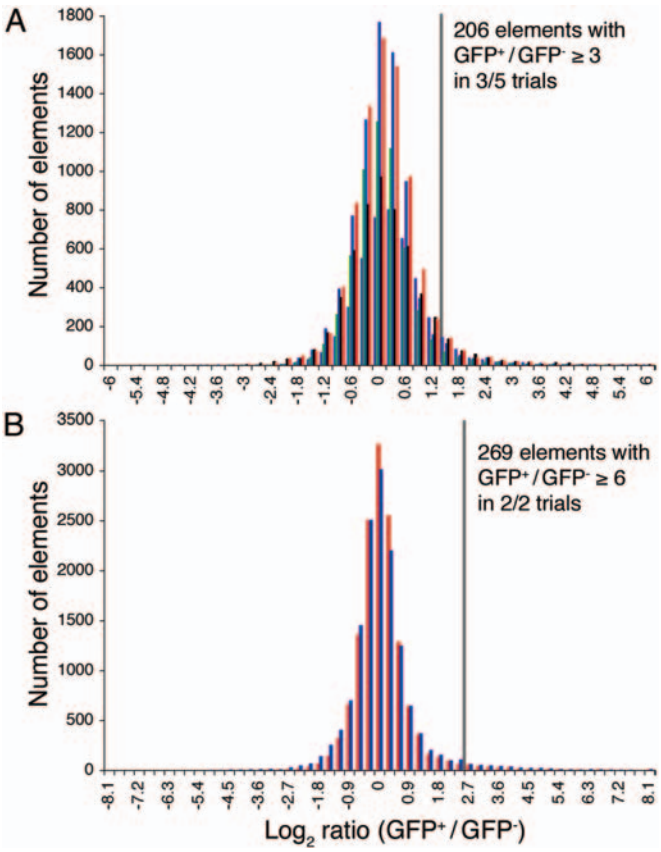
A
Number of elements
206 elements with
GFP+ / GFP- ≥ 3
in 3/5 trials
B
Number of elements
269 elements with
GFP+ / GFP- ≥ 6
in 2/2 trials
Log2 ratio (GFP+ / GFP-)

*Figure 3***.** Merkel cells express pre-synaptic proteins *in vivo*. Confocal micrographs show immunohistochemical staining of touch domes in *Math1/nGFP* skin cryosections. Each row includes antibody staining (red, left), GFP fluorescence (green, middle) and a merged image (right). (*A*) An anti-NF200 antibody labeled sensory afferents that contacted Merkel cells. Dermal fluorescence reflects autofluorescence that is independent of GFP expression. Scale bar: 10 μm. (*B*) Low magnification micrographs demonstrate that, in the skin, Rab3C staining was detectable only in Merkel cells (arrowhead). Scale bar: 25 μm. (*C – E*) High magnification images show immunoreactivity of Rab3C (*C*), CCK8 (*D*) and Piccolo (PCLO, *E*) in Merkel cells. Scale bar in *C* is 5 μm and applies to *C – E*.

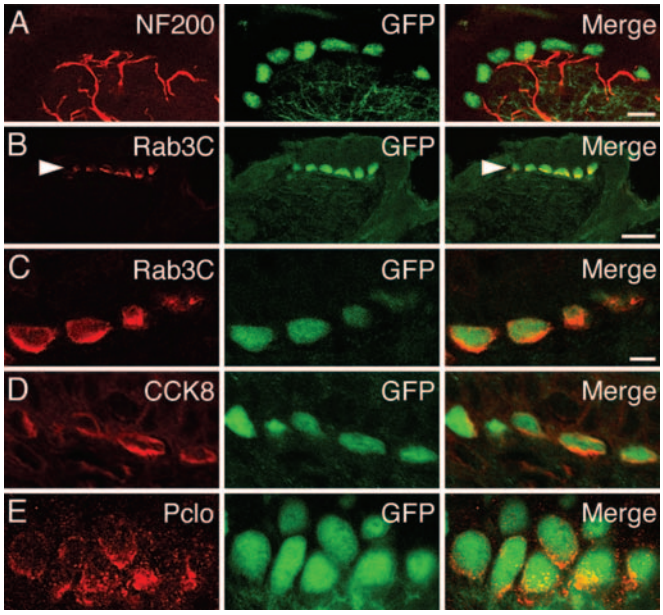
A
NF200
GFP
Merge
B
Rab3C
GFP
Merge
C
Rab3C
GFP
Merge
D
CCK8
GFP
Merge
E
Pclo
GFP
Merge

Figure 4. Merkel cells express VGLUT2 protein. An antibody against VGLUT2 (red, *A, D* and *E*) labeled KRT1-18-positive (blue, *B, D* and *E*), GFP-expressing Merkel cells (green, *C, D* and *E*) in a touch dome. DRG fibers that contacted Merkel cells and those that formed palisade endings around hair shafts displayed weak VGLUT2 staining (arrowheads in *E*). The image in *E* is a projection of a confocal z-series collected with 2-μm axial steps. Scale bars: 5 μm (*D*), 20 μm (*E*).

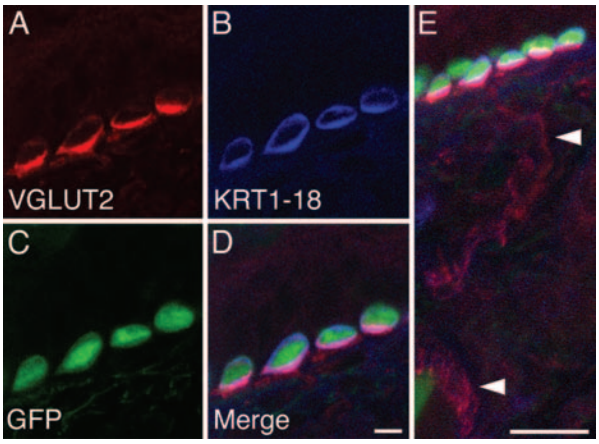
A
VGLUT2
B
KRT1-18
E
C
GFP
D
Merge

Figure 5. Merkel cells have functional P/Q- and L-type Ca^{2+} channels. (*A*) PCR products were amplified from sorted Merkel cells using primers specific for the indicated voltage-gated Ca^{2+}-channel α_1 subunits. (*B – D*) An epifluorescence micrograph shows sorted GFP^+ cells after 2 d in culture (*B*). Pseudocolor images of fura-2 fluorescence ratio (F_{340}/F_{380}) just before (*C*) and 6 s after (*D*) perfusion with high-K^+ Ringer's solution. Pseudocolor scale (*C – D*) denotes F_{340}/F_{380} from 0.1 (black) to 3 (white). Scale bar: 100 μm. (*E – G*) Plots of mean fura-2 ratios versus time in the absence (dashed line) or presence (solid line) of Ca^{2+} channel antagonists. Cells were exposed to drugs for 15 – 20 min before depolarization. Application of high-K^+ solution began at $t = 0$ and lasted throughout the recording. Each trace represents the average fura-2 ratio of 57 – 119 cells. Error bars indicate SEM. Antagonists: 10 μM nimodipine (Nim; *E*), 1 μM ω-agatoxin IVA (Aga; *F*), 10 μM nimodipine plus 1 μM ω-agatoxin IVA (*G*). (*H*) Quantification of the effects of Ca^{2+} channel antagonists ($n = 4 – 5$ experiments per group). Responses of Merkel cells exposed to antagonists were normalized to those measured from control cells. The effect of ω-agatoxin IVA or nimpodipine was significantly different from that of ω-conotoxin GVIA (Ctx; $P \leq 0.002$). Inhibition by ω-agatoxin IVA plus nimodipine was significantly greater than that achieved with either alone ($P \leq 8 \text{ X } 10^{-4}$).

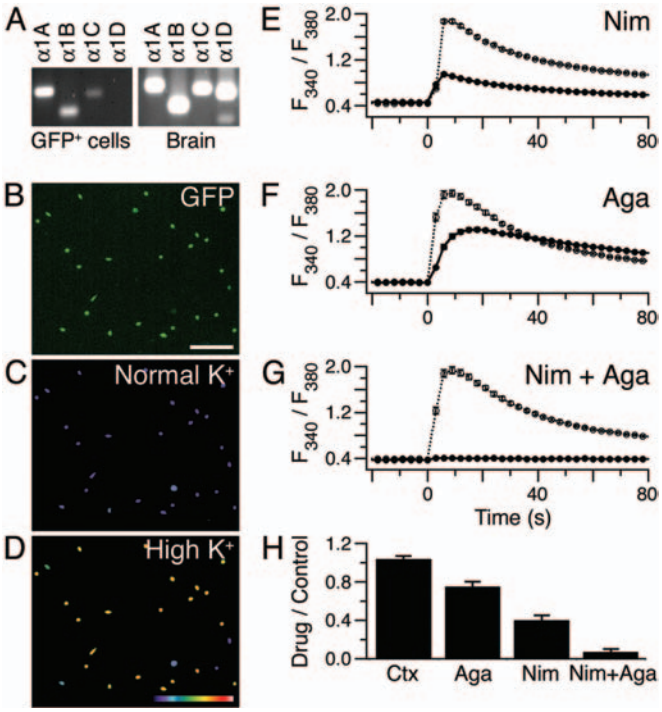
A
α1A
α1B
α1C
α1D
α1A
α1B
α1C
α1D
GFP+ cells
Brain
B
GFP
C
Normal K+
D
High K+
E
Nim
F
Aga
G
Nim + Aga
F340 / F380
2.0
1.2
0.4
0
40
80
Time (s)
H
Drug / Control
1.2
0.8
0.4
0.0
Ctx
Aga
Nim
Nim+Aga

Figure 6. Acutely dissociated Merkel cells have functional P/Q- and L-type Ca^{2+} channels ($n = 5$ experiments). Merkel cells were imaged < 5 h after FACS collection. (*A*) Plot of mean fura-2 ratios versus time in the absence (dashed line) or presence (solid line) of 10 μM nimodipine plus 1 μM ω-agatoxin IVA. (*B*) Plot of mean fura-2 ratios versus time for the same cells 1 h after washout (solid line) of Ca^{2+} channel antagonists. The average response of control cells imaged in parallel is shown (dashed line). Application of high-K^+ solution began at $t = 0$ and lasted for the duration of the recording. Each trace represents the average fura-2 ratio of 28 – 40 cells. Error bars indicate SEM. The effects of ω-agatoxin IVA plus nimpodipine on acutely dissociated and cultured Merkel cells (Fig. 5*G*) were indistinguishable. The time course of Merkel cells' responses to depolarization was similar in acutely dissociated and cultured Merkel cells. The average peak response was lower for acutely dissociated cells than for cultured Merkel cells because fewer acutely dissociated cells (~70%) responded with observable Ca^{2+} signals and those signals were smaller. This likely reflects the fact that cells had not fully recovered from damage due to FACS.

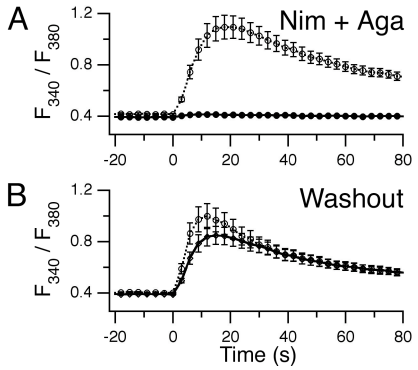
A
Nim + Aga
B
Washout
F_{340} / F_{380}
1.2
0.8
0.4
-20
0
20
40
60
80
Time (s)

Table 1. Results from RIKEN cDNA microarrays (20,423 elements). Blanks indicate elements whose sums of median Cy3 and Cy5 signals were < 500 units.

Table 1. Fold enrichment in Merkel cells (GFP+ cells / GFP- cells) in RIKEN cDNA micro Blanks indicate elements whose sums of median Cy3 and Cy5 signals were < 500 units. Top 100 hits

RIKEN ID	Trial 1	Trial 2	Trial 3	Trial 4	Trial 5
0610040B07	222.6	35.8	90.9	208.6	171.8
5730409J20	82.9	40	46.7	64.2	80.7
2010107O15	58.3	41.1	57.6	56.3	36.2
2900010B03	52.9	24.4	25.6	35.2	40.1
0710001C04	50.5	33.2	25.8	45.8	
2010003O17	48.1	35.9	48.3	37.8	64.4
2010009P05	39	17.3	22	31.7	35.5
1110012J17	30.4	7.6	18.9	36.7	20.9
2900026H06	28.2	21.2	20.9	52.3	50
1500004I01	27.6	13.1	18.5	23.7	22.1
2810422A08	25.6	16.8	41	53.8	49.2
A930009E05	25.3	10.5	22.9	19.9	29.2
2700029M09	23.9	20.5	37	14.8	11.4
2310011G17	22.1	0.5	0.6	0.4	0.6
1810064N08	20.3	0.8	0.9	0.9	0.9
0710008K14	19.4	15.1	20.2	13.3	
2900082I03	19.3	14.9	19.2	33.2	24.4
2610209N05	18.7	16.6	15.2	14.6	9.8
1110003P13	17.2	6.3	12.6	25	9.2
9630005A06	16.6	25.2	25.3	123.7	25.4
1110033I23	14.9	8.6	11.6	6	6.8
0610025N19	14.4	5	5.8	6.2	7.6
A230103D18	14.2	6.7	15.7	29.5	23.5
2410004M13	14	17.1	23.1	66.3	48.4
1500032A09	13.7	11.5	8.8	12.1	18.3
7.10E+23	13	4.5	12.6	16.1	14.5
2700088D09	12.2	7.4	8.7	17	6.8
2900042M13	11.7	7.5	10.1	17.8	
4921531N22	11.4	8.2	7.3	9.6	6.9
1110029F20	11.2	6.7	4.4	5.7	5.5
1110063G11	10.9	5.5	12	16.6	7.8
2610100B16	10.8	8.6	5	13.6	7.9
2010306I20	10.7	3.5	3.2	5.7	2.6
A230103K18	10.3	3.6	10.7	14.1	11.5
2310012G06	10.1	8.7	6.9	15.2	10.2
5430425M22	9.9	7.7	16.5	19.9	15.7
2610027C14	9.9	12.8	13.2	14.8	14.7
2300009C08	9.6	10.9	15.3	11.7	10
1500031O04	9.2		16.9	14.3	15.3
6330411F23	9.2	14.7	13.2	15.4	12.4
1110012H21	9.1	16	11.9	22.5	14.4
1500009L16	9		11.2	29.8	8.9
7.10E+18	9		15.3	16	25.4
2410012C07	9	6.1	6.6	9.9	10.6

1.30E+15	9	4.2	6.7	6	4.3
6330403K07	8.9		9.3	17	12.7
2.40E+10	8.7		6	13.8	4
0610006O14	8.4	6.5	5.5	6.9	8.3
1110069M14	8.2	1.3	1.3	0.8	0.9
C030023P10	8.1	6	7.5	4.2	9.6
2810432N10	8.1	4.7	7.5	8.4	6.1
2810422P17	7.9	6.1	31.9	23.1	13.2
2410001K24	7.7	6.4	8	15.5	7.7
2010200C07	7.7	8.3	9.9	6.7	14.3
1500040L08	7.7	7	10.1	25	15.2
2410020A08	7.6		7.3	15.3	7.1
1.21E+17	7.4		5.6	7.9	9.6
2700060H17	7.2	5.9	11.8	10.5	5.8
2600002F02	7.1	6.9	7.4	4	6.2
1210002B07	6.9	3	3.2	3.8	3.4
6330562O12	6.9	3.9	3.7	4.6	4.6
4.93E+23	6.7	2.2	1.8		2.6
2900074L19	6.6	6	5.9	16.1	11.4
1300016D08	6.5	7.8	7.9	6.7	6.6
2410041A17	6.3	6.6	5.3	4.3	4.8
2.21E+20	6.3	5.1	5.4	8.9	5.6
2310043N10	6.1	4	4.2	3	3
1810006K23	6.1	9.8	7.2	5	9.2
0610037K01	6.1	4.3	5.3	5.8	
2210414F18	6	8.6	5.8	6.7	4.7
2310001B08	5.9	1.5	0.6	1.4	1.4
1110008L10	5.9	7.1	7.8	8.9	5.4
2310042I22	5.9	1.4	1.5		2.5
1600016C16	5.9	3.4	5.5	10.9	7.8
A330042I05	5.7	6.3	6.3	8.3	7.6
3110070H17	5.7	8.8	4.8	7.3	5.5
9.13E+13	5.7	4	3.2	10.9	7.1
1600010D10	5.7	4.7	4	6.4	4.2
2.70E+16	5.6	11	25.9	17.9	22.5
9430041P20	5.6	4.9	6.2	6.5	4.2
2610022J01	5.6	3.5	2.7	1.7	1.7
1110008N23	5.6	4.4	5.5	8	3.2
1.11E+23	5.5	3.5	4.4	4.9	3.6
1500010J12	5.5	4.5	4.2	3	2.5
0910001K20	5.5	5.9	4.4	7.3	6.6
2300002D11	5.4	5	4.4	5.1	5.7
5430406J05	5.4	4.8	7.6	3.8	5.6
2.51E+26	5.4	11.7	19	3.3	5.2
2900059O22	5.4	4	6.7	5.2	3.9
2700084L11	5.4	2.2	2	2	1.8
0610007J12	5.3	3.5	3.6	7	2.8
1110062G02	5.2	5.4	5.1	4.7	3.9
2.51E+25	5.2	2.2	3.2	3.1	3

2310068P04	5.2	3	4.8	6.7	4.9
3.23E+08	5.1	3.9	4.3	4.9	4.1

Table 2. Results from two Affymetrix GeneChip trials (36,899 probe sets).

Haeberle Supplemental Table 2. Fold enrichment in Merkel cells (GFP+ cells / GFP- cells) in two Affymetrix GeneChip trials. Table displays top 100 hits

Affy ID	Gene name	Description	Trial 1 Present	Trial 1 Ratio	Trial 1 Change	Trial 1 Change P	Trial 2 Present	Trial 2 Ratio	Trial 2 Change	Trial 2 Change P
168404_at	Atoh1	atonal homolog 1 (Drosophila)	P	3327	I	0	P	168.9	I	0
165624_i_at	4930568N03R	RIKEN cDNA 4930568N03 gene	P	831.7	I	0	P	548.7	I	0
96055_at	Cck	cholecystokinin	P	238.9	I	0	P	1024	I	0
138453_at		Mus musculus 6 days neonate skin cDNA, RIKEN full-le	P	388	I	0	P	675.6	I	0
94334_f_at			P	128	I	0	P	776	I	0
101009_at	Krt2-8	keratin complex 2, basic, gene 8	P	256	I	0	P	630.3	I	0
132118_at		ESTs, Weakly similar to otoferlin [Mus musculus] [M.m	P	362	I	0	P	415.9	I	0
166904_at	2410012C07R	RIKEN cDNA 2410012C07 gene	P	181	I	0	P	315.2	I	0
138492_at		Mus musculus adult male medulla oblongata cDNA, RIK	P	207.9	I	0	P	238.9	I	0
95766_f_at	Defcr16	defensin related cryptdin 16	P	111.4	I	0	P	315.2	I	0
166854_at	4833424K13R	RIKEN cDNA 4833424K13 gene	P	168.9	I	0	P	256	I	0
163530_at		ESTs	P	137.2	I	0	P	274.4	I	0
165471_f_at	1100001E04R	RIKEN cDNA 1100001E04 gene	P	315.2	I	0	P	90.5	I	0
95621_at	9030623C06R	RIKEN cDNA 9030623C06 gene	P	222.9	I	0	P	128	I	0
167630_f_at	2410012C07R	RIKEN cDNA 2410012C07 gene	P	256	I	0	P	73.5	I	0
165671_f_at	Fn3k	fructosamine 3 kinase	P	157.6	I	0	P	168.9	I	0
135249_at	Pde1c	phosphodiesterase 1C	P	294.1	I	0	P	24.3	I	0
167615_s_at		Mus musculus adult male brain cDNA, RIKEN full-lengt	P	207.9	I	0	P	90.5	I	0
95347_at	Myt1	myelin transcription factor 1	P	157.6	I	0	P	137.2	I	0
92841_f_at	Chgb	chromogranin B	P	104	I	0	P	168.9	I	0
138052_g_at		ESTs, Moderately similar to ANM1_MOUSE Protein argi	P	128	I	0	P	137.2	I	0
130616_at		ESTs	P	111.4	I	0	P	147	I	0
100009_r_at	Sox2	SRY-box containing gene 2	P	111.4	I	0	P	128	I	0
166831_i_at		ESTs, Moderately similar to ANM1_MOUSE Protein argi	P	55.7	I	0	P	181	I	0
99339_r_at	Kcnd2	potassium voltage-gated channel, Shal-related family,	P	181	I	0	P	52	I	0
102431_at	Mapt	microtubule-associated protein tau	P	111.4	I	0	P	119.4	I	0
108813_at	AI987662	expressed sequence AI987662	P	90.5	I	0	P	137.2	I	0
160899_at	Pcp4	Purkinje cell protein 4	P	137.2	I	0	P	68.6	I	0
165795_f_at	Gpr85	G protein-coupled receptor 85	P	90.5	I	0	P	111.4	I	0
138946_at		Mus musculus 18-day embryo whole body cDNA, RIKEI	P	29.9	I	0	P	168.9	I	0
103259_at	Gfi1	growth factor independent 1	P	78.8	I	0	P	111.4	I	0
99561_f_at	Cldn7	claudin 7	P	36.8	I	0	P	147	I	0
110465_at	6332401O19R	RIKEN cDNA 6332401O19 gene	P	59.7	I	0	P	119.4	I	0
166763_at		ESTs	P	97	I	0	P	73.5	I	0
117306_at	6330548O06R	RIKEN cDNA 6330548O06 gene	P	64	I	0	P	104	I	0
107298_at		Mus musculus adult male brain cDNA, RIKEN full-lengtl	P	59.7	I	0	P	104	I	0
171068_f_at	C130057K09	hypothetical protein C130057K09	P	128	I	0	P	29.9	I	0
130696_f_at	0610040J01Ri	RIKEN cDNA 0610040J01 gene	P	90.5	I	0	P	64	I	0
168117_i_at	5730414M22R	RIKEN cDNA 5730414M22 gene	P	26	I	0	P	128	I	0
92989_f_at	Cadps	Ca<2+>dependent activator protein for secretion	P	64	I	0	P	78.8	I	0
167171_at	Kcnv1	potassium channel, subfamily V, member 1	P	90.5	I	0	P	52	I	0
108864_at	Gpr22	G protein-coupled receptor 22	P	45.3	I	0	P	97	I	0
165407_f_at	2010016F14Ri	RIKEN cDNA 2010016F14 gene	P	97	I	0	P	42.2	I	0
138495_f_at		ESTs, Moderately similar to synapsin 3 [Mus musculus	P	48.5	I	0	P	90.5	I	0
97235_f_at	Apobec2	apolipoprotein B editing complex 2	P	64	I	0	P	73.5	I	0
115745_at	Aspa	aspartoacylase (aminoacylase) 2	P	52	I	0	P	84.4	I	0
100536_at	Mobp	myelin-associated oligodendrocytic basic protein	A	45.3	I	0	P	90.5	I	0
167714_at		Mus musculus 16 days neonate thymus cDNA, RIKEN f	P	90.5	I	0	P	45.3	I	0
97753_at	Pclo	piccolo (presynaptic cytomatrix protein)	P	52	I	0	P	78.8	I	0
99197_at	Gc	group specific component	P	90.5	I	0	P	32	I	0
160170_at	Stmn3	stathmin-like 3	P	104	I	0	P	17.1	I	0
102918_at	Muc1	mucin 1, transmembrane	P	36.8	I	0	P	78.8	I	0
167342_r_at	B230215L15R	RIKEN cDNA B230215L15 gene	P	34.3	I	0	P	73.5	I	0
92515_at	Isl1	ISL1 transcription factor, LIM/homeodomain (islet 1)	P	11.3	I	0	P	90.5	I	0
109427_at	C730029A08R	RIKEN cDNA C730029A08 gene	P	64	I	0	P	36.8	I	0
165743_at	Syn2	synapsin II	P	34.3	I	0	P	55.7	I	0
129038_at		Mus musculus 15 days embryo head cDNA, RIKEN full-	P	18.4	I	0	P	68.6	I	0
102085_at	Insm1	insulinoma-associated 1	P	8	I	0	P	78.8	I	0
115271_at		ESTs, Weakly similar to chromosome 11 open reading	P	26	I	0	P	59.7	I	0
160868_at	Rab3b	RAB3B, member RAS oncogene family	A	26	I	0	P	59.7	I	0
99842_at	Col19a1	procollagen, type XIX, alpha 1	P	68.6	I	0	P	16	I	0
110829_at	Syt13	synaptotagmin 13	P	32	I	0	P	52	I	0
171390_i_at	AI504353	expressed sequence AI504353	P	55.7	I	0	P	27.9	I	0
163903_at		Mus musculus 12 days embryo embryonic body betwee	P	48.5	I	0	P	34.3	I	0
102249_at	Avil	advillin	P	7.5	I	0	P	73.5	I	0
94756_at			P	24.3	I	0	P	55.7	I	0
100047_at	Snap25	synaptosomal-associated protein 25	P	39.4	I	0	P	39.4	I	0
166817_i_at	6330509G02R	RIKEN cDNA 6330509G02 gene	P	48.5	I	0	A	27.9	I	0
166821_r_at	1500001L12Ri	RIKEN cDNA 1500001L12 gene	P	39.4	I	0	P	36.8	I	0
163639_at	B230343H07R	RIKEN cDNA B230343H07 gene	P	12.1	I	0	P	64	I	0
110980_at		Mus musculus 10 days neonate cerebellum cDNA, RIKE	P	64	I	0	P	9.8	I	0
110850_f_at	3021401A05R	RIKEN cDNA 3021401A05 gene	P	17.1	I	0	P	55.7	I	0
113811_at	Calcb	calcitonin-related polypeptide, beta	P	59.7	I	0	P	13	I	0
162451_r_at	Fbxo3	F-box only protein 3	A	68.6	NC	0.03	A	2.8	NC	0.47
104825_g_at	2210011C24R	RIKEN cDNA 2210011C24 gene	P	39.4	I	0	P	32	I	0
162192_f_at	Chga	chromogranin A	A	36.8	I	0	A	34.3	I	0
108901_at		ESTs	P	27.9	I	0	P	42.2	I	0
104383_at	Crmp1	collapsin response mediator protein 1	P	6.1	I	0	P	64	I	0
165581_at	0710005M24R	RIKEN cDNA 0710005M24 gene	P	45.3	I	0	P	24.3	I	0
138417_f_at	Slc17a6	solute carrier family 17 (sodium-dependent inorganic p	P	39.4	I	0	P	29.9	I	0
129028_at	C530050I23Ri	RIKEN cDNA C530050I23 gene	P	32	I	0	P	36.8	I	0
167395_r_at	D330017J20R	RIKEN cDNA D330017J20 gene	P	36.8	I	0	P	29.9	I	0
138513_at		Mus musculus 10 days neonate medulla oblongata cDN	P	45.3	I	0	P	19.7	I	0
94335_r_at			P	36.8	I	0	P	27.9	I	0
163809_r_at	1500011B03R	RIKEN cDNA 1500011B03 gene	P	48.5	I	0	A	16	NC	0
164178_i_at	Grm3	glutamate receptor, metabotropic 3	M	59.7	I	0	P	4.6	I	0
161089_r_at	Akap8	A kinase (PRKA) anchor protein 8	A	64	NC	0.14	A	0.2	NC	0.58
114443_at	C630004H02R	RIKEN cDNA C630004H02 gene	P	8	I	0	P	55.7	I	0
102967_at	Gdap1	ganglioside-induced differentiation-associated-protein	M	39.4	I	0	P	24.3	I	0
104564_at	Scg3	secretogranin III	P	14.9	I	0	P	48.5	I	0
167869_f_at	Rtn1	reticulon 1	P	21.1	I	0	P	42.2	I	0
113587_at	Syt1	Mus musculus, synaptotagmin 1, clone MGC:36169 IM,	P	27.9	I	0	P	34.3	I	0
138490_at		ESTs	P	42.2	I	0	P	18.4	I	0
92293_at		Mus musculus adult male spinal cord cDNA, RIKEN full-	P	26	I	0	P	34.3	I	0
137572_f_at	Smarca1	SWI/SNF related, matrix associated, actin dependent r	A	32	I	0	P	26	I	0
130656_at		ESTs	P	29.9	I	0	P	27.9	I	0
92945_at	Gria2	glutamate receptor, ionotropic, AMPA2 (alpha 2)	P	42.2	I	0	P	14.9	I	0
105240_at	Pde1c	phosphodiesterase 1C	P	13.9	I	0	P	42.2	I	0
104932_at	6530403A04	hypothetical protein 6530403A04	P	34.3	I	0	P	21.1	I	0
94731_at	Stac	src homology three (SH3) and cysteine rich domain	P	16	I	0	P	39.4	I	0

Table 3. List of 362 unique transcripts enriched in Merkel cells from five RIKEN and two Affymetrix trials. GFP+/GFP- ratio is the mean fold enrichment over all biological replicates for Affymetrix or RIKEN arrays. Number of independent elements representing a transcript is indicated if >1.

Table 3. List of unique transcripts enriched in Merkel cells from five RIKEN and two Affymetrix trials. Mean ratio is the average fold enrichment over all trials. Number of independent hits is indicated if >1.

ID	Mean ratio (Gl	Gene Symbol	# indep. hits	Other IDs
168404_at	1748	Atoh1		
165624_i_at	690	4930568N03		
96055_at	631	Cck		
138453_at	532	Ubce8		
101009_at	443	Krt2-8		
132118_at	389	Mm.77737		
138492_at	223	6330582C22		
95766_f_at	213	Defcr16		
166854_at	212	4833424K13		
163530_at	206	Mm.37750		
165471_f_at	203	1.10E+10		
171599_f_at	170	Ina	3	94335_r_at, 94334_f_at
135249_at	159	Pde1c		
92841_f_at	136	Chgb		
130616_at	129	Mm.89971		
138052_g_at	125.5	Mm.39750	2	166831_i_at
100009_r_at	120	Sox2		
99339_r_at	117	Kcnd2		
108813_at	114	C820005A15		
160899_at	103	Pcp4		
165795_f_at	101	2900026B03		
138946_at	99	1190003C09		
6230421J19	96.9	Frcl1		
166904_at	96.4	2410012C07	3	167630_f_at, 2410012C07
103259_at	95	Gfi1		
99561_f_at	92	Cldn7		
110465_at	90	6332401O19		
95347_at	86.3	Myt1	2	169294_s_at
166763_at	85	Mm.36691		
117306_at	84	6330548O06		
108830_at	83.3	Aspa	4	115745_at, 0610040B07, 2010107O15
167615_s_at	79.4	3632434I06	3	107298_at, 139503_at
130696_f_at	77	0610040J01		
168117_i_at	77	5730414M22		
165407_f_at	70	2010016F14k		
95621_at	69	9030623C06	3	9030623C06, 2010003O17
165671_f_at	68.4	Fn3k	2	2310074G21
167714_at	68	A130018G07		
97753_at	65	Pclo		
99197_at	61	Gc		
160170_at	61	Stmn3		
102918_at	58	Muc1		
110829_at	56.9	Syt13	2	5730409J20
167342_r_at	54	B230215L15		
92515_at	51	Isl1		
109427_at	50	C730029A08		
171068_f_at	49.7	C130057K09	2	138377_at
102431_at	48.4	Mapt	3	102742_g_at, 116406_at
167171_at	47	Kcnv1	2	2810422A08
108864_at	46.6	2900068K05	2	135327_at
92989_f_at	46.5	Cadps	2	92988_i_at
129038_at	43	D930002I12		
102085_at	43	Insm1		
160868_at	43	Rab3b		
115271_at	43	Mm.29035		
99842_at	42	Col19a1		
171390_i_at	42	AI504353		
163903_at	41	9430092A10		
102249_at	40	Avil		
9630005A06	40.4	9630005A06	2	9330179O15
94756_at	40	Hist1h3f		
100536_at	39.6	Mobp	2	99046_at
100047_at	39	Snap25		
163639_at	38	9330127N12		
110980_at	37	B930094H20		
110850_f_at	36	3021401A05		
113811_at	36	Calcb		
104825_g_at	36	2210011C24		
108901_at	35	Mm.69080		
104383_at	35	Crmp1		
165581_at	35	0710005M24		
129028_at	34	C530050I23		
167395_r_at	33	D330017J20		

2900026H06	32.9	2900026H06	2	6330404L05
163809_r_at	32	1500011B03		
114443_at	32	C630004H02		
113587_at	31	Syt1		
138490_at	30	Mm.40399		
92293_at	30	C030017F07		
2010009P05	29.1	2010009P05		
137572_f_at	29	Smarca1		
130656_at	29	Mm.26134		
92945_at	29	Gria2		
93021_at	29	Rex3	2	2410004M13
105240_at	28	C230032E05		
99642_i_at	28	Cpe	4	99643_f_at, 0710001C04, 2900010B03
97235_f_at	27.9	Apobec2	2	2300009C08
104932_at	28	C230052D13		
94731_at	28	Stac		
138495_f_at	27.6	Syn2	4	165743_at, 2900074L19, 2900082I03
101058_at	27	Amy1		
163911_at	26	Nptx1		
165509_at	26	1.70E+24		
96591_at	26	Reln		
105823_at	25	Cdh10		
164023_at	25	Cacng5		
170227_at	25	Mm.131516		
94194_s_at	25	Hcn2		
104564_at	24.5	Scg3	2	162237_f_at
92757_at	24	Sez6		
108807_at	24	1500016O10		
163844_at	24	Rims2		
136288_at	23	Farsl		
129217_at	23	Mm.23240		
166821_r_at	22.3	1500001L12	3	171439_at, 1500001L12
99524_at	22	Slc8a1		
A930009E05	21.6	A930009E05		
2700029M09	21.5	2700029M09		
113747_at	21	Mm.206054		
1500004I01	21	Cyfip2		
104375_at	21	Gcnt2		
138513_at	20.8	B830032F12	2	137348_at
105742_at	21	AI851531		
105715_at	21	A830039N20		
97920_at	20	Krt2-7		
167869_f_at	20.4	Rtn1	2	94545_at
131405_at	20	4930526B11		
137677_at	20	Caln1		
114389_at	20	Gabrb3		
138417_f_at	19.4	Slc17a6	3	108915_at, 2900073D12
165753_at	19	Mm.40489		
171195_f_at	19	Nhlh1		
102902_at	19	Lhx3		
166895_s_at	19	6430519O13		
93287_at	19	Biklk		
114497_at	18.4	1110012J17	2	1110012J17
102296_at	18	Pcsk2		
108796_at	18	MGC38336		
102774_at	18	EGF		
94270_at	18	Krt1-18		
93863_f_at	18	Defcr6		
114949_at	18	Kcnmb1		
167388_f_at	17	9430010P06		
106071_at	17	9430078I07		
166011_i_at	17.3	Rab3c	3	3110037E15, A230103D18
166817_i_at	17.3	6330509G02	2	6330414G02
163248_at	17	Mm.25672		
100351_f_at	17	Defcr3		
112876_at	17	2900052J15		
6720420G18	16.7	6720420G18		
100131_at	16.6	Sgne1	4	0710008K14, 1500031O04, 2610209N05
2.70E+16	16.6	2.70E+16		
101786_at	16	Kcna4		
110516_at	16	Mm.82645		
106290_at	16	AI415330		
160236_at	16	AA675320		
163743_at	16.2	Map 1b	2	1500009L16
166819_at	16.1	6330411F23	2	6330411F23
92420_at	16	Ntf3		
109975_at	16	2310045A20		

104510_at	16	Cacna2d1		
163539_at	16	Mm.38269		
93155_at	15.3	1500032A09	2	1500032A09
166048_r_at	15	5.73E+21		
2810422P17	15.2	Cntnap2	2	5430425M22
135364_at	15	E030017G24		
165510_f_at	15	Art1		
106075_at	15	Cplx1		
163572_at	15	Gng4		
92200_at	15	Adcyap1		
114393_at	14.5	Ppp1r1c	2	7.10E+18
110346_at	14	1700020G04		
1190003P12	14.3	Pgcp-pending		
114999_at	14	Dach1		
160819_at	14	Ndr4		
163632_at	14	A2bp1-pending		
160413_at	13.5	Nsg2	3	0710008E18, 2610027C14
104280_at	13.4	Sncg	2	161859_f_at
167470_i_at	13	6430601K09		
109362_at	13	3.11E+20		
117125_at	13	Mm.41044		
133732_at	13	Pou4f2		
114766_at	13	9330127H16		
103543_at	13	Aig1-pending		
160610_at	13	Pcdha4		
114845_s_at	13	Pepf-pending		
102967_at	12.7	Gdap1	2	9630008H22
160695_i_at	12.6	Homer2	2	1110012H21
135696_f_at	13	Syt14r		
117096_at	12	C030033F14		
163664_at	12	Fads2	2	2900042M13
105861_at	12	ARP3beta		
108786_at	12	LOC230904		
106855_at	12	D430041D05		
137043_r_at	12	Mm.37240		
133909_at	11	Mm.33217		
107855_at	11	A330086D10		
92498_at	11	Unc13h1		
102009_at	11	6430511D02		
114119_at	11	Mtap2		
111336_at	11	Sepm-pending	3	A230103K18, 1500040L08
131792_s_at	11	Entpd3		
163642_at	10.9	Gng2	3	1110003P13, 1110008L10
1190004M23	10.8	1190004M23		
99510_at	11	Prkcb		
1110063G11	10.6	1110063G11		
2700010L09	10.6	2700010L09		
92349_at	10	2810011G06		
170825_i_at	10	7530419J18		
98488_at	10	Myh4		
2310012G06	10.2	2310012G06		
95559_at	10.2	6330403K07	2	6330403K07
111519_at	10	Atp8a2		
160185_at	10	Tagln3		
92812_f_at	10	Defcr1		
116691_at	10	Mm.38576		
105882_at	10	Mm.40506		
96780_at	9.5	2410022L05	2	96779_f_at
96244_at	9.5	Uchl1	3	1110033I23, 2900059O22
2010200C07	9.4	Mcf2l		
139497_at	9	5033430I15R		
167583_at	9	Mm.259070		
98457_at	9.2	Slc4a4	2	113013_s_at
2610100B16	9.2	2610100B16		
166562_r_at	9	Mm.100454		
113306_at	9	9130020G22		
2410001K24	9.1	2410001K24		
95546_g_at	9	Igf1		
104778_at	9	4930428B12		
103960_at	9	Rap2ip	3	106502_at, 0610040A09
2.51E+26	8.9	2.51E+26		
162578_at	9	Smpd3		
2410020A08	8.7	Cldn6	2	2410046F06
4921531N22	8.7	4921531N22		
166760_s_at	9	C230094B15		
138068_at	9	Mm.39876		
138554_at	9	Mm.40940		

103506_f_at	8	Dsc2	2	9030618P22
161431_i_at	8	Rmp-pending		
166513_at	8.4	5730592G18	2	5730592G18
169241_i_at	8	Mm.62358		
162949_at	8	6620401M08		
2700060H17	8.2	2700060H17		
5730443M18	8.2	Ank3		
2.40E+10	8.1	2.40E+10		
113857_at	8	6.43E+15		
109490_at	8	9130024F11		
162963_at	8	1810006K23	3	1810006K23, C030023P10
6430411K14	8	6430411K14		
116395_at	8	9430096I18		
95453_f_at	7.9	S100a1	3	2700088D09, 5430406J05
162620_at	8	9830160H19		
110393_at	7.8	2810432N10	3	165794_at, 2810432N10
105407_at	8	9330120H11		
1.21E+17	7.6	1.21E+17		
92402_at	8	Mm.409		
168115_f_at	8	C130036G08		
106505_at	8	C630030B20		
104045_at	8	2610102M01		
2610507K20	7.5	Slc14a1		
104337_f_at	7	1200008D14		
105812_at	7	Doc2g		
136737_r_at	7	A230011M16		
106583_at	7	Plekha2		
98005_at	7	Pkia		
103743_at	7	Mm.24441		
92626_at	7	Npdc1		
166600_at	7	Khdrbs3		
104299_at	7	Zdhhc14		
103536_at	7	Tmeff2		
163268_at	7	A930006B11		
105162_at	7	A830080H07		
0610006O14	7.1	0610006O14		
1300016D08	7.1	1300016D08		
0610025N19	7.1	Nrp	2	2600002F02
103843_at	7	Gnao		
4933405M22	7	4933405M22		
111553_at	7	Crmp5-pending		
107460_at	7	6230400G14		
A330042I05	6.9	A330042I05		
2810407D22	6.8	Anxa6	2	5930413M14
1110029F20	6.7	1110029F20		
1600016C16	6.7	1600016C16		
4930455F09	6.6	Prok2		
163796_at	7	Dact1		
161619_f_at	7	Mapk8ip		
2410011K10	6.5	2410011K10		
3110070H17	6.4	3110070H17		
0610041C11	6.4	Tagln		
5430425K04	6.4	5430425K04		
2900084I15	6.3	2900084I15		
2010010B23	6.3	Myo1a		
115348_i_at	6	A830059A17		
2210414F18	6.2	2210414F18	2	2.31E+14
1.30E+15	6	1.30E+15		
2610037C02	6	Olfm1		
0910001K20	5.9	0910001K20		
1500003B06	5.8	Tcfap2b	2	5430431G23
2.21E+20	5.8	Arl6	2	1110018H24
4921511C13	5.7	Tmod2		
1300008P18	5.6	1300008P18	2	2600017J23
1700048I17	5.5	Hist2	2	4.93E+24
9430041P20	5.5	9430041P20		
2410041A17	5.5	2410041A17		
104534_at	5.4	3.23E+08	3	3230402E02, 1110057K12
0610037K01	5.4	0610037K01		
1110008N23	5.4	1110008N23		
1810012I01	5.3	1810012I01		
1110032F04	5.1	1110032F04		
2010306I20	5.1	Chuk		
2300002D11	5.1	2300002D11		
1600010D10	5	1600010D10		
1500031H04	4.9	1500031H04		
2310068P04	4.9	2310068P04		

1110062G02	4.9	1110062G02		
1810009G19	4.8	1810009G19		
165462_at	4.8	2900046G09	2	2900046G09
1700030B06	4.8	1700030B06		
D030020D09	4.8	D030020D09		
6330562O12	4.7	6330562O12		
2410008A19	4.7	Zmynd1		
2410045I01	4.7	2410045I01		
2810423I09	4.6	2810423I09		
3110009G19	4.6	3110009G19		
9.13E+13	4.6	9.13E+13	2	9230104K21
0610034M08	4.6	S100a13	2	2210411D22
1110037D04	4.5	1110037D04		
2010109N16	4.5	Ctsz	2	2510005D09
0610005D09	4.4	Ctsl	2	2610028H05
4930558F19	4.4	4930558F19		
1.11E+23	4.4	1.11E+23		
0610007J12	4.1	Atp6v0b	3	2310024H13, C530010I21
1210002B07	4.1	1210002B07		
2310043N10	4.1	2310043N10		
D930014C06	4.1	Schip1		
0610038J11	4	0610038J11	2	1700030O21
2810005F16	4	Cldn3	2	1700029O03
0610012F20	3.9	Gabarapl2		
1700003H21	3.9	Necab1		
1100001C17	3.9	Col1a2		
2610009I02	3.9	2610009I02		
4930534G10	3.8	4930534G10		
2610303L14	3.8	Gabarapl1	2	9130422N19
1300019I11	3.8	1300019I11		
2.51E+13	3.7	2.51E+13		
0610042I08	3.7	0610042I08		
5730405G19	3.7	Hip1R		
C330001N20	3.7	C330001N20		
1600009N02	3.7	H2bfs	3	1500011O09, 1500010J12
3110082B06	3.7	Kif1b		
5730551K18	3.6	5730551K18		
1110017I03	3.6	Tde2	2	0610039M12
3930402F23	3.5	3930402F23		
2310069N01	3.5	2310069N01		
2010015A02	3.5	2010015A02		
3830403N01	3.4	3830403N01		
0610039C21	3.4	0610039C21		
1110034C02	3.4	Stat3		
2.31E+07	3.4	2.31E+07		
2900093H08	3.4	2900093H08	2	2810457N15
1810020L16	3.4	Aga		
2.51E+25	3.3	Sdc2		
2600017F15	3.3	Aldo1		
1700054C17	3.3	Asb1		
2010001M06	3.3	2010001M06		
1.70E+13	3.3	1.70E+13	2	1810073O09
1810017B18	3.3	1810017B18		
0610008C09	3.3	H1f2		
1.11E+10	3.2	Sprrl2		
1110005K06	3.2	1110005K06	2	0610010O12
1110058A15	3.2	1110058A15	2	1110018O07
2310020L01	3.1	Sprrl9	2	2310066F03
1110007B04	3.1	1110007B04		
2310076K21	3.1	2310076K21		
2310042L19	3.1	2310042L19		
2210416B11	3	2210416B11		
2410012A13	3	2410012A13		
B230219D22	3	B230219D22		
2210416O15	3	2210416O15		
1810073P09	3	1810073P09		
1110059L13	2.8	1110059L13		

CHAPTER 4

SWELLING-ACTIVATED Ca^{2+} CHANNELS TRIGGER Ca^{2+} TRANSIENTS IN MERKEL CELLS

Introduction

Since their discovery, epithelial Merkel cells have been proposed to be mechanosensory cells that transduce mechanical stimuli and then transmit sensory information to underlying sensory afferents (Iggo and Findlater, 1984). This hypothesis stems from their location adjacent to sensory afferent terminal s in highly touch sensitive areas of skin. This anatomy resembles that of hair cells, the force-sensitive cells of the inner ear that make synaptic contacts with afferent terminal s. Moreover, Merkel cells express presynaptic molecules essential for synaptic transmission (Haeberle *et al*., 2004; Hitchcock *et al*., 2004). Finally, Merkel cells have functional L- and P/Q-type VACCs (Yamashita *et al*., 1992; Haeberle *et al*., 2004), which trigger vesicle release at neuronal synapses. Despite this anatomical and biochemical evidence, physiological experiments have failed to conclusively determine if Merkel cells are required for the SAI response (Halata *et al*., 2003). Eliminating Merkel cells by laser ablation or genetic deficiency abolished the SAI response in some studies (Pacitti and Findlater, 1988; Ikeda *et al*., 1994) but not others (Mills and Diamond, 1995; Kinkelin *et al*., 1999). Previous reports exploring Merkel-cell mechanosensitivity *in vivo* and *in vitro* have been likewise inconclusive (Baumann *et al*., 1996; Tazaki and Suzuki, 1998)

To determine if Merkel cells are mechanosensory cells, we asked if purified Merkel cells directly respond to mechanical stimuli *in vitro*. When the skin is displaced, forces must alter Merkel-cell shape, though the exact nature of this deformation is not known. Here we chose osmotic stimuli because they permit simultaneous stimulation of many cells. Also, this is a robust stimulus known to activate force-sensitive ion channels

(Colbert et al., 1997; Kim et al., 2003; Gong et al., 2004) as well as hair cells and mechanosensory neurons (Crist et al., 1993; Viana et al., 2001a). Moreover, the mechanosensitive channel whose structure and function is best understood, MscL, is directly activated by hypotonic stimuli *in vivo* (Kung and Blount, 2004). Our findings demonstrate that hypotonic stimuli cause Ca^{2+} influx in Merkel cells, and indicate that this Ca^{2+} influx is initiated by swelling-activated ion channels. We used RT-PCR and pharmacology to identify candidate ion channels that may mediate this response. Our results demonstrate that Merkel cells are directly mechanosensitive, which supports the hypothesis that they function as touch receptors in the Merkel cell-neurite complex.

Results

Hypotonic stimuli evoke cytoplasmic Ca^{2+} transients in Merkel cells

To determine if Merkel cells respond to changes in osmolality, we monitored intracellular Ca^{2+} with the ratiometric, fluorescent indicator fura-2. In epidermal-cell suspensions, Merkel cells represent ≈0.2% of dissociated cells. Using FACS we enriched GFP^+ Merkel cells to approximately 85% percent: the remaining 15% consisted predominately of GFP-negative keratinocytes. Cells were subjected to Ringer's solutions of varying osmolality. Most Merkel cells showed an increase in free $[Ca^{2+}]$ in response to 20% hypotonic stimuli (65±3% cells, *N*=19 experiments, 10–33 cells/experiment, Fig. 1A–C). In responding Merkel cells, the peak cytoplasmic Ca^{2+} transients ranged from threshold to 4 μM above resting Ca^{2+} levels (0.51±0.06 μM, mean ± SEM, *N*=19 experiments, 7–28 responding cells/experiment). Merkel cells showed no response to 30% hypertonic solutions (*N*=35 cells). Keratinocytes showed no change in free $[Ca^{2+}]$ to

osmotic strength changes (*N*=30 cells, Fig. 1A–C, arrow head). Our results indicate that Merkel cells, but not keratinocytes, respond to hypotonic solutions.

We next characterized the time course of the hypotonic response in Merkel cells. Hypotonic solutions triggered Ca^{2+} transients with an initial rise in global [Ca^{2+}] 16.4±1.5 s after onset of perfusion (Fig. 1D, *N*=19 experiments, 7–28 cells/experiment). In control experiments with fluorescent perfusion solutions, we found that it took 5.5 s to replace ≥ 95% of the volume of the bath solution. Subtracting this perfusion time from Merkel cells' response times indicates that on average 10.9±1.5 s elapsed before the initial observable rise in [Ca^{2+}] in response to a hypotonic stimulus. Merkel cells responded to hypotonic Ringer's solution with a sigmoidal increase in [Ca^{2+}], followed by an exponential decay to an elevated [Ca^{2+}] significantly above baseline (p<0.0001, *N*=68 cells, paired Wilcoxon test). After the hypotonic stimulus ended, cytoplasmic free [Ca^{2+}] recovered to baseline. The time course of recovery was fit with a single exponential with a time constant of 22±2.6 s (mean ± SD).

To characterize the dose-response of the hypotonic-triggered Ca^{2+} rise in Merkel cells, we challenged Merkel cells with solutions of progressively decreasing osmolality. Ringer's solutions of decreasing osmolality induced larger peak Ca^{2+} transients in individual Merkel cells (Fig. 1E). Merkel cells with the largest Ca^{2+} transient at 10% hypotonic Ringer's solution had the largest Ca^{2+} influx at 20 or 30% hypotonic Ringer's solution. In addition, solutions of progressively lower osmotic strength elicited responses in a greater proportion of Merkel cells than mildly hypotonic solutions (261 mmol·kg^{-1} recruited 29% of cells, 232 mmol·kg^{-1} recruited 52% of cells, 203 mmol·kg^{-1} recruited 71% of cells, Fig. 1F). Our data indicate that Merkel cells respond to relatively mild 10%

changes in osmolality, yet, even 30% hypotonic solutions do not appear to saturate Merkel cells' response.

Hypotonic solutions induce cell swelling which activates stretch-sensitive channels in bacteria (Blount et al., 1996), so we asked whether similar hypotonic-induced swelling occurred in Merkel cells. To ascertain if hypotonic solutions altered Merkel-cell volume, we monitored cell shape in three dimensions with fluorescent microspheres attached to the plasmalemma of Merkel cells while perfusing cells with a 20% hypotonic bath solution. Microspheres settled onto Merkel cells and the surrounding coverslip within 30 min of bath application and remained tightly coupled during solution changes (Fig. 2A). Microspheres were imaged with high-speed confocal microscopy, and their positions were used to model the location of Merkel-cell surfaces in relation to the coverslip. By integrating the volume between reconstructed cell surfaces and the coverslip, we estimated that Merkel cells' volume in isotonic Ringer's solution was 334±39 μm^3 (mean ± SD, N=8). To determine if Merkel cells swelled in response to a hypotonic stimulus, we imaged Merkel cells in time series while perfusing 20% hypotonic Ringer's solution (Fig. 2B). This stimulus caused Merkel cells to swell 7.3±2.9% (mean ± SD, N=8, $p<0.001$, paired Student's t test). Merkel cells began swelling within 7 s of the onset of hypotonic perfusion, which was the temporal resolution of the three-dimensional imaging. Merkel cells remained enlarged throughout the hypotonic stimulus and relaxed to their original volume after recovery to isotonic Ringer's solution (data not shown).

Comparing the timecourse of hypotonic-induced cell swelling with hypotonic-induced increase in cytoplasmic [Ca^{2+}] would help indicate whether there is a

causal link between cell swelling and Ca^{2+} rise. Unfortunately the experimental design necessitated the use of different chambers in the two different experiments preventing direct comparison of timecourse, although general conclusions can be drawn. The chamber used to determine cell size was very small, and likely had an extremely fast replacement time. This indicates that significant swelling occurs within 7 seconds of the hypotonic stimulus, which precedes the foot of the [Ca^{2+}] transients by several seconds. However, these Ca^{2+} measurements were averages of the entire cytoplasm of the cell, subcellular cytoplasm transients below threshold could occur with a less latency.

Hypotonic-induced Ca^{2+} transients are concentrated in processes

Mechanosensitive channels are often located within specialized cellular processes that are thought to help leverage forces to the mechanosenstive ion channels. Hair cells have mechanoelectric transduction channels near the tips of modified microvilli called stereocilia (Lumpkin and Hudspeth, 1995), and kidney cells detect fluid flow with mechanosensitive channels located in their cilia (Nauli et al., 2003). Similarly, Merkel cells *in vivo* have actin-filled processes that penetrate overlying keratinocytes (Smith, 1967; Iggo and Muir, 1969). To determine if Merkel cells extend analogous processes *in vitro*, we stained Merkel cells with fluorescent sphingolipids, to visualize membrane morphology, and fluorescent phalloidin, to label filamentous-actin (F-actin). We found that cultured Merkel cells have processes arranged in a branch like pattern, with smaller processes at the terminal s of larger processes (Fig. 3A). The F-actin-filled processes were up to 8 μm long, and were $\approx$0.5 to 2 μm in diameter (Fig. 3B-D).

Since these actin-filled processes *in vivo* are proposed to be sites of mechanotransduction (Iggo and Findlater, 1984), we asked whether cultured Merkel cells

display subcellular Ca^{2+} transients in their processes in response to hypotonic solutions. During hypotonic stimuli, Merkel cells had elevated [Ca^{2+}] in their processes, and around the nucleus (Fig. 4A, B). Furthermore, [Ca^{2+}] increased first in regions adjacent to the plasmalemma and then in regions located deeper within the cytoplasm (Fig. 4C, D). Superficial regions had higher [Ca^{2+}] than interior regions during the first 30 s of the stimulus; however, both regions displayed similar peak [Ca^{2+}] and similar time courses of relaxation. The increase in [Ca^{2+}] near the plasmalemma of Merkel cells implies Ca^{2+} influx across the cell membrane. Furthermore, localized [Ca^{2+}] increases in Merkel-cell processes suggest that they are the initial sites of mechanotransduction.

Hypotonic-induced Ca^{2+} transients are amplified by VACCs and Ca^{2+}-induced Ca^{2+} release

To identify the source of hypotonic-triggered increases in cytoplasmic [Ca^{2+}], we treated Merkel cells with hypotonic Ringer's solution while either blocking Ca^{2+} influx across the cell membrane or eliminating Ca^{2+} release from internal stores. We blocked Ca^{2+} influx across the membrane by chelating extracellular Ca^{2+} with 10 mM EGTA. Extracellular EGTA completely abolished hypotonic-induced Ca^{2+} transients (99.0±0.3%, mean ± SEM, *N*=3 experiments, Fig. 5A, D) and was fully reversible upon reintroduction of external Ca^{2+}. These data indicate that extracellular Ca^{2+} influx contributes to hypotonic-triggered Ca^{2+} transients.

To ascertain whether voltage-activated Ca^{2+} channels (VACCs) also contribute to hypotonic-induced increases in free [Ca^{2+}], we blocked these channels with a cocktail containing 10 μM conotoxin MVIIC to block N- and P/Q-type Ca^{2+} channels and 10 μM nimodipine to block L-type Ca^{2+} channels (Haeberle et al., 2004). The efficacy of this

cocktail was tested by depolarizing Merkel cells with high-K^+ Ringer's solution (Fig. 5B). The blocking cocktail inhibited peak high-K^+-induced Ca^{2+} transients by 96±1% (mean ± SEM, *N*=4 experiments). By contrast, the blocking cocktail only curtailed peak hypotonic-induced Ca^{2+} transients by 51±13% (mean ± SEM, *N*=4 experiments). Thus, in the presence of VGCC blockers, 60% of Merkel cells had larger hypotonic-induced transients than high-K^+ induced transients (Fig. 5B). This partial inhibition of the high-K^+ response by VACC blockers indicates that VACCs contribute to, but are not the sole source of, hypotonic-induced Ca^{2+} influx across the plasma membrane.

To determine whether Ca^{2+} release from internal stores contributes to the hypotonic-induced Ca^{2+} transient, we designed an experimental protocol to empty internal stores of Ca^{2+} and analyzed the hypotonic response (Fig. 5C). We blocked Ca^{2+} reuptake into internal stores with 1 μM thapsigargin, which inhibits the sarco/endoplasmic reticulum Ca^{2+}-ATPase. We then emptied internal stores by depolarizing the membrane with high-K^+ Ringer's solution, activating Ca^{2+}-induced Ca^{2+}-release from internal stores. Store depletion was verified at the end of experiments by first chelating extracellular Ca^{2+} with EGTA and then permeabilizing cell membranes with the Ca^{2+} ionophore ionomycin. Pre-treatment with thapsigargin reduced Ca^{2+} transients from hypotonic stimuli 80±3% (mean ± SEM, *N*=4 experiments). As a result, the peak amplitudes of hypotonic-induced transients in the presence of thapsigargin and VACC antagonists, though reduced, were significantly larger than those in the presence of 10 mM EGTA ($p<0.05$, paired Student's *t* test, *N*=3–4 experiments, Fig. 5D). Thus, internal Ca^{2+} stores amplify Ca^{2+} influx induced by hypotonic solutions.

K^+ channels modulate the hypotonic response

Voltage-activated K^+ channels regulate hypo-osmotic signaling in Merkel cells

Our previous gene-profiling studies indicated that Merkel cells express transcripts encoding multiple K^+ channel isoforms, including an accessory subunit of BK_{Ca} channels ((Haeberle et al., 2004)). Since voltage-activated K^+ channels in Merkel cells shape and limit membrane excitation in neurons, I asked if K^+ might also shape Ca^+ influx in response to hypo-osmotic solutions.

Merkel cells were bathed in a 20% hypotonic extracllular solution either in the presence or absence of 30 mM TEA. In Merkel cells stimulated with 20% hypotonic solutions, we observed elevated $[Ca^{2+}]_{in}$ (Fig 6A), the peaks of which were significantly increased in the presence of TEA (Fig 6B; mean ± S.E.M.: control, 1.25 ± 0.25; TEA, 2.30 ± 0.19). TEA also significantly increased the rate of onset of hypotonic-induced Ca^{2+} transients (Fig 6C; mean ± S.E.M.: control, 20.9 ± 2.1 s; TEA, 12.6 ± 3.2 s). Surprisingly, we found that the relaxation time during the hypotonic challenge was significantly shortened in the presence of TEA (Fig 6D; mean ± S.E.M., control: 13.2 ± 2.6 s; TEA: 5.2 ± 1.7 s). These results indicate that voltage-activated K^+ channels limit the extent and prolong the duration of Ca^{2+} transients in Merkel cells.

To ask specifically if BK_{Ca} channels modulate Ca_{2+} transients in Merkel cells, we incubated Merkel cells in 100 nM IBTX for ≥10 min. We found that this treatment increased the resting fura-2 ratios by 10.5 ± 0.4%, (N = 119 cells). This suggests that BK_{Ca} channels regulate Ca^{2+} influx in Merkel cells by contributing to the resting membrane potential; however, this resting Ca^{2+} increase confounded the interpretation of Ca^{2+} transients in Merkel cells

Pharmacology of the hypotonic response

Hypotonic induced extracellular Ca^{2+} influx implies the presence of a swelling-activated, plasmalemma ion channel, but does not speak to its identity. The most obvious candidate is TRPV4 (GenBank accession number NM_022017), which is expressed in Merkel cells (Liedtke et al., 2000) and is activated by hypotonic solutions when expressed in human embryonic kidney (HEK) cells (Strotmann et al., 2000; Liedtke et al., 2003). To determine if TRPV4 is required for hypotonic responses, we analyzed hypotonic-induced Ca^{2+} transients in Merkel cells from TRPV4-deficient mice (Fig. 6). The magnitude and time course of Ca^{2+} transients in Merkel cells from TRPV4 -/- mice were indistinguishable from those of heterozygous littermate controls (Fig. 6) and from wild-type responses. Thus, TRPV4 is unlikely to mediate the hypotonic response in Merkel cells.

We next broadened our search for the molecular identity of the swelling-activated channels in Merkel cells. Two ion channel families have been implicated in mechanotransduction in mammals: transient receptor potential (TRP) channels and Degenerin/Epithelial Na^+ channels (DEG/ENaC), (Gillespie and Walker, 2001). Ruthenium red is a broad-spectrum blocker of many channels, including TRPV channels. We found that 10 μM ruthenium red inhibited the osmotic response by 71±8% (mean ± SEM, *N*=2 experiments, *N*=9–10 cells/experiment); however, ruthenium red inhibited high-K^+-induced Ca^{2+} transients to the same extent (68±12%). Because ruthenium red did not fully block hypotonic-induced Ca^{2+} transients, we sought to determine if the hypotonic response was sensitive to the DEG/ENaC antagonist, amiloride. Amiloride (50

μM) did not inhibit the hypotonic-induced Ca^{2+} transient (¯8± 13%, *N*=2 experiments, *N*=20–27cells/experiment).

Merkel cells express TRP ion channels

Since amiloride did not inhibit the hypotonic response, we used RT-PCR to screen for amiloride-insensitive non-selective cation channels expressed in Merkel cells. We focused on channels from the TRP family because many of these channels fit this profile and because they function in diverse modes of sensory transduction. Primer efficacy was tested against cDNA derived from brain, skin, or a mixture of liver, skin, heart, spleen and kidney (Fig. 7). Merkel-cell cDNA yielded robust amplicons for six TRP channels and occasional amplicons for an additional five channels (Table 1). Notably, we discovered amplicons for TRPC1 (GenBank accession number NM_011643), PKD1 (NM_013630) and PKD2 (NM_008861), channels previously implicated in mechanotransduction in other cell types (Hanaoka et al., 2000; Maroto et al., 2005).

Discussion

This study demonstrates that dissociated Merkel cells are mechanosensitive cells directly activated by cell swelling. Our results indicate hypotonic-induced cell swelling triggers Ca^{2+} entry through an as yet unknown cation channel; the resultant depolarization activates VACCs and together these two sources of Ca^{2+} influx activate Ca^{2+} release from internal stores. We identified 11 TRP channels expressed in Merkel-cells of which seven have pharmacological profiles matching the hypotonic response we observed. Of these, PKD1 and PKD2 are promising candidates because they have been previously implicated in mechanotransduction in cilia of kidney cells (Hanaoka et al., 2000). Moreover, we

identified actin-filled process as sites of Ca^{2+} influx in Merkel cells, suggesting that transduction channels cluster there. Our data support a model in which skin indentation applies force to Merkel-cell processes, whose mechanosensitive channels allow Ca^{2+} influx. This Ca^{2+} influx is amplified by VACCS and Ca^{2+} induced Ca^{2+} release (CICR) and could trigger synaptic signaling to the underlying sensory afferent. Finally this signaling is modified by voltage-activated K^+ channels, which seem to modulate the dynamics of hypotonic-evoked Ca^2 influx.

Merkel cells express hypotonic-activated ion channels

Several lines of evidence indicate that Ca^{2+} permeable ion channels generate hypotonic-induced Ca^{2+} transients in Merkel cells. First, the requirement for extracellular Ca^{2+} suggests Ca^{2+} ions enter across the plasma membrane. Second, blocking VACCs or emptying intracellular stores curtails, but does not eliminate, the hypotonic response, suggesting other sources of Ca^{2+} entry. Although it is formally possible that a hypotonic-activated G-protein coupled receptor could induce membrane depolarization *and* Ca^{2+} release from stores, our results indicate such a hypotonic-activated receptor would need to be inactivated by extracellular EGTA. We know of no receptors that match these requirements. Thus, the most parsimonious interpretation of our data is that Merkel cells express hypotonic-activated, Ca^{2+}-permeable cation channels.

If hypotonic solutions activate the same channel complexes in dissociated Merkel cells that are activated by touch *in vivo,* one might expect a similar time course of activation. Instead, the latency of hypotonic-induced Ca^{2+} influx in Merkel cells is ≈11 s, much longer than the 200 μs latency of the SAI response (Gottschaldt and Vahle-Hinz, 1981). Several possibilities could explain this latency difference. For example, Merkel

cells may respond rapidly to touch-evoked pressure, whereas osmotic stimuli might take longer to develop sufficient membrane distortion to activate channels. Although our volumetric data indicate that Merkel cells begin to swell within 7 s of hypotonic-solution perfusion, they continue to swell for >30 s so it may take the observed 11 s to generate sufficient membrane tension to activate mechanotransduction channels. Alternatively, Merkel cells' transduction channels, like other force-activated cell types, may require extracellular linkages or specialized extracellular matrices present *in vivo* that are not present in culture. In hair cells, stereociliary deflection tugs extracellular links that transmit force to mechanotransductive channels (Gillespie and Walker, 2001), and body touch neurons in *Caenorhabditis elegans* require extracellular proteins to respond to touch (Du et al., 1996). Hypotonic-induced membrane stretch in Merkel cells might constitute a global mechanical stimulus sufficient to activate force-transducing machinery independent of these extracellular linkages. The lack of extracellular linkages might also explain why blunt pressure failed to generate responses in isolated Merkel cells under whole-cell voltage clamp in previous work (Yamashita et al., 1992). Finally, the latency of mechanotransduction is unknown in Merkel cells *in vivo*. Although the SAI response has 200 μs latency, it is possible that the initial dynamic phase of the SAI response is generated by the nerve afferent, with Merkel cells mediating the slowly adapting element (Ogawa, 1996).

Does osmosensitivity imply that Merkel cells are mechanosensory cells? Although altering cell volume by application of anisotonic extracellular solutions induces Ca^{2+} influx in a variety of excitable and non-excitable cells (Oike et al., 1994; Chen et al., 1996; Altamirano et al., 1998), these responses have 1–5 minute latencies followed by 2–

10 minute time to peak. By contrast, a subset of sensory cells isolated from the trigeminal nucleus has robust responses that develop within seconds and these neurons have been proposed to be the mechanosensitive subset of neurons in the trigeminal nucleus (Viana et al., 2001b). We found that hypotonic solutions induced a Ca^{2+} signal similar to this rapidly activating neuronal population. This observation suggests that this response is associated with mechanotransduction, and not a ubiquitous regulatory volume response.

Modulation of hypotonic signaling by voltage-activated K^+ channels in Merkel cells

Because voltage-activated K^+ channels generally limit excitability in neuroendocrine cells, it seems paradoxical that blocking BK_{Ca} and other voltage-activated K^+ channels shortens hypotonic-evoked Ca^{2+} transients in Merkel cells. Such counterintuitive effects of BK_{Ca} blockers have been reported in other cell types ((Warbington et al., 1996; Pattillo et al., 2001; Skinner et al., 2003; Xu and Slaughter, 2005)). The Ca^{2+} transients we observe in Merkel cells reflects a balance between Ca^{2+} flux into the cytosol and sequestration by buffering and extrusion ((Berridge et al., 2003)). These processes are all modulated by Ca^{2+} ((Berridge et al., 2003)) and are therefore potential sites of regulation by BK_{Ca} and voltage-activated K^+ channels. For example, by limiting membrane depolarization and $[Ca^{2+}]_{in}$, K^+ channels may delay inactivation of voltage-activated Ca^{2+} channel thereby prolonging the Ca^{2+} transient. Furthermore, BK_{Ca} and Cl^- channels have been found to link intracellular Ca^{2+} dynamics during regulatory volume decrease after hypotonic stimulation ((Weskamp et al., 2000; Jakab and Ritter, 2006)).

Evidence for microvilli as the site of mechanotransduction in Merkel cells

In vivo, Merkel cells' superficial surfaces are studded with actin-rich microvilli are proposed to be sites of mechanotransduction (Iggo and Findlater, 1984). In culture, we observed Merkel cells with two cell shapes: cells with large processes 2–15 μm in length that branch into smaller processes 1–8 μm in length and spherical cells with smaller 1–8 μm processes. Both cell shapes are observed *in vivo,* where they are termed "dendritic" and "non-dendritic" Merkel cells, respectively (Garcia-Anoveros et al., 1995; Tachibana et al., 1997; Nakafusa et al., 2006). The slender processes, present in all Merkel cells though not visible in our fura-2 ratio images, could be the source of Ca^{2+} influx. If Ca^{2+} influx was concentrated in slender processes Ca^{2+} would flow to the filopodial-like, visible processes before the entering the soma. We often observed hypotonic-triggered Ca^{2+} transients in processes before global cytoplasmic Ca^{2+} levels increased, providing the first evidence substantiating the hypothesis that Merkel-cell actin-filled processes are sites of mechanotransduction.

Candidate transduction channels in Merkel cells

Several gene families have been implicated in vertebrate mechanotransduction, including members of the TRP family and the DEG/ENaC family. In particular, TRPV4 responds to hypotonic solutions in HEK cells (Strotmann et al., 2000; Liedtke et al., 2003) and is expressed in Merkel cells (Liedtke et al., 2000). However, our finding that TRPV4 deficient mice have normal hypotonic responses indicates TRPV4 is not required for swelling-activated Ca^{2+} transients. Thus, we used pharmacology to elucidate the molecular nature of Merkel cells' hypotonic-activated channel. Amiloride (50 μM), a DEG/ENaC antagonist with an IC_{50} of < 5 μM, does not block the hypotonic response,

making these channels unlikely candidates for Merkel-cell transduction channels. Ruthenium red is a broad-spectrum inhibitor that blocks some TRP channels, including TRPV channels. We found that 10 μM ruthenium red inhibits both hypotonic and high-K^+ induced Ca^{2+} transients in Merkel cells. Since ruthenium red has also been shown to inhibit both VACCs and Ca^{2+} store release in some cell types (Nagasaki and Fleischer, 1989; Cibulsky and Sather, 1999), it is unclear to what extent ruthenium red directly inhibits swelling-activated channels or downstream amplification. Because ruthenium red does not completely block hypotonic-induced Ca^{2+} transients, the hypotonic response cannot be solely mediated by ruthenium-red-sensitive channels, including the TRPV subfamily.

Because other TRP channels play prominent roles in sensory transduction, including mechanotransduction in zebrafish and invertebrates, they remain attractive candidates for investigation. Moreover, many of these channels are not blocked by ruthenium red. We demonstrated with RT-PCR that Merkel cells express robust transcripts encoding six TRP channels, and transcripts were occasionally found for an additional five channels. Among these channels, TRPC1 and PKD2 have been previously implicated in mechanotransduction. Both are Ca^{2+} permeable, and neither is known to be blocked by ruthenium red (Zitt et al., 1996; Hanaoka et al., 2000; Launay et al., 2002). Although PKD2 is blocked by amiloride, its IC_{50} is 80 μM, larger than the concentrations than we tested here (see methods, (Gonzalez-Perrett et al., 2001)). Interestingly, PKD1 and PKD2 form Ca^{2+} permeable complexes that transduce fluid flow in the kidney (Nauli et al., 2003). In human polycystic kidney disease, patients are heterozygous for either PKD1 or PKD2 mutations and suffer from cyst formation and

eventual kidney failure (Arnaout, 2001). As homozygous deletion in PKD1 or PKD2 in mice causes embryonic death, examination of touch sensitivity in PKD-deficient mice will require a conditional knockout (Piontek et al., 2004). TRPC1 is activated by membrane tension in CHO- cells and *Xenopus laevis* oocytes (Maroto et al., 2005); however, the role of TRPC1 *in vivo* is still undetermined (Dietrich et al., 2007). Many of the TRP channels we found expressed in Merkel cells are orphans: little is known of their biophysical properties, let alone their physiological roles *in vivo*. Consequently, they are all possible candidates for the transduction channel. Thus, our findings set the stage for future gene disruption experiments to identify which of these channels are required for hypotonic responses and for touch sensitivity of Merkel-cell neurite complexes *in vivo*.

Merkel cell mechanotransduction and signaling in the Merkel cell-neurite complex

How might Merkel cells contribute to mechanotransduction in the Merkel-cell neurite complex? The anatomical organization of the complex, with roughly a dozen Merkel cells connected to a single afferent neuron, could explain the irregular distribution of impulses characteristic of the sustained component of the SAI response if each individual Merkel is capable of depolarizing an afferent to threshold (Iggo and Findlater, 1984). Our finding that Merkel cells directly respond to mechanical stimuli *in vitro* suggest they contribute to this depolarization. Our observation that hypotonic-induced Ca^{2+} transients originate in processes provides the first physiological evidence supporting the hypothesis that Merkel-cell processes are sites of mechanotransduction. These processes are presumably deformed by touch *in vivo*. In the few published reports of dissociated Merkel cells and in our preparations, most of these slender processes are bereft of extracellular contacts beyond the collagen-coated coverslip (Fradette et al.,

2003; Shimohira-Yamasaki et al., 2006). How Merkel cells co-cultured with contacting keratinocytes respond to direct touch is explored in the next chapter.

Figures

Figure 1. GFP^+ Merkel cells, but not keratinocytes, show cytoplasmic $[Ca^{2+}]$ increases in response to hypotonic solutions. (A) An epiflourescence micrograph shows GFP^+ Merkel cells after two days in culture (scale bar: 20 μm). (B, C) Pseudocolor images of fura-2 fluorescence ratios (F_{340}/F_{380}) of cells just before perfusion (B) with a 20% hypotonic solution (232 $mmol \cdot kg^{-1}$), and 26 s after perfusion onset (C). Pseudocolor scale bar represents F_{340}/F_{380} (range 0.3–3.0). (D) Plot of $[Ca^{2+}]$ in a keratincocyte (denoted by arrowhead in C, black) and a Merkel cell (arrow in C, green) marked in (B) and (C). (E) Plot of cytoplasmic $[Ca^{2+}]$ versus time for three representative Merkel cells perfused with bath solutions of decreasing osmolality. (F) Quantification of the proportion of total Merkel cells (N=104) that responded. (see methods, 10%: 263 $mmol \cdot kg^{-1}$; 20%: 232 $mmol \cdot kg^{-1}$: 30%: 203 $mmol \cdot kg^{-1}$).

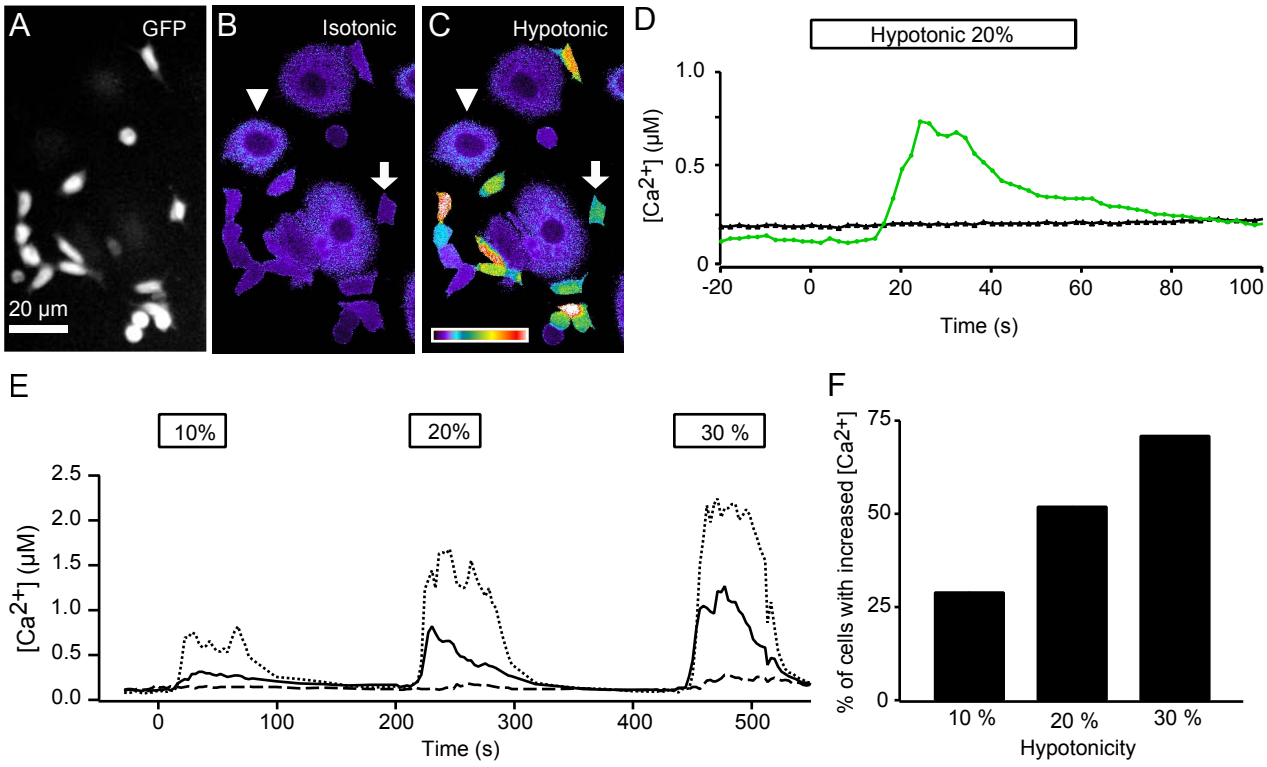
A
GFP
20 µm
B
Isotonic
C
Hypotonic
D
Hypotonic 20%
[Ca2+] (µM)
Time (s)
E
10%
20%
30 %
[Ca2+] (µM)
Time (s)
F
% of cells with increased [Ca2+]
10 %
20 %
30 %
Hypotonicity

Figure 2. Hypotonic solutions cause Merkel cells to swell. Shape changes were monitored with plasmalemma-bound fluorescent microspheres using confocal microscopy. (A) A three-dimensional plot of fluorescent microspheres (black spots) coating the surfaces of a representative Merkel cell and the coverslip. The surface of the Merkel cell was reconstructed from the location of the micropheres (topographic scalebar: navy blue denotes the coverslip surface; dark red=6 μm above the coverslip). Areas of low bead density are keratinocytes, which are poorly bound by the beads. (B) Plot of cell volume versus time for the cell shown in (A). The 20% hypotonic solution was administered at t=0.

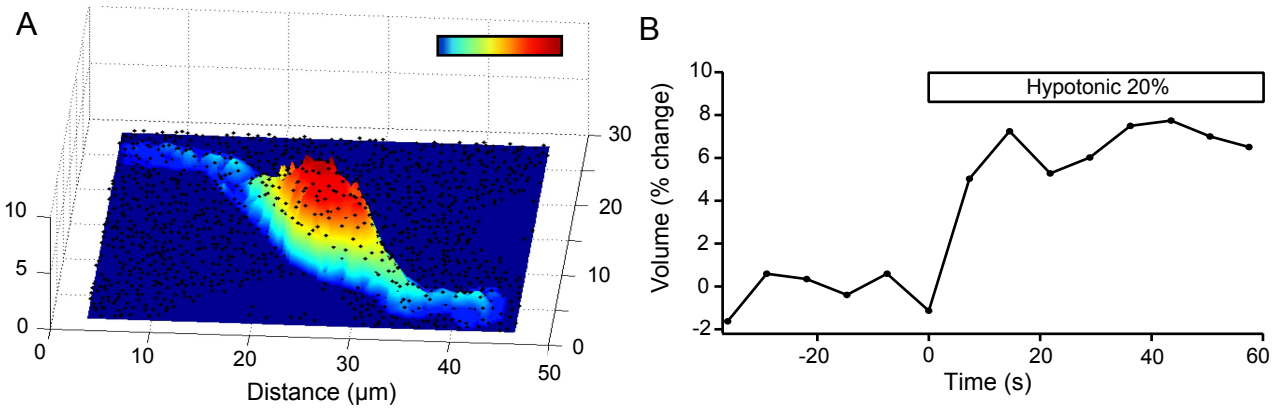
A
B
Hypotonic 20%
Volume (% change)
Time (s)
Distance (µm)

Figure 3. Cultured Merkel cells have cytoplasmic processes. (A) Projections of confocal z-series of cells stained with fluorescencent sphingolipids. Processes 1–8 μm in length jutted from the Merkel–cell surface (arrowhead). By comparison, the keratinocyte showed a smooth cell surface. (B–D) Projections of a confocal z-series of a Merkel cell labeled with rhodamine-phalloidin to visualize F-actin-filled processes in Merkel cells. Images depict (B) GFP fluorescence, (C) phalloidin, and (D) merge. Scale bar in (A) applies to all panels.

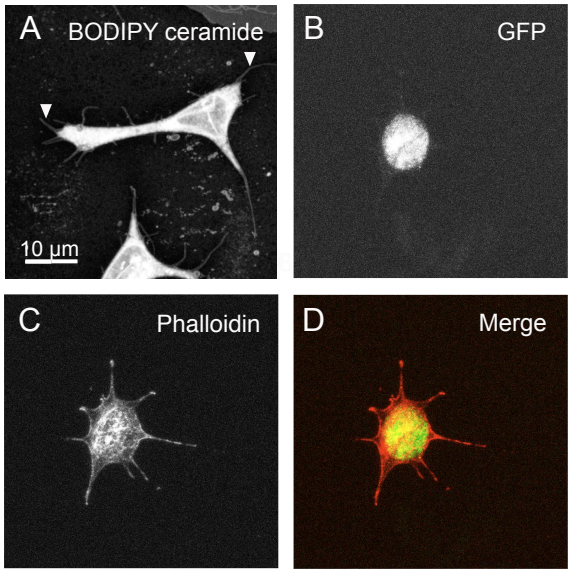
A
BODIPY ceramide
10 µm
B
GFP
C
Phalloidin
D
Merge

Figure 4. Merkel cells display increased [Ca^{2+}] near the plasmalemma of processes in response to hypotonic stimuli. (A, B) Pseudocolor images of fura-2 fluorescence ratios in a Merkel cell before (A) and 16 s after (B) perfusion onset with a 20% hypotonic solution (232 mmol·kg^{-1}). Pseudocolor scale bar shows F_{340}/F_{380} and applies to (A–C). (C) Pseudocolor kymograph of the line shown in (A) and (B). Each pixel along the ordinate corresponds to a point on the line shown in (A) and (B). Pixels near the top and bottom of the kymograph show F_{340}/F_{380} near the plasmalemma, whereas pixels in the middle correspond to the interior of the process. Time proceeds along the abscissa. The time points of (A) and (B) are indicated by arrows pointing to the kymograph in (C). Black lines denote the beginning and end of hypotonic perfusion. (D) Plot of [Ca^{2+}] versus time for three positions along the cell process. Colored lines indicate the average of the corresponding colored box in (C). Red and green traces signify regions near the plasmalemma, whereas blue represents a region deeper in the cytoplasm.

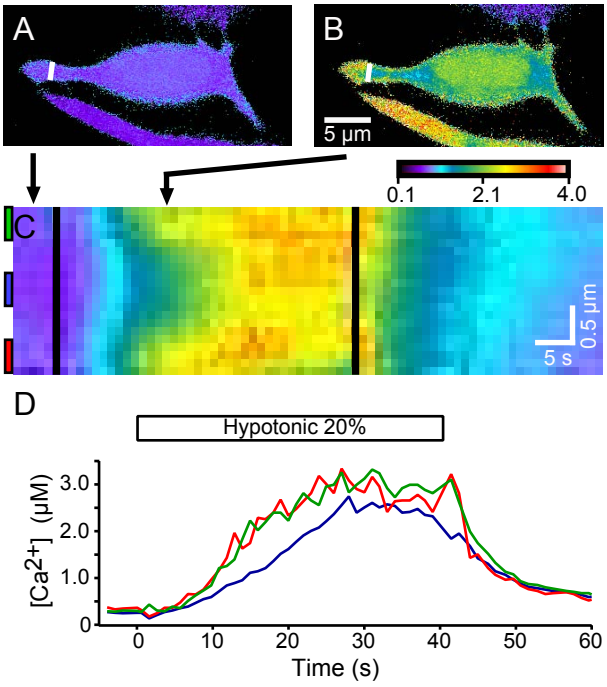
A
B
5 µm
0.1
2.1
4.0
C
0.5 µm
5 s
D
Hypotonic 20%
[Ca2+] (µM)
3.0
2.0
1.0
0
0
10
20
30
40
50
60
Time (s)

Figure 5. Extracellular Ca^{2+} is required for hypotonic-triggered Ca^{2+} transients. These Ca^{2+} transients are composed in part by Ca^{2+} influx through voltage-activated Ca^{2+} channels and Ca^{2+} released from internal stores. (A–C) Plots depict [Ca^{2+}] versus time of representative cells. "Hypo" denotes perfusion of 20% hypotonic solution (232 mmol·kg^{-1}). (A) Labeled boxes indicate the time period of perfusion. Bath Ca^{2+} was replaced with 10 mM EGTA. (B) Cells were depolarized with high-K^+ solution (140 mM K^+). The voltage-activated Ca^{2+} channel (VACC) toxin cocktail contained 10 μM nimodipine and 10 μM ω-conotoxin MVII-C. (C) Thapsigargin was used at 1 μM. The box labeled "Ion" indicates wash with 10 mM EGTA, followed by perfusion of 10 μM ionomycin, a Ca^{2+} ionophore. (D) Quantification of the effects of EGTA, VACC antagonists, and thapsigargin upon peak hypotonic induced Ca^{2+} influx (N=3–5 experiments per group). Hypotonic responses of Merkel cells exposed to these compounds were normalized to control hypotonic responses. Error bars indicate SEM. Asterisks denote statistically significant differences between EGTA and VACC or thapsigargin treated responses ($p \leq 0.04$, paired Student's t test). The EGTA, VACC and thapsigargen treated responses were significantly different from control ($p \leq 0.05$, Student's t test).

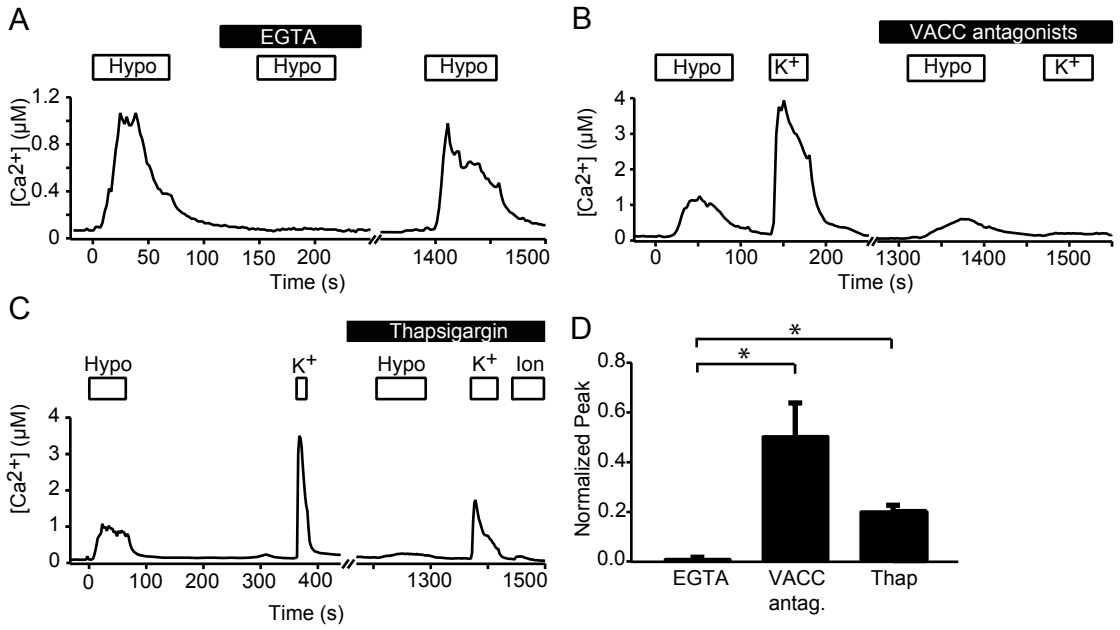
A
EGTA
Hypo
Hypo
Hypo
[Ca2+] (μM)
1.2
0.8
0.4
0
0
50
100
150
200
1400
1500
Time (s)
B
VACC antagonists
Hypo
K+
Hypo
K+
[Ca2+] (μM)
4
3
2
1
0
0
100
200
1300
1400
1500
Time (s)
C
Thapsigargin
Hypo
K+
Hypo
K+
Ion
[Ca2+] (μM)
4
3
2
1
0
0
100
200
300
400
1300
1500
Time (s)
D
*
*
Normalized Peak
0.8
0.6
0.4
0.2
0.0
EGTA
VACC antag.
Thap

Figure 6. K^+ channels control hypotonic-evoked Ca^{2+} transients in Merkel cells. (A) Increases in Fura-2 fluorescent ratios (F_{340}/F_{380}) were elicited by bathing cells in a 20% hypotonic solution (232 mmol kg^{-1}) in the absence or presence of 30 mM TEA. Responses of two representative cells are shown. (B) In the presence of TEA, the hypotonic-induced, peak fluorescence increase was significantly greater than in control conditions. (C and D) Both the rise time and relaxation time of hypotonic-evoked fluorescence increase were significantly faster than in control conditions. Rise time was defined as the elapsed time between 10% and 90% of the peak value ($N = 27$ cells). Relaxation time was defined as the elapsed time between 100% and 80% of the peak value ($N = 8$ cells). Data are derived from two independent experiments. Error bars represent SEM. Asterisks indicate statistically different populations ($p < 0.03$, paired Wilcoxon signed rank test).

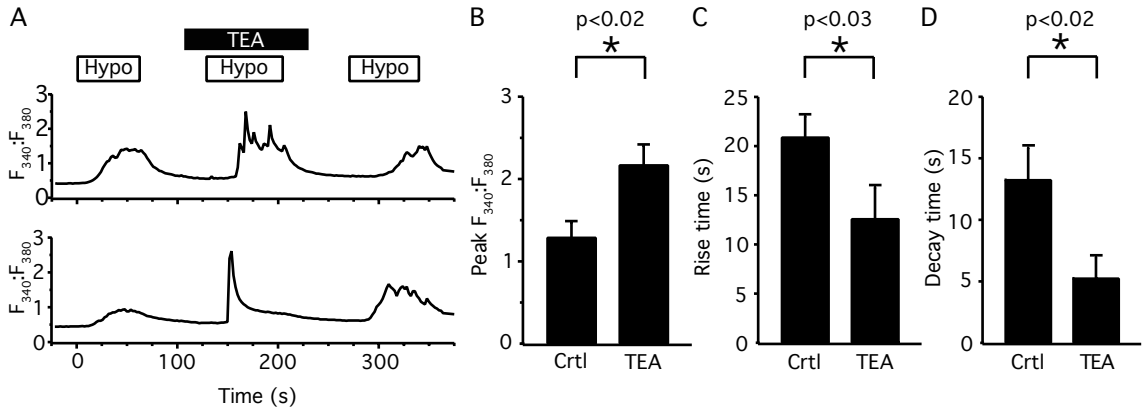
A
TEA
Hypo
Hypo
Hypo
$F_{340}:F_{380}$
$F_{340}:F_{380}$
0
1
2
3
0
100
200
300
Time (s)
B
p<0.02
*
Peak $F_{340}:F_{380}$
Crtl
TEA
C
p<0.03
*
Rise time (s)
0
5
10
15
20
25
Crtl
TEA
D
p<0.02
*
Decay time (s)
0
5
10
15
20
Crtl
TEA

Figure 7. TRPV4 is not required for hypotonic-evoked [Ca^{2+}] transients in Merkel cells. The paired histograms display pooled peak osmotic responses (*N*= 37–43 cells).

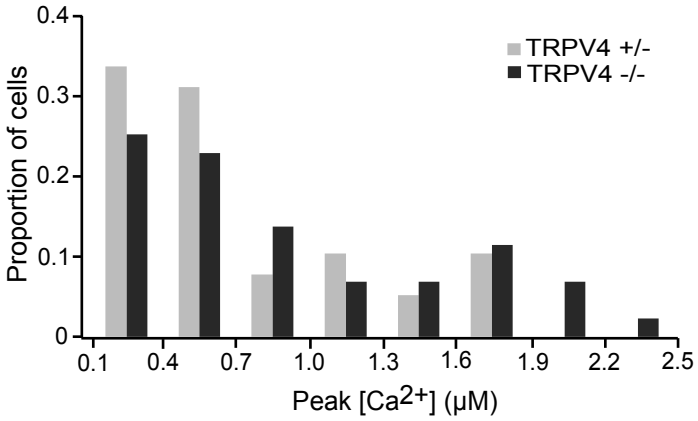
0.4
0.3
0.2
0.1
0
Proportion of cells
TRPV4 +/-
TRPV4 -/-
0.1
0.4
0.7
1.0
1.3
1.6
1.9
2.2
2.5
Peak [Ca2+] (μM)

Figure 8. TRP channel transcripts are expressed in Merkel cells. Representative RT-PCR of the data summarized in *Table 1*. Bars at base of figure mark lanes with products amplified from GFP^+ Merkel cells or control cDNA, respectively. Control cDNA was derived from brain or skin.

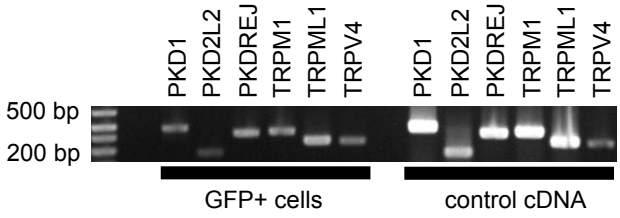
PKD1
PKD2L2
PKDREJ
TRPM1
TRPML1
TRPV4
PKD1
PKD2L2
PKDREJ
TRPM1
TRPML1
TRPV4
500 bp
200 bp
GFP+ cells
control cDNA

CHAPTER 5:

DIRECT TOUCH TRIGGERS Ca^{2+} TRANSIENTS IN MERKEL CELLS

Introduction

We have demonstrated that Merkel cells respond to hypotonic stimuli. However, many mechanosensitive cells respond not only to hypotonic solutions but also to direct mechanical manipulation of their membranes. Such stimulation may more closely approximate the mechanical forces experienced by the cells *in vivo*. Merkel cell-neurite complexes respond robustly to indentation, but not stretch *in vivo* (Iggo and Muir, 1969). We wished to determine whether dissociated Merkel cells have a similar mechanical response profile. We used blunt probes to determine whether Merkel cells respond to direct touch *in vitro*. We also subjected Merkel cells to stretch by culturing them on elastic membranes linked to a machine that provides radial stretch. We find that Merkel cells, when contacting keratinocytes, respond to mechanical indentation, but are minimally responsive to radial stretch.

Results

Indentation of keratinocyte/Merkel cell complexes causes Ca^{2+} transients in Merkel cells

To determine if Merkel cells respond to plasmalemma indentation, we monitored cytoplasmic [Ca^{2+}] with the fluorescent Ca^{2+} indicator fura-2. Using FACS we enriched Merkel cells to approximately 70%: the remaining 30% consisted predominately of GFP-negative keratinocytes. Under such conditions Merkel cells were surrounded by contacting keratinocytes. Using a blunt, ≈1μm wide glass probe, we applied ≈0.4 μm indentation to Merkel cell bodies and processes. Keratinocytes were often ruptured by

mechanical stimulation, and all Merkel cells had ruptured keratinocytes within 30 μm. Some Merkel cells showed an increase in cytoplasmic [Ca^{2+}] levels in response to sustained plasmalemmal indentation (5/8 cells). Responding Merkel cells reacted to indentation of both the cell body (*N*=3 cells) and cytoplasmic processes (*N*=2 cells). These cells showed dynamic rise in [Ca^{2+}] in response to indentation (Fig. 1). After variable delay, Merkel cells' [Ca^{2+}] rose exponentially to a peak, followed occasionally by damped ringing. Keratinocytes did not respond to indentation (*N*=3 cells).

To clarify if these mechanically evoked responses in Merkel cells require extracellular contacts provided by the surrounding keratinocytes, I mechanically stimulated isolated Merkel cells, bereft of any contacting cells. No isolated Merkel cells responded to plasmalemmal indentation (*N*=16 cells). These Merkel cells were grown in identical culturing conditions as those Merkel cells with contacting keratinocytes, indicating differences in gross cell culture conditions did not contribute to this lack of mechanical sensitivity.

Merkel cells respond minimally to stretch

The Merkel cell neurite-complex is highly responsive to skin indentation, but not stretch, *in vivo* (Iggo and Muir, 1969), so I examined if Merkel cells were activated by stretch *in vitro*. Merkel cells were stretched by culturing them on elastic, silicon membranes, which were than fitted to a vacuum driven apparatus that pulled the membranes over a circular post (Flexcell, Indianna). This apparatus was mounted on the sate of an upright microscope so that cells could be monitored before, during, and after stretch. I found that most Merkel cells (*N*=61) displayed no increase in [Ca^{2+}] in response to radial stretch, though two cells responded minimally (fig. 2). Since one keratinocyte

had a minimal response as well (*N=1)* it is not clear if these responses are reflective of physiological function or cellular damage.

Discussion

Merkel cells require keratinocytes to respond to direct indentation

This chapter provides evidence that Merkel cells are mechanosensitive cells directly activated by touch. I observed that Merkel cells respond to plasmalemma indentation, and this response requires the presence of contacting keratinocytes; Merkel cells bereft of cellular contact were uniformly unresponsive to indentation. This dependence stands in obvious contrast to hypo-osmotic stimuli, which induced [Ca^{2+}] transients in Merkel cells irrespective of the presence of abutting keratinocytes (Chapter 4). These two modalities of mechanical stimulation may be activating two entirely different physiological processes, with indentation sensitivity requiring cellular contact, and osmosensitivity acting cell autonomously. This explanation implies that Merkel cells have robust signaling mechanisms for the detection of osmolality changes independent of their putative role in mechanotransduction. I find this explanation unsatisfactory because it fails to account for the frequency of overlap between mechanically sensitive and osmosensitive cell types. Hair cells (Harada et al., 1993), somatosensory neurons in mouse (Viana et al., 2001b) and mechanically sensitive neurons in *c. elegans* (Colbert et al., 1997) are all osmosensitive. In addition, neurons underlying hyrosensation in *Drosophila Melanogaster* are mechanosensitive (Liu et al., 2007). This functional linkage implies both modalities of mechanical stimulation may be acting upon a common cell signaling mechanism.

What explains the requirement of abutting keratinocytes for touch sensitivity but not osmosensitivity? Perhaps hypo-osmotic stimuli constitute a robust mechanical signal, capable of activating mechanotransduction channels even in the absence of surrounding keratinocytes, while touch-evoked mechanotransduction requires the extracellular matrix provided by surrounding keratinocytes. There is precedent for the requirement of extracellular matrix in other mechanosensitive systems: in hair cells, stereociliar deflection tugs extracellular links that transmit force to mechanosensitve channels (Gillespie and Walker, 2001), and body touch neurons in c. elegans require extracellular matrix proteins to respond to touch (Du et al., 1996). Keratinocytes might also modulate the nature of the mechanical stimulus; they might diffuse or focus force applied to their exterior and thereby aid mechanotransduction in Merkel cells. Such sophisticated force transfer mechanisms are used in bone where macro bone stress is transduced into microscopic deflections of osteopaths (Malone et al., 2007).

Merkel cells are specifically sensitive to compression, and not stretch, *in vitro*

Merkel cell neurite complexes are highly sensitive to specific mechanical stimuli *in vivo*. They respond to indentations of the skin of as little as 0.5 μm, but are almost insensitive to skin stretch (Iggo and Muir, 1969). My finding that Merkel cells respond minimally to stretch *in vitro* implies that this specificity of function is retained in culture. Merkel cell insensitivity to radial stretch *in vitro* was common even in the presence of abutting keratinocytes. Thus the specificity of Merkel cell neurite signaling to indentation, rather than stretch, is likely a function of the Merkel cell neurite complex and adjacent keratinocytes, rather than a macroscopic feature of the surrounding epidermis.

mouse (Viana et al., 2001b) and mechanically sensitive neurons in *c. elegans* (Colbert et al., 1997) are all osmosensitive. In addition, neurons underlying hyrosensation in *Drosophila Melanogaster* are mechanosensitive (Liu et al., 2007). This functional linkage implies both modalities of mechanical stimulation may be acting upon a common cell signaling mechanism.

What explains the requirement of abutting keratinocytes for touch sensitivity but not osmosensitivity? Perhaps hypo-osmotic stimuli constitute a robust mechanical signal, capable of activating mechanotransduction channels even in the absence of surrounding keratinocytes, while touch-evoked mechanotransduction requires the extracellular matrix provided by surrounding keratinocytes. There is precedent for the requirement of extracellular matrix in other mechanosensitive systems: in hair cells, stereociliar deflection tugs extracellular links that transmit force to mechanosensitve channels (Gillespie and Walker, 2001), and body touch neurons in c. elegans require extracellular matrix proteins to respond to touch (Du et al., 1996). Keratinocytes might also modulate the nature of the mechanical stimulus; they might diffuse or focus force applied to their exterior and thereby aid mechanotransduction in Merkel cells. Such sophisticated force transfer mechanisms are used in bone where macro bone stress is transduced into microscopic deflections of osteopaths (Malone et al., 2007).

Merkel cells are specifically sensitive to compression, and not stretch, *in vitro*

Merkel cell neurite complexes are highly sensitive to specific mechanical stimuli *in vivo*. They respond to indentations of the skin of as little as 0.5 μm, but are almost insensitive to skin stretch (Iggo and Muir, 1969). My finding that Merkel cells respond minimally to stretch *in vitro* implies that this specificity of function is retained in culture.

Merkel cell insensitivity to radial stretch *in vitro* was common even in the presence of abutting keratinocytes. Thus the specificity of Merkel cell neurite signaling to indentation, rather than stretch, is likely a function of the Merkel cell neurite complex and adjacent keratinocytes, rather than a macroscopic feature of the surrounding epidermis.

Figures

Figure 1. Membrane indentation triggers [Ca^{2+}] transients in Merkel cells. Plot of cytoplasmic [Ca^{2+}] versus time for a representative Merkel cell. Time course of mechanical stimulation is inset at top.

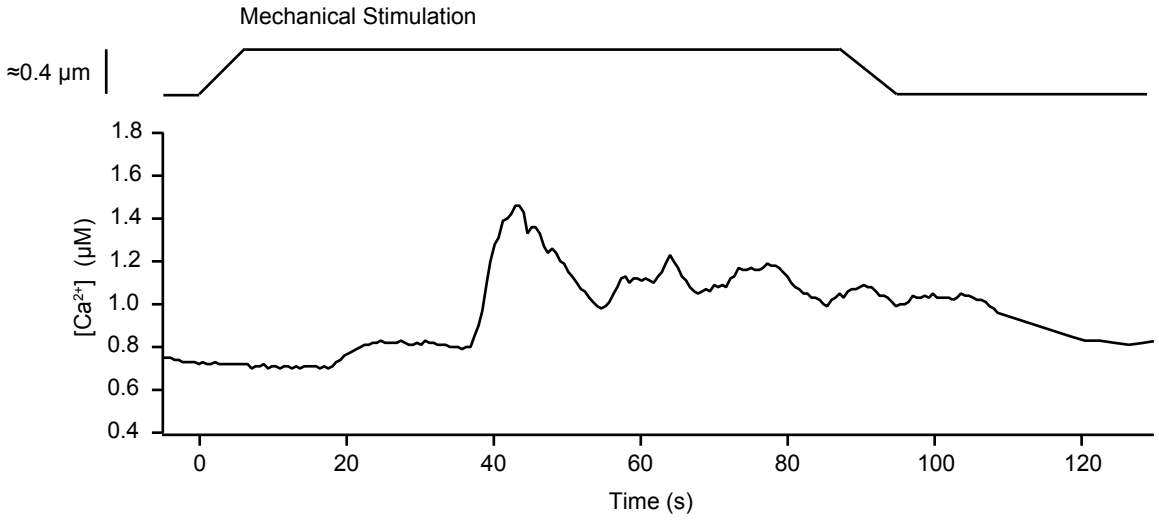
Mechanical Stimulation
≈0.4 µm
1.8
1.6
1.4
1.2
1.0
0.8
0.6
0.4
[Ca2+] (µM)
0
20
40
60
80
100
120
Time (s)

Figure 2. Membrane stretch induces minimal [Ca^{2+}] transients in Merkel cells. Plot of cytoplasmic [Ca^{2+}] versus time for two GFP^{+} Merkel cells and one GFP^{-} cell. Stretching the membrane induced focal plane shifts, rendering several timepoints at the beginning and terminus of the stimulus unobservable.

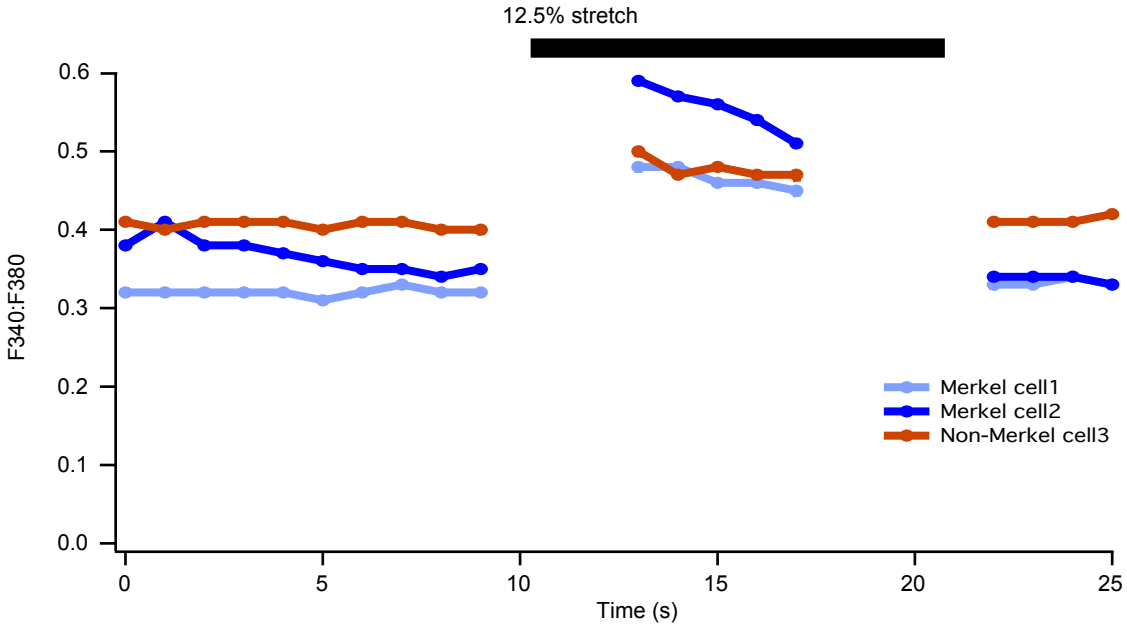
12.5% stretch
0.6
0.5
0.4
0.3
0.2
0.1
0.0
F340:F380
0
5
10
15
20
25
Time (s)
Merkel cell1
Merkel cell2
Non-Merkel cell3

CHAPTER 6:

GENERAL CONCLUSIONS AND FUTURE DIRECTIONS

Ultrastructural evidence suggests Merkel cells signal the nerve afferent via chemical synaptic transmission (Mihara et al., 1979). My colleagues and I demonstrate that Merkel cells express the presynaptic proteins necessary for vesicle release (Chapter 3). Furthermore, we and others have established that Merkel cells express the vesicular glutamate transporter (Haeberle et al., 2004; Hitchcock et al., 2004; Nunzi et al., 2004), VGLUT2, which is a hallmark of a glutamatergic synapse. Although unusual, large dense-core vesicles have been shown to release small, classical neurotransmitters, including glutamate (Morimoto et al., 2003). Semi-intact preparations have suggested that glutamatergic signaling plays a role in SAI signaling (Cahusac et al., 2005), although the evidence is incomplete. Our own attempts to measure glutamate release from Merkel cells *in vitro* have been inconclusive (unpublished observations). Observing the SAI response in mice deficient in VGLUT2 may help resolve the role of glutamate signaling in Merkel cell-neurite mechanotransduction. This does not rule out the role of other neurotransmitters at the Merkel cell-neurite synapse. Indeed, we find extremely high levels of the neuropeptide cholecystokinin octapeptide (CCK 8). Determining whether CCK antagonists inhibit the SAI response would illuminate the role of this neuropeptide in Merkel cell-neurite signaling.

If Merkel cells are mechanosensitive, how might synaptic transmission specify mechanotransduction in the Merkel cell-neurite complex? Some have noted that the 0.3 ms latency of the SAI response is too fast to be mediated by chemical synaptic transmission (Gottschaldt and Vahle-Hinz, 1981) which has been sighted as evidence that Merkel cells do not contribute to the SAI response (Gottschaldt and Vahle-Hinz, 1981;

Diamond et al., 1986). However, others have noted that both the nerve terminal and Merkel cells could be mechanosensitive, with the nerve terminal generating the first action potentials following mechanical stimulation, and Merkel cells contributing the later, sustained element (Ogawa, 1996). Presumably, Merkel cells have cellular signaling machinery that would support them in this role. My colleagues and I have demonstrated that Merkel cells express L- and P/Q-type Ca^{2+} channels, which have both Ca^{2+} and voltage dependent inactivation (Piskorowski et al.). How this inactivation contributes to signaling in the Merkel cell-neurite complex is an unresolved question, likely requiring genetic manipulations of calcium channel inactivation in semi-intact preparations.

The long-standing controversy over whether the Merkel cell contributes to mechanotransduction stems from the inability to directly measure and manipulate mechanotransduction *in situ*. Identification of the proteins essential for mechanotransduction would side-step this problem and provide a tool for characterizing mechanotransduction directly *in vivo*. We find that an ion channel likely underlies hypotonic responses in Merkel cells, which may also mediate mechanotransduction *in vivo* (Gillespie and Walker, 2001). Furthermore, we provide evidence that this channel is a TRP channel, and enumerate several promising candidates, including PKD1 and PKD2, which are thought to transduce mechanical stimuli in the kidney (Nauli et al., 2003).

Conclusive molecular identification of this channel constitutes the most important extension of this research. Candidates in which deficient mouse lines are available can be tested directly. Merkel cells from such mice can be tested for sensitivity to hypotonic solutions *in vitro*. For other candidates, small inhibitory RNAs can be used to disrupt their expression in Merkel cells *in vitro*. Since the activity of voltage-activated Ca^{2+}

channels is highly reduced immediately post dissociation (Chapter 3), likely most channels on the surface of Merkel cells *in vivo* do not survive the dissociation. Given reasonable rates of protein degredation, Merkel cells treated with such inhibitory RNAs should lack the target protein after several days in culture, and can then be rapidly screened for mechanosensitivity using our hypotonic response paradigm.

Once a channel necessary for hypotonic sensitivity is identified, several experimental lines of evidence would determine if the channel contributes to mechanotransduction *in vivo*. First, mice deficient in the putative mechanosensitive channel should have altered touch-based behaviors. Behavioral assays to test texture detection have been designed for mice (Wetzel et al., 2006). Second, the skin-nerve preparation should display deficits in mechanoreceptor responses, specifically the SAI. If other cutaneous response profiles are disrupted, the native expression pattern of the protein should match the disrupted responses. While neuron subtypes that innervate particular cutaneous structures have not been identified, general distinctions based on neuron cell body size can be made: large-diameter neurons innervate innocuous mechanoreceptors and proprioceptors, while small diameter neurons are generally polymodal nociceptive afferents. Fourth, candidate mechanoreceptors should localize to known sites of mechanotransduction, which for most cutaneous receptors is the afferent terminal .

It is quite possible that multiple channel subunits heteromultermize to form a force-sensitive complex in mammals. In *Drosophila melanogaster*, the mechanosensitive channels *nanchung* and *inactive* are both required for hearing (Gong et al., 2004). The authors note that disruption of either protein prevents localization of the other to the

sensory cilia, and argue that the two gene products form heteromultimers. Additionally, two channel subunits, MEC-4 and MEC-10, form a force-sensitive ion channel in *Caenorhabditis elegans* (Goodman and Schwarz, 2003).

Identification of a force-sensitive channel would help to resolve the recalcitrant issue of the Merkel cell's role in mechanotransduction: if the channel is required for normal SAI responses, then expression of the channel exclusively in the Merkel cells would argue for an essential role of Merkel cells in mechanotransduction. If the channel is more widely expressed, its expression could be conditionally disrupted in Merkel cells using *Math1:CRE* mice to settle the matter. More importantly, if a channel is definitively identified, it would provide the first mechanosensitive channel in a mammalian system, finally providing a molecular handle for touch and hearing, the least molecularly described of Aristotle's five cardinal senses.

REFERENCES

Adrian ED, Zotterman Y (1926) The impulses produced by sensory nerve endings: Part 3. Impulses set up by Touch and Pressure. J Physiol 61:465-483.

Altamirano J, Brodwick MS, Alvarez-Leefmans FJ (1998) Regulatory volume decrease and intracellular Ca2+ in murine neuroblastoma cells studied with fluorescent probes. J Gen Physiol 112:145-160.

Arnaout MA (2001) Molecular genetics and pathogenesis of autosomal dominant polycystic kidney disease. Annu Rev Med 52:93-123.

Baumann KI, Chan E, Halata Z, Senok SS, Yung WH (1996) An isolated rat vibrissal preparation with stable responses of slowly adapting mechanoreceptors. Neurosci Lett 213:1-4.

Bekirov IH, Needleman LA, Zhang W, Benson DL (2002) Identification and localization of multiple classic cadherins in developing rat limbic system. Neuroscience 115:213-227.

Bell J, Bolanowski S, Holmes MH (1994) The structure and function of Pacinian corpuscles: a review. Prog Neurobiol 42:79-128.

Ben-Arie N, Hassan BA, Bermingham NA, Malicki DM, Armstrong D, Matzuk M, Bellen HJ, Zoghbi HY (2000) Functional conservation of atonal and Math1 in the CNS and PNS. Development 127:1039-1048.

Bermingham NA, Hassan BA, Price SD, Vollrath MA, Ben-Arie N, Eatock RA, Bellen HJ, Lysakowski A, Zoghbi HY (1999) Math1: an essential gene for the generation of inner ear hair cells. Science 284:1837-1841.

Berridge MJ, Bootman MD, Roderick HL (2003) Calcium signalling: dynamics, homeostasis and remodelling. Nat Rev Mol Cell Biol 4:517-529.

Blount P, Sukharev SI, Moe PC, Nagle SK, Kung C (1996) Towards an understanding of the structural and functional properties of MscL, a mechanosensitive channel in bacteria. Biol Cell 87:1-8.

Boring EG (1942) Sensation and perception in the history of experimental psychology. New York: Appleton Century Crofts Inc.

Brakebusch C, Grose R, Quondamatteo F, Ramirez A, Jorcano JL, Pirro A, Svensson M, Herken R, Sasaki T, Timpl R, Werner S, Fassler R (2000) Skin and hair follicle integrity is crucially dependent on beta 1 integrin expression on keratinocytes. Embo J 19:3990-4003.

Brown AG, Iggo A (1967) A quantitative study of cutaneous receptors and afferent fibres in the cat and rabbit. J Physiol 193:707-733.

Cahusac PM, Senok SS, Hitchcock IS, Genever PG, Baumann KI (2005) Are unconventional NMDA receptors involved in slowly adapting type I mechanoreceptor responses? Neuroscience 133:763-773.

Caterina MJ, Julius D (2001) The vanilloid receptor: a molecular gateway to the pain pathway. Annu Rev Neurosci 24:487-517.

Catterall WA (2000) Structure and regulation of voltage-gated Ca^{2+} channels. Annu Rev Cell Dev Biol 16:521-555.

Chan E, Yung WH, Baumann KI (1996) Cytoplasmic Ca^{2+} concentrations in intact Merkel cells of an isolated, functioning rat sinus hair preparation. Exp Brain Res 108:357-366.

Chen Y, Simasko SM, Niggel J, Sigurdson WJ, Sachs F (1996) Ca2+ uptake in GH3 cells during hypotonic swelling: the sensory role of stretch-activated ion channels. Am J Physiol 270:C1790-1798.

Chu PG, Weiss LM (2002) Keratin expression in human tissues and neoplasms. Histopathology 40:403-439.

Cibulsky SM, Sather WA (1999) Block by ruthenium red of cloned neuronal voltage-gated calcium channels. J Pharmacol Exp Ther 289:1447-1453.

Colbert HA, Smith TL, Bargmann CI (1997) OSM-9, a novel protein with structural similarity to channels, is required for olfaction, mechanosensation, and olfactory adaptation in Caenorhabditis elegans. J Neurosci 17:8259-8269.

Crist JR, Fallon M, Bobbin RP (1993) Volume regulation in cochlear outer hair cells. Hear Res 69:194-198.

Dalsgaard CJ, Rydh M, Haegerstrand A (1989) Cutaneous innervation in man visualized with protein gene product 9.5 (PGP 9.5) antibodies. Histochemistry 92:385-390.

DeCarvalho AC, Cappendijk SL, Fadool JM (2004) Developmental expression of the POU domain transcription factor Brn-3b (Pou4f2) in the lateral line and visual system of zebrafish. Dev Dyn 229:869-876.

DeRisi JL, Iyer VR, Brown PO (1997) Exploring the metabolic and genetic control of gene expression on a genomic scale. Science 278:680-686.

Diamond J, Holmes M, Nurse CA (1986) Are Merkel cell-neurite reciprocal synapses involved in the initiation of tactile responses in salamander skin? J Physiol 376:101-120.

Dietrich A, Kalwa H, Storch U, Mederos YSM, Salanova B, Pinkenburg O, Dubrovska G, Essin K, Gollasch M, Birnbaumer L, Gudermann T (2007) Pressure-induced and store-operated cation influx in vascular smooth muscle cells is independent of TRPC1. Pflugers Arch.

Dodt E, Zotterman Y (1952) Mode of action of warm receptors. Acta Physiol Scand 26:345-357.

Du H, Gu G, William CM, Chalfie M (1996) Extracellular proteins needed for C. elegans mechanosensation. Neuron 16:183-194.

Duggan A, Ma C, Chalfie M (1998) Regulation of touch receptor differentiation by the Caenorhabditis elegans mec-3 and unc-86 genes. Development 125:4107-4119.

Fagan BM, Cahusac PM (2001) Evidence for glutamate receptor mediated transmission at mechanoreceptors in the skin. Neuroreport 12:341-347.

Fradette J, Larouche D, Fugere C, Guignard R, Beauparlant A, Couture V, Caouette-Laberge L, Roy A, Germain L (2003) Normal Human Merkel Cells are Present in Epidermal Cell Populations Isolated and Cultured from Glabrous and Hairy Skin Sites. J Invest Dermatol 120:313-317.

Fremeau RT, Jr., Troyer MD, Pahner I, Nygaard GO, Tran CH, Reimer RJ, Bellocchio EE, Fortin D, Storm-Mathisen J, Edwards RH (2001) The expression of vesicular glutamate transporters defines two classes of excitatory synapse. Neuron 31:247-260.

Garcia-Anoveros J, Ma C, Chalfie M (1995) Regulation of Caenorhabditis elegans degenerin proteins by a putative extracellular domain. Curr Biol 5:441-448.

Garcia-Caballero A, Gallego R, Garcia-Caballero T, Fraga M, Blanco M, Fernandez-Redondo V, Beiras A (1997) Cellular and subcellular distribution of 7B2 in porcine Merkel cells. Anat Rec 248:159-163.

Gillespie PG, Walker RG (2001) Molecular basis of mechanosensory transduction. Nature 413:194-202.

Gong Z, Son W, Chung YD, Kim J, Shin DW, McClung CA, Lee Y, Lee HW, Chang DJ, Kaang BK, Cho H, Oh U, Hirsh J, Kernan MJ, Kim C (2004) Two interdependent TRPV channel subunits, inactive and Nanchung, mediate hearing in Drosophila. J Neurosci 24:9059-9066.

Gonzalez-Perrett S, Kim K, Ibarra C, Damiano AE, Zotta E, Batelli M, Harris PC, Reisin IL, Arnaout MA, Cantiello HF (2001) Polycystin-2, the protein mutated in autosomal dominant polycystic kidney disease (ADPKD), is a Ca2+-permeable nonselective cation channel. Proc Natl Acad Sci U S A 98:1182-1187.

Goodman MB, Schwarz EM (2003) Transducing touch in Caenorhabditis elegans. Annu Rev Physiol 65:429-452.

Gottschaldt KM, Vahle-Hinz C (1981) Merkel cell receptors: structure and transducer function. Science 214:183-186.

Gottschaldt KM, Vahle-Hinz C (1982) Evidence against transmitter function of met-enkephalin and chemosynaptic impulse generation in "Merkel cell" mechanoreceptors. Exp Brain Res 45:459-463.

Haag ML, Glass LF, Fenske NA (1995) Merkel cell carcinoma: diagonsis and treatment. Dematological Surgery 21:669-683.

Haeberle H, Fujiwara M, Chuang J, Medina MM, Panditrao M, Bechstedt S, Howard J, Lumpkin EA (2004) Molecular profiling reveals synaptic release machinery in Merkel cells. Proc Natl Acad Sci U S A 101:14503-14508.

Halata Z, Grim M, Bauman KI (2003) Friedrich Sigmund Merkel and his "Merkel cell", morphology, development, and physiology: Review and new results. Anat Rec 271A:225-239.

Hamann W (1995) Mammalian cutaneous mechanoreceptors. Prog Biophys Mol Biol 64:81-104.

Hanaoka K, Qian F, Boletta A, Bhunia AK, Piontek K, Tsiokas L, Sukhatme VP, Guggino WB, Germino GG (2000) Co-assembly of polycystin-1 and -2 produces unique cation-permeable currents. Nature 408:990-994.

Harada N, Ernst A, Zenner HP (1993) Volume regulation in guinea pig outer hair cells and the role of intracellular calcium. Acta Otolaryngol Suppl 500:39-41.

Hartschuh W, Weihe E (1980) Fine structural analysis of the synaptic junction of Merkel cell-axon-complexes. J Invest Dermatol 75:159-165.

Hartschuh W, Weihe E, Egner U (1990) Electron microscopic immunogold cytochemistry reveals chromogranin A confined to secretory granules of porcine Merkel cells. Neurosci Lett 116:245-249.

Hayashi Y, Zviman MM, Brand JG, Teeter JH, Restrepo D (1996) Measurement of membrane potential and [Ca2+]i in cell ensembles: application to the study of glutamate taste in mice. Biophys J 71:1057-1070.

Helms AW, Abney AL, Ben-Arie N, Zoghbi HY, Johnson JE (2000) Autoregulation and multiple enhancers control Math1 expression in the developing nervous system. Development 127:1185-1196.

Hensel H, Boman KK (1960) Afferent impulses in cutaneous sensory nerves in human subjects. J Neurophysiol 23:564-578.

Hitchcock IS, Genever PG, Cahusac PM (2004) Essential components for a glutamatergic synapse between Merkel cell and nerve terminal in rats. Neurosci Lett 362:196-199.

Hunt CC, Mc IA (1960) An analysis of fibre diameter and receptor characteristics of myelinated cutaneous afferent fibres in cat. J Physiol 153:99-112.

Iggo A, Muir AR (1969) The structure and function of a slowly adapting touch corpuscle in hairy skin. J Physiol 200:763-796.

Iggo A, Findlater GS (1984) A review of Merkel cell mechanisms. In: Sensory receptor mechanisms (Hamann W, Iggo A, eds), pp 117-131. Singapore: World Scientific Publ. Co.

Ikeda I, Yamashita Y, Ono T, Ogawa H (1994) Selective phototoxic destruction of rat Merkel cells abolishes responses of slowly adapting type I mechanoreceptor units. J Physiol 479 (Pt 2):247-256.

Ikeda K, Saito Y, Nishiyama A, Takasaka T (1991) Effect of neuroregulators on the intracellular calcium level in the outer hair cell isolated from the guinea pig. ORL J Otorhinolaryngol Relat Spec 53:78-81.

Jakab M, Ritter M (2006) Cell volume regulatory ion transport in the regulation of cell migration. Contrib Nephrol 152:161-180.

Jarman AP (2002) Studies of mechanosensation using the fly. Hum Mol Genet 11:1215-1218.

Johnson KO, Hsiao SS (1992) Neural mechanisms of tactual form and texture perception. Annu Rev Neurosci 15:227-250.

Johnson KO, Yoshioka T, Vega-Bermudez F (2000) Tactile functions of mechanoreceptive afferents innervating the hand. J Clin Neurophysiol 17:539-558.

Kawai J, Shinagawa A, Shibata K, Yoshino M, Itoh M, Ishii Y, Arakawa T, Hara A, Fukunishi Y, Konno H, Adachi J, Fukuda S, Aizawa K, Izawa M, Nishi K, Kiyosawa H, Kondo S, Yamanaka I, Saito T, Okazaki Y, Gojobori T, Bono H, Kasukawa T, Saito R, Kadota K, Matsuda H, Ashburner M, Batalov S, Casavant T, Fleischmann W, Gaasterland T, Gissi C, King B, Kochiwa H, Kuehl P, Lewis S, Matsuo Y, Nikaido I, Pesole G, Quackenbush J, Schriml LM, Staubli F, Suzuki R, Tomita M, Wagner L, Washio T, Sakai K, Okido T, Furuno M, Aono H, Baldarelli R, Barsh G, Blake J, Boffelli D, Bojunga N, Carninci P, de Bonaldo MF, Brownstein MJ, Bult C, Fletcher C, Fujita M, Gariboldi M, Gustincich S, Hill D, Hofmann M, Hume DA, Kamiya M, Lee NH, Lyons P, Marchionni L, Mashima J, Mazzarelli J, Mombaerts P, Nordone P, Ring B, Ringwald M, Rodriguez I, Sakamoto N, Sasaki H, Sato K, Schonbach C, Seya T, Shibata Y, Storch KF, Suzuki H, Toyo-oka K, Wang KH, Weitz C, Whittaker C, Wilming L, Wynshaw-Boris A, Yoshida K, Hasegawa Y, Kawaji H, Kohtsuki S, Hayashizaki Y (2001) Functional annotation of a full-length mouse cDNA collection. Nature 409:685-690.

Kim J, Chung YD, Park DY, Choi S, Shin DW, Soh H, Lee HW, Son W, Yim J, Park CS, Kernan MJ, Kim C (2003) A TRPV family ion channel required for hearing in Drosophila. Nature 424:81-84.

Kinkelin I, Stucky CL, Koltzenburg M (1999) Postnatal loss of Merkel cells, but not of slowly adapting mechanoreceptors in mice lacking the neurotrophin receptor p75. Eur J Neurosci 11:3963-3969.

Klebes A, Biehs B, Cifuentes F, Kornberg TB (2002) Expression profiling of Drosophila imaginal discs. Genome Biol 3:RESEARCH0038.

Knibestol M, Vallbo AB (1980) Intensity of sensation related to activity of slowly adapting mechanoreceptive units in the human hand. J Physiol 300:251-267.

Kung C, Blount P (2004) Channels in microbes: so many holes to fill. Mol Microbiol 53:373-380.

Launay P, Fleig A, Perraud AL, Scharenberg AM, Penner R, Kinet JP (2002) TRPM4 is a Ca2+-activated nonselective cation channel mediating cell membrane depolarization. Cell 109:397-407.

Leem JW, Willis WD, Weller SC, Chung JM (1993) Differential activation and classification of cutaneous afferents in the rat. J Neurophysiol 70:2411-2424.

Lewis RS, Hudspeth AJ (1983) Voltage- and ion-dependent conductances in solitary vertebrate hair cells. Nature 304:538-541.

Liedtke W, Tobin DM, Bargmann CI, Friedman JM (2003) Mammalian TRPV4 (VR-OAC) directs behavioral responses to osmotic and mechanical stimuli in Caenorhabditis elegans. Proc Natl Acad Sci U S A 100 Suppl 2:14531-14536.

Liedtke W, Choe Y, Marti-Renom MA, Bell AM, Denis CS, Sali A, Hudspeth AJ, Friedman JM, Heller S (2000) Vanilloid receptor-related osmotically activated channel (VR-OAC), a candidate vertebrate osmoreceptor. Cell 103:525-535.

Liu L, Li Y, Wang R, Yin C, Dong Q, Hing H, Kim C, Welsh MJ (2007) Drosophila hygrosensation requires the TRP channels water witch and nanchung. Nature 450:294-298.

Lumpkin EA, Hudspeth AJ (1995) Detection of Ca^{2+} entry through mechanosensitive channels localizes the site of mechanoelectrical transduction in hair cells. Proc Natl Acad Sci U S A 92:10297-10301.

Lumpkin EA, Collisson T, Parab P, Omer-Abdalla A, Haeberle H, Chen P, Doetzlhofer A, White P, Groves A, Segil N, Johnson JE (2003) Math1-driven GFP expression in the developing nervous system of transgenic mice. Gene Expr Patterns 3:389-395.

Malone AM, Anderson CT, Tummala P, Kwon RY, Johnston TR, Stearns T, Jacobs CR (2007) Primary cilia mediate mechanosensing in bone cells by a calcium-independent mechanism. Proc Natl Acad Sci U S A 104:13325-13330.

Maroto R, Raso A, Wood TG, Kurosky A, Martinac B, Hamill OP (2005) TRPC1 forms the stretch-activated cation channel in vertebrate cells. Nat Cell Biol 7:179-185.

Merkel F (1875) Tastzellen und Tastkorperchen bei den, Haustehieren und beim Menschen. Arch Mikrosk Anat 11:636-652.

Mihara M, Hashimoto K, Ueda K, Kumakiri M (1979) The specialized junctions between Merkel cell and neurite: an electron microscopic study. J Invest Dermatol 73:325-334.

Mills LR, Diamond J (1995) Merkel cells are not the mechanosensory transducers in the touch dome of the rat. J Neurocytol 24:117-134.

Moll I, Kuhn C, Moll R (1995) Cytokeratin 20 is a general marker of cutaneous Merkel cells while certain neuronal proteins are absent. J Invest Dermatol 104:910-915.

Mollon HBBaJD (1982) The senses.

Morimoto R, Hayashi M, Yatsushiro S, Otsuka M, Yamamoto A, Moriyama Y (2003) Co-expression of vesicular glutamate transporters (VGLUT1 and VGLUT2) and their association with synaptic-like microvesicles in rat pinealocytes. J Neurochem 84:382-391.

Mountcastle VB (1967) The problem of sensing and the neural coding of sensory events. In: The Neurosciences (Quarton GC mT, Schmitt FO, ed), pp 393-408. New York: Rockfeller University Press.

Munger BL (1965) The intraepidermal innervation of the snout skin of the opossum. A light and electron microscope study, with observations on the nature of Merkel's Tastzellen. J Cell Biol 26:79-97.

Nagasaki K, Fleischer S (1989) Modulation of the calcium release channel of sarcoplasmic reticulum by adriamycin and other drugs. Cell Calcium 10:63-70.

Nakafusa J, Narisawa Y, Shinogi T, Taira K, Tanaka T, Inoue T, Misago N (2006) Changes in the number of Merkel cells with the hair cycle in hair discs on rat back skin. Br J Dermatol 155:883-889.

Nauli SM, Alenghat FJ, Luo Y, Williams E, Vassilev P, Li X, Elia AE, Lu W, Brown EM, Quinn SJ, Ingber DE, Zhou J (2003) Polycystins 1 and 2 mediate mechanosensation in the primary cilium of kidney cells. Nat Genet 33:129-137.

Nordin M (1990) Low-threshold mechanoreceptive and nociceptive units with unmyelinated (C) fibres in the human supraorbital nerve. J Physiol 426:229-240.

Nunzi MG, Pisarek A, Mugnaini E (2004) Merkel cells, corpuscular nerve endings and free nerve endings in the mouse palatine mucosa express three subtypes of vesicular glutamate transporters. J Neurocytol 33:359-376.

Ogawa H (1996) The Merkel cell as a possible mechanoreceptor cell. Prog Neurobiol 49:317-334.

Oike M, Droogmans G, Nilius B (1994) Mechanosensitive Ca2+ transients in endothelial cells from human umbilical vein. Proc Natl Acad Sci U S A 91:2940-2944.

Pacitti EG, Findlater GS (1988) Calcium channel blockers and Merkel cells. Prog Brain Res 74:37-42.

Pasche F, Merot Y, Carraux P, Saurat JH (1990) Relationship between Merkel cells and nerve endings during embryogenesis in the mouse epidermis. J Invest Dermatol 95:247-251.

Pattillo JM, Yazejian B, DiGregorio DA, Vergara JL, Grinnell AD, Meriney SD (2001) Contribution of presynaptic calcium-activated potassium currents to transmitter release regulation in cultured Xenopus nerve-muscle synapses. Neuroscience 102:229-240.

Petit D, Burgess PR (1968) Dorsal column projection of receptors in cat hairy skin supplied by myelinated fibers. J Neurophysiol 31:849-855.

Phillips JR, Johnson KO (1981) Tactile spatial resolution. II. Neural representation of Bars, edges, and gratings in monkey primary afferents. J Neurophysiol 46:1192-1203.

Piontek KB, Huso DL, Grinberg A, Liu L, Bedja D, Zhao H, Gabrielson K, Qian F, Mei C, Westphal H, Germino GG (2004) A functional floxed allele of Pkd1 that can be conditionally inactivated in vivo. J Am Soc Nephrol 15:3035-3043.

Piskorowski RA, Haeberle H, Panditrao M, Lumpkin EA Voltage-activated calcium channels control excitability in Merkel cells by regulating calcium-activated potassium channels and calcium-induced calcium release. Under revision.

Reuter H (1996) Diversity and function of presynaptic calcium channels in the brain. Curr Opin Neurobiol 6:331-337.

Roberts WM, Jacobs RA, Hudspeth AJ (1990) Colocalization of ion channels involved in frequency selectivity and synaptic transmission at presynaptic active zones of hair cells. J Neurosci 10:3664-3684.

Senok SS, Baumann KI, Halata Z (1996) Selective phototoxic destruction of quinacrine-loaded Merkel cells is neither selective nor complete. Exp Brain Res 110:325-334.

Shimohira-Yamasaki M, Toda S, Narisawa Y, Sugihara H (2006) Merkel cell-nerve cell interaction undergoes formation of a synapse-like structure in a primary culture. Cell Struct Funct 31:39-45.

Skinner LJ, Enee V, Beurg M, Jung HH, Ryan AF, Hafidi A, Aran JM, Dulon D (2003) Contribution of BK Ca2+-activated K+ channels to auditory neurotransmission in the Guinea pig cochlea. J Neurophysiol 90:320-332.

Smith KR, Jr. (1967) The structure and function of the Haarscheibe. J Comp Neurol 131:459-474.

Strotmann R, Harteneck C, Nunnenmacher K, Schultz G, Plant TD (2000) OTRPC4, a nonselective cation channel that confers sensitivity to extracellular osmolarity. Nat Cell Biol 2:695-702.

Szeder V, Grim M, Kucera J, Sieber-Blum M (2003) Neurotrophin-3 signaling in mammalian Merkel cell development. Dev Dyn 228:623-629.

Tachibana M, Okada T, Arimura T, Kobayashi K, Piccolino M (1993) Dihydropyridine-sensitive calcium current mediates neurotransmitter release from bipolar cells of the goldfish retina. J Neurosci 13:2898-2909.

Tachibana T, Nawa T (2002) Recent progress in studies on Merkel cell biology. Anat Sci Int 77:26-33.

Tachibana T, Endoh M, Nawa T (2001) Immunohistochemical expression of G protein alpha-subunit isoforms in rat and monkey Merkel cell-neurite complexes. Histochem Cell Biol 116:205-213.

Tachibana T, Endoh M, Kumakami R, Nawa T (2003) Immunohistochemical expressions of mGluR5, P2Y2 receptor, PLC-beta1, and IP3R-I and -II in Merkel cells in rat sinus hair follicles. Histochem Cell Biol.

Tachibana T, Yamamoto H, Takahashi N, Kamegai T, Shibanai S, Iseki H, Nawa T (1997) Polymorphism of Merkel cells in the rodent palatine mucosa: immunohistochemical and ultrastructural studies. Arch Histol Cytol 60:379-389.

Tazaki M, Suzuki T (1998) Calcium inflow of hamster Merkel cells in response to hyposmotic stimulation indicate a stretch activated ion channel. Neurosci Lett 243:69-72.

Vallbo AB, Johansson RS (1984) Properties of cutaneous mechanoreceptors in the human hand related to touch sensation. Hum Neurobiol 3:3-14.

Vallbo AB, Olsson KA, Westberg KG, Clark FJ (1984) Microstimulation of single tactile afferents from the human hand. Sensory attributes related to unit type and properties of receptive fields. Brain 107 (Pt 3):727-749.

Van Gele M, Boyle GM, Cook AL, Vandesompele J, Boonefaes T, Rottiers P, Van Roy N, De Paepe A, Parsons PG, Leonard JH, Speleman F (2004) Gene-expression profiling reveals distinct expression patterns for Classic versus Variant Merkel cell phenotypes and new classifier genes to distinguish Merkel cell from small-cell lung carcinoma. Oncogene 23:2732-2742.

Viana F, de la Pena E, Pecson B, Schmidt RF, Belmonte C (2001a) Swelling-activated calcium signalling in cultured mouse primary sensory neurons. Eur J Neurosci 13:722-734.

Viana F, de la Pena E, Pescon B, Schmidt RF, Belmonte C (2001b) Swelling-activated calcium signalling in cultured mouse primary sensory neurons. Eur J Neurosci 13:722-734.

Vielkind U, Sebzda MK, Gibson IR, Hardy MH (1995) Dynamics of Merkel cell patterns in developing hair follicles in the dorsal skin of mice, demonstrated by a monoclonal antibody to mouse keratin 8. Acta Anat (Basel) 152:93-109.

von Poser C, Südhof TC (2001) Synaptotagmin 13: structure and expression of a novel synaptotagmin. Eur J Cell Biol 80:41-47.

Wallis D, Hamblen M, Zhou Y, Venken KJ, Schumacher A, Grimes HL, Zoghbi HY, Orkin SH, Bellen HJ (2003) The zinc finger transcription factor Gfi1, implicated in lymphomagenesis, is required for inner ear hair cell differentiation and survival. Development 130:221-232.

Warbington L, Hillman T, Adams C, Stern M (1996) Reduced transmitter release conferred by mutations in the slowpoke-encoded Ca2(+)-activated K+ channel gene of Drosophila. Invert Neurosci 2:51-60.

Werner G, Mountcastle VB (1965) Neural Activity in Mechanoreceptive Cutaneous Afferents: Stimulus-Response Relations, Weber Functions, and Information Transmission. J Neurophysiol 28:359-397.

Weskamp M, Seidl W, Grissmer S (2000) Characterization of the increase in [Ca(2+)](i) during hypotonic shock and the involvement of Ca(2+)-activated K(+) channels in the regulatory volume decrease in human osteoblast-like cells. J Membr Biol 178:11-20.

Wetzel C, Hu J, Riethmacher D, Benckendorff A, Harder L, Eilers A, Moshourab R, A. K, Labuz D, Caspani O, Erdmann B, Machelska H, Heppenstall PA, Lewin GR (2006) A stomatin-domain protein essential for touch sensation in the mouse. Nature In press.

Woodbury CJ, Koerber HR (2007) Central and peripheral anatomy of slowly adapting type I low-threshold mechanoreceptors innervating trunk skin of neonatal mice. J Comp Neurol 505:547-561.

Xu JW, Slaughter MM (2005) Large-conductance calcium-activated potassium channels facilitate transmitter release in salamander rod synapse. J Neurosci 25:7660-7668.

Yamashita Y, Akaike N, Wakamori M, Ikeda I, Ogawa H (1992) Voltage-dependent currents in isolated single Merkel cells of rats. J Physiol 450:143-162.

Zhang Y, Ma C, Delohery T, Nasipak B, Foat BC, Bounoutas A, Bussemaker HJ, Kim SK, Chalfie M (2002) Identification of genes expressed in C. elegans touch receptor neurons. Nature 418:331-335.

Zitt C, Zobel A, Obukhov AG, Harteneck C, Kalkbrenner F, Luckhoff A, Schultz G (1996) Cloning and functional expression of a human Ca2+-permeable cation channel activated by calcium store depletion. Neuron 16:1189-1196.

Zotterman Y (1939) Touch, pain and tickling: an electro-physiological investigation on cutaneous sensory nerves. J Physiol 95:1-28.

APPENDICES

Merkel cell Isolation Protocol

Henry Haeberle and Rebecca Piskorowski

Lumpkin Lab, based on procedure from Hanson Zhen (Oro lab, Stanford University)

11.2006

Solutions and Media:

1. 10% Hibiclens

	Quantities:	Final concentration:
Sterile Water	450 mL	
Hibiclens (Fisher cat # 19-037)	50 mL	10%

2 Washing Solution

HBSS (Complete or Ca^{2+} Mg^{2+} Free) (invitrogen 24020117)	495 mL	
Penicillin/Streptomycin, with fungizone (amphotericin B) (invitrogen 15240062) 100X	5 mL	100U and .25 µg/ml

3. Dispase Solution

HBSS (CMF) 100 mL

(invitrogen14170112)

Dispase 100 mL 50 %

(BD biosciences #354235)

4. Trypsin-EDTA*

0.25% Trypsin and 1 mM EDTA-4Na 5mL

(invitrogen 25200056)

HBSS (CMF) 15mL

*(Diluted before each experiment. Final concentration varies by lot, usually between .05 and .15% Trypsin)

5. TNS (Trypsin Neutralizing Solution)

HBSS (CMF) 425 mL

Fetal Bovine Serum 75 mL 15%

(Gibco cat#26400-36)

6. Launching Media

CNT-02 (Chemicon, cat# CNT02)

7. Sorting & Landing Media

CNT-02

(Chemicon, cat# CNT02) (50% by volume)

FBS (50% by volume)

(Hyclone, ordered through fisher SH3007002)

Procedure

1. Euthanize mice appropriately. Until you get the skin in dispase, work quickly. If you don't have to dehair, you should be able to finish the dissection portion in 20-25 minutes.

2. If the animals are hairy, dehair by shaving and applying depilatory (surgicreme) for 5 minutes. Rub the surgicreme in well with latex gloves. Wash the surgicreme off with warm tap water and rub the skin with your gloves.

3. Clean the skin with 10% Hibiclens.

4. Separate skin from body with forceps and scissors. Get rid of as much of the fat and extra tissue as possible.

5. Wash skin in 10% Hibiclens by placing it dermis side down into the solution for about 1 minute.

6. Wash skin in the wash solution by placing it dermis side down and agitating. Let it soak in the wash solution for at least 3 minutes.

7. Move the skin to fresh wash solution and carefully remove fat and connective tissue from the dermis with a scalpel. (Total of three washes in three dishes).

8. Move the skin to a third wash solution and cut into 1-2 mm wide strips. This is a critical step, as the dispase solution works most effectively close to cut edges. Generally the thinner the strips are, the more cells the prep yields

for a given amount of digestion time. If the mice are entering the hair cycle, make sure to cut the dark skin in small pieces, as it will digest slower, lighter skin can be cut into slightly larger pieces in order to save time. Furthermore, the dispase is relatively gentle, unlike trypsin, higher yields from this digestion do not negatively impact cell viability.

9. Leave skin in dispase solution, covered, at room temperature for 1-2 hrs in the dark (Dispase is light-sensitive). P0-P1 animals should not require more then 1 hour digestion. P1-P3 animals require no more then 1h15m. P3-P6 animals may take up to 1 h 30 min. Once the epidermis easily separates from the dermis, start peeling.

10. Peel the epidermis away from the dermis with sharp forceps. Epidermis is white, transparent, and tough, dermis is fleshy, easily torn, and fleshy colored. Place the peeled epidermal pieces in a bit of dispase solution until you are finished with the peeling. The skin should separate easily, if there is resistance your yields will not be optimal. If the mouse is beginning the hair cycle (P3-P8), work on the lighter skin first, as that skin will peel more easily, and the darker skin, which requires more dispase digestion, remains in the dispase longer.

11. Split the peeled epidermis into 15ml conical tubes (3 tubes for 2 P3-P6 mice), each containing 7 mL of 0.07-0.15% trypsin-EDTA, depending on the strength of the lot of trypsin. Incubate in a 37°C water bath for 11-15 minutes, depending on the strength of the trypsin. Make sure the pH doesn't change significantly. We briefly vortex the tubes (1-2 seconds) every 2 minutes. Keep

the skin in the trypsin until cloudy – then neutralize soon after, as over trypsinization will kill the cells.

12. Neutralize the trypsin by adding 4 mL TNS per tube. Combine aliquots of trypsinized skin in a 50mL conical tube, and triturate the skin ~15 times with a 10mL serological pipette. Be careful not to introduce bubbles, as bubbles will kill cells.

13. Filter with a 70 μm filter to remove skin fragments. Spin filtrate at 400 x g for 12 minutes.

14. Resuspend cells in 1.5 ml of CnT-02 with DNAse. Use enough (>1,000 units/prep) DNAse to make resuspension of the pellet easy, but not so much that the pH of the solution changes.

15. Sort with Fluorescence Activated Cell Sorting (FACS). Merkel cells survive better in co-culture with keratinoctyes, therefore, it is better to sort for yield rather than purity, to maximize the number of cells collected, and to include some keratinocytes in the culture. Sort by comparing FITC (green) fluorescence vs. Cy-3 (red) fluorescence.

16. Collect cells in landing media that is 60 μl Hyclone FBS and 60 μl CnT-02 keratinocyte media. Yields and Merkel cell concentration will vary with the age of the animals: P0 animals will often have Merkel cells consisting of .4-1% of total cells, yielding 2-5*10^5 Merkel cells/mouse. P1-P2 animals should have 0.2-0.4% of total cells, yielding at least 10,000 Merkel cells/mouse. P3-P6 animals should have .2% of total cells, yielding about 10,000 cells/mouse. If on average Merkel cells consist of <.2% of total cells, the skin has either not been cut

into small enough pieces, or it has been under digested with dispase or trypsin. If there are more then 3*10^5 MCs/mouse the cells may be over digested and not healthy enough for electrophysiology. The cell sorter is aseptic but not completely sterile, so it often contaminates preperations. Sterilize the sorter with bleach. Keep Merkel cells cold when possible; before sorting place on ice, and sort into a refrigerated container.

17. Spot Merkel cells on collagen coated coverslips immediately after sorting, and culture in CnT-02 media. Merkel cells take a long time to sit down; yet the high FBS levels kill keratinocytes, therefore I plate for ½ hour, than place media (CNT-02) carefully into the chamber, so as not to disturb the Merkel cells and keratinocytes.

18. Merkel cells like to be co-cultured with Keratinocytes. They are more likely to survive and more likely to grow processes when in co-culture. They grow well on PDL as well as collagen. They spread out in large star formations on Matrigel.

Ca^{2+} imaging calibration protocol

Solutions (all concentrations in mM).

R_{max}: 135 KCl, 2 $MgCl_2$, 10 HEPES, 10 $CaCl_2$

R_{min}: 135 KCl, 2 $MgCl_2$, 10 HEPES, 10 EGTA

R_{mid}: 135 KCl, 2 $MgCl_2$, 10 HEPES, 8.6 EGTA, 1.4 $CaCl_2$

1. Calibrate fura-2 salt concentration for the microscope. Fura-2 salt should not be frozen, store 1 mM stocks at 4C°. Dilute stock to 10 µM in R_{max} and $R_{min.}$

2. Record R_{max} and R_{min} F_{340}:F_{380} with consistent exposure times and regions. The region should include the relatively flat fluorescence profile in the center of field of view.

3. Record Q: The average intensity value of the region for R_{max} and divide by the average intensity value of R_{min}.

4. Record R_{mid} F_{340}:F_{380}. Use the recorded R_{max} and R_{min} values to determine the free [Ca^{2+}] of R_{mid}. [Ca^{2+}]= $Kd\cdot(R-R_{min})/(R_{max}-R)*Q$. In these solutions, assume fura-2 Kd is 250 nM (Diana Bautista, UC Berkeley). Make sure the R_{mid} [Ca^{2+}] is near the Kd* of fura-2 *in vivo*, which should be about 1µM.

5. Culture and load Merkel cells with Fura-2 AM as normal.

6. Perfuse Merkel cells with R_{min} solution supplemented with 2mM 2-deoxy-D-glucose for ½ hour.

7. Perfuse R_{min} solution with 1 µM ionomycin.

8. Allow Ca^{2+} concentrations to return to baseline, record the R_{min} Fura-2 ratio.

9. Transfer cells to R_{max} solution supplemented with 1 μM ionomycin. Cell $[Ca^{2+}]$ should rise exponentially to a stable R_{max} level. If cells do not rise to R_{max}, add 0.01–0.015% triton X-100 to further permeabilize cells. Higher concentrations of triton X-100 will lyse cells. Leave cells in high $[Ca^{2+}]$ for as short of time as possible. Verify that cells have not lost dye by determining if raw F_{340} or F_{380} values are stable. Record R_{max} fura-2 ratio.

10. Transfer cells to R_{mid} solution with 1 μM ionomycin. F_{340}:F_{380} should decrease, and will likely decrease back to baseline, if any pumps are still active.

11. If fura-2 ratios return to baseline, or a value significantly lower than expected, Ca^{2+} pumps are still active. Add between .01–0.15% triton X-100 to help permeabilize cells, and 2mM 2-deoxy-D-glucose to terminate ATP synthesis. Fura-2 ratios should slowly rise; wait for up to 1 h for high, stable fura-2 ratios, without loss of fura-2.

12. Establish Kd* where R_{mid} $[Ca^{2+}]= Kd^{*}\cdot(R_{mid}-R_{min})/(R_{max}-R_{mid})$

Ca^{2+} Imaging Data Analysis

Data was acquired with Metafluor software, Meta Imaging series, (version 6.4.7, Molecular Devices) and analyzed with custom algorithms written in Igor Pro (version 5.03, Wavemetrics).

1) Set gain to max. Set exposure time such that 380 emission use all of the dynamic range. Exposure times should be between 70 and 300 ms, longer exposure times will likely induce photodamage, while exposure times less than 30 ms likely indicate that the cells are overloaded with fura-2, and small [Ca^{2+}] signals will be buffered.

2) Subtract backgrounds. Divert emission to the eyepieces, and record background images under the subtract background command on the control panel. Subtract these backgrounds.

2) Design regions around GFP positive cells, such that they include all cytoplasmic processes.

3) Set thresholds for fura-2 emission from both 340 nm and 380 nm excitation such that background is eliminated.

4) Log Fura-2 ratio data it's a check box under the command panel. Data exported from Metaflour has the following format:

"Header information in quotes, denoting location of regions"

Time (s); Ratio cell 1; Ratio cell 2; Ratio cell 3; … etc

Time (s); Ratio cell 1; Ratio cell 2; Ratio cell 3; … etc

"event Marks, with Time(s) in quotes"

Time (s); Ratio cell 1; Ratio cell 2; Ratio cell 3; … etc

…

5) Cut the event marks from the .log file and place them in a second file, named events.txt. Remove the remaining lines that begin with quotes from the .log file, and rename it .txt. This process can be done by hand, or the following bash shell script can be used:

```
for x in `find . -name '*.LOG' | cut -f 2 -d . | cut -c 2-` ; do grep -v \" $x.LOG > $x.txt; grep -v : $x. LOG | grep \" | grep -v "R1 R2" | sed s/\"//g > $x"Events.txt"; done; for x in `find . -name '*.log' | cut -f 2 -d . | cut -c 2-` ; do grep -v \" $x.log > $x.txt; grep -v : $x.LOG | grep \" | grep -v "R1 R2" | sed s/\"//g > $x"Events.txt"; done
```

5) Launch Igor, and open the Ca^{2+} imaging analysis program. The program is designed to read the two files previously described. Toggle the “load file” button to launch the loading procedure.

6) Select the active experiment with the “Select Experiment” toggle button. Individual cells will be displayed in the active window. If you want to load additional experiments, toggle “load file” an additional time. The second experiment will show up in the “Select Experiment” list. “Display Average” will graph average of all traces in experiment ± SEM.

7) Perform further analysis from the command line. The program has function windows open that explain how to perform the analysis, such as determining responding cells, finding peak responses, and converting fura-2 ratios to $[Ca^{2+}]$.

Publishing Agreement

It is the policy of the University to encourage the distribution of all theses and dissertations. Copies of all UCSF theses and dissertations will be routed to the library via the Graduate Division. The library will make all theses and dissertations accessible to the public and will preserve these to the best of their abilities, in perpetuity.

Please sign the following statement:

I hereby grant permission to the Graduate Division of the University of California, San Francisco to release copies of my thesis or dissertation to the Campus Library to provide access and preservation, in whole or in part, in perpetuity.

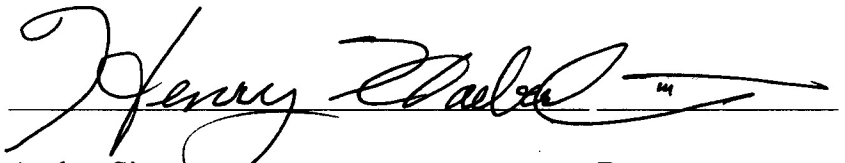

Author Signature 12/21/2007

Date